



Contents lists available at ScienceDirect

Arabian Journal of Chemistry

journal homepage: [www.sciencedirect.com](http://www.sciencedirect.com)

Review article

# Thiazole ring- the antimicrobial, anti-inflammatory, and anticancer active scaffold

Seyedmohammad Hosseini-zhad<sup>a,b</sup>, Ali Ramazani<sup>a,c,\*</sup><sup>a</sup> Department of Chemistry, Faculty of Science, University of Zanjan, Zanjan 45371-38791, Iran<sup>b</sup> Department of Chemistry, Faculty of Science, Babol Noshirvani University of Technology, Babol, Iran<sup>c</sup> Research Institute of Modern Biological Techniques (RIMBT), University of Zanjan, Zanjan 4537138791, Iran

## ARTICLE INFO

### Article history:

Received 4 April 2023

Accepted 31 August 2023

Available online 6 September 2023

### Keywords:

Antifungal  
Antibacterial  
Biological activity  
Antitumor  
Thiazoles  
Drug discovery

## ABSTRACT

**Background:** Thiazole ring is one of the most important heterocycle scaffolds in organic and medicinal chemistry due to this scaffold being the backbone of numerous drugs and their significant activities against various diseases have made it one of the best candidates for industrial production. According to the literature, the number of drugs that have this ring on their structures is increasing. In fact, drugs containing thiazole scaffold have taken a significant share in the last decade, which reached its maximum number of 8 drugs in 2019. **Objective:** In This current review, we focus on essential advances of antimicrobial, anti-inflammatory, and anticancer activities of structures containing thiazole scaffold and various groups' effects on this scaffold against the broad spectrum of bacterial strains, fungal strains, inflammatory cells, and cancer cells. Also, we analyzed and investigated thiazole hybrids with potential antimicrobial, anti-inflammatory, and anticancer activities. **Results:** More than 100 research articles were found, we selected about 100 research articles from 2014 to 2022 that had outstanding results.

© 2023 The Author(s). Published by Elsevier B.V. on behalf of King Saud University. This is an open access article under the CC BY license (<http://creativecommons.org/licenses/by/4.0/>).

## 1. Introduction

Organic and medicinal chemistry are important majors in the field of synthesis and development of structures with biological activity (Sani and Zanda, 2022; Wentrup, 2022). In recent years, researchers focusing on structures that have scaffolds containing heterocycles atoms, and rings. There are a lot of molecules with five, six, and so on membered heterocycle rings containing hetero atoms (Kaur, 2018a,b; Kaur and Kishore, 2014; Kaur et al., 2021). Meanwhile, the thiazole ring is one of the types of heterocyclic rings with different biological properties (Ali and Sayed, 2021). **Scheme 1.**

Research illustrates Thiazole rings have an excellent wide range of pharmaceutical applications such as antimalarial (Bueno et al., 2016), antifungal (Lino et al., 2018), anticancer (Jain et al., 2018),

anti-inflammatory (Moldovan et al., 2011), antibacterial (Li et al., 2014), antioxidant (Grozav et al., 2017), and so on. According to the Njardarson group reports, five drugs with thiazole scaffold exist in the top two hundred brand name drugs by retail sales in 2015, namely: Viekira Pak, Sprycel, Augmentin, Kaletra, and Olysio/Sovriad. Five drugs exist in the top two hundred brand name drugs by retail sales in 2016, namely: Stribild, Sprycel, Genvoya, Myrbetriq, and Augmentin. In 2018, seven drugs exist in the top two hundred brand name drugs by retail sales, namely: Genvoya, Sprycel, Prezcoibix, Myrbetriq, Tafinlar, Lixiana, and Augmentin. The number of drugs increased to eight in 2019, which are Genvoya, Sprycel, Prezista, Myrbetriq, Edoxaban, Tafinlar/Mekinist, Lixiana, and Augmentin. This trend decreased to 5 drugs in 2020, but again from 2021 this trend increased until it increased to 7 drugs in 2022. According to the information in the Fig. 1, it can be seen that after every decreasing trend, there is an increasing trend. Also, the highest number of drugs containing the thiazole ring was in 2019, and in 2015, 2016 and 2020, the number of drugs was fixed at 5 (Fig. 1) (J. Chem. Ed. 2010).

The purpose of the present review is to collect and analysis of important studies that investigate of antimicrobial, anti-inflammatory, and anticancer activity of structures that have thiazole scaffold from 2014 to 2022 and show their advance for more effectiveness.

\* Corresponding author.

E-mail addresses: [hossinichemistry1397@gmail.com](mailto:hossinichemistry1397@gmail.com), [M.hosseini-zhad@stu.nit.ac.ir](mailto:M.hosseini-zhad@stu.nit.ac.ir) (S. Hosseini-zhad), [aliramazani@znu.ac.ir](mailto:aliramazani@znu.ac.ir) (A. Ramazani).

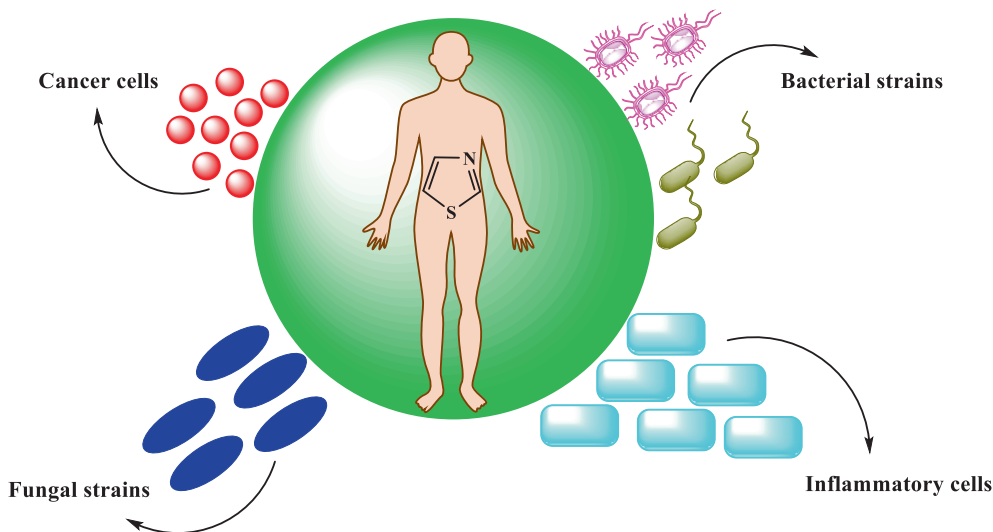
Peer review under responsibility of King Saud University.



Production and hosting by Elsevier

<https://doi.org/10.1016/j.arabjc.2023.105234>

1878-5352/© 2023 The Author(s). Published by Elsevier B.V. on behalf of King Saud University. This is an open access article under the CC BY license (<http://creativecommons.org/licenses/by/4.0/>).



**Scheme 1.** The thiazole ring has the characteristic of resisting the inflammatory cells of various bacterial and fungal strains, as well as all types of cancer cells, and it can even be used to treat these pathogens in industrial drugs. Therefore, the thiazole ring is a suitable protective medicine for humans from these pathogenic agents.

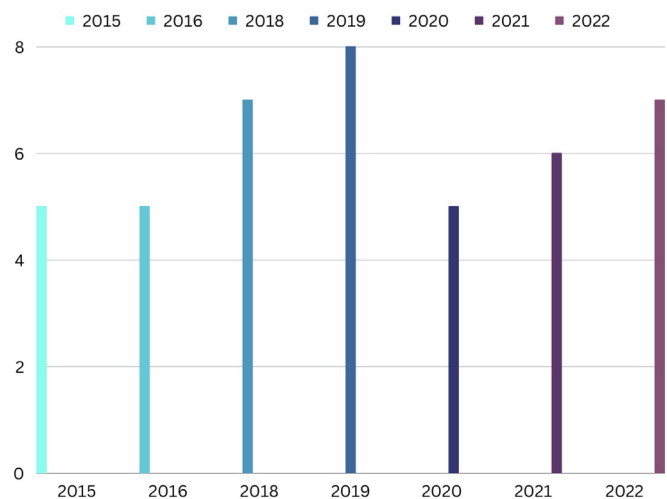


**Fig. 1.** The number of drugs containing thiazole scaffold in between two hundred brand drugs by retail sales from 2015 to 2022.

## 2. Thiazole derivatives with antimicrobial activity

For a long time, we didn't have very many new drugs to treat bacteria. This led to a lack of drugs that work against bacteria that are resistant to drugs. So now we need to synthesize new drugs that work in different ways and that can treat both sensitive and resistant strains of bacteria (Holmes et al., 2016).

In 2014, Liaras and co-workers synthesized two thiazole-based aminopyrimidine derivatives and eight N-phenylpyrazoline derivatives (Fig. 2). Ten derivatives were tested against 9 g-positive and negative bacteria and 9 fungal strains. The evaluations showed all structures have antibacterial activities. In addition, two structures (1a and 1b) among all structures had excellent activity but had no good yield (15% – 27%) (Table 1 and Fig. 2). Streptomycin and ampicillin were used as reference drugs. Most of the derivatives showed comparable or better activities than the reference drugs. Among all derivatives, structure 1a had the best activity (Table 1 and Fig. 2). Structure 1b showed the best inhibitory effect against gram-positive bacteria (Table 1 and Fig. 2). The best antibacterial activity against gram-positive and negative bacteria showed by structure 1a (Table 1 and Fig. 2). In addition, structure

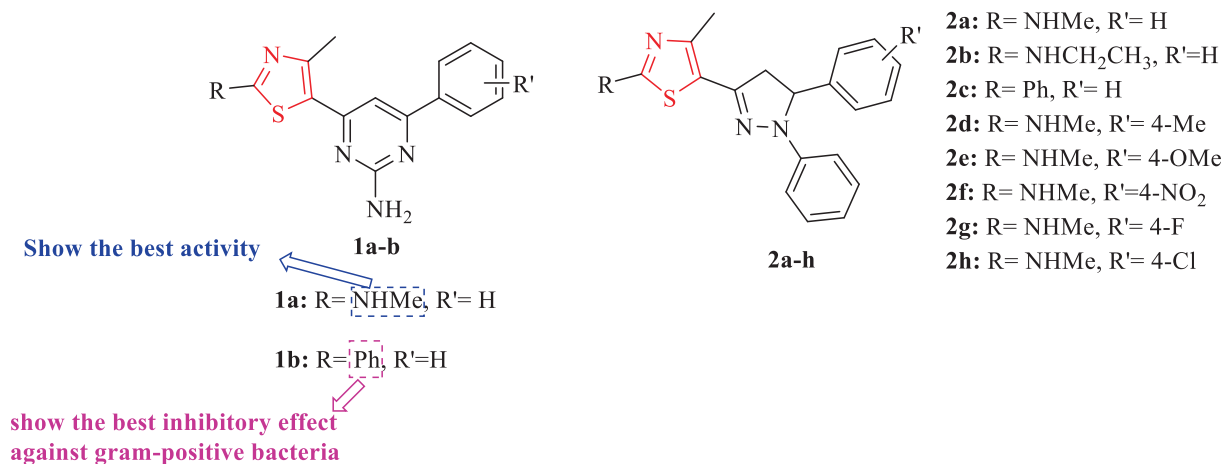


**Fig. 2.** Chemical structures 1a-b and 2a-h (Liaras et al., 2014)

**Table 1**  
Antimicrobial activity (MIC, MBC, and MFC =  $\mu\text{mol ml}^{-1} \times 10^{-2}$ ) of The structures 1a and 1b (Liaras et al., 2014)

Cpd. no.	Gram-Positive bacteria					Gram-Negative bacteria				
	S. a.	B. c.	M. f.	L. m.	Ps. aer.	S. typh.	E. coli	En. f.	En. cl.	
1a	MIC	8.41 ± 0.02	3.37 ± 0.02	3.37 ± 0.02	10.10 ± 0.10	3.37 ± 0.02	3.37 ± 0.02	3.37 ± 0.00	NT	6.74 ± 0.08
	MBC	10.10 ± 0.03	6.74 ± 0.10	8.41 ± 0.10	11.81 ± 0.10	6.74 ± 0.08	6.74 ± 0.02	6.74 ± 0.00	NT	8.41 ± 0.10
1b	MIC	1.45 ± 0.00	5.80 ± 0.10	5.80 ± 0.10	1.45 ± 0.00	29.00 ± 0.30	29.00 ± 0.00	34.80 ± 0.10	29.00 ± 0.07	NT
	MBC	5.80 ± 0.07	40.60 ± 0.10	29.00 ± 0.00	36.25 ± 0.00	40.60 ± 0.00	34.80 ± 0.30	40.60 ± 0.20	34.80 ± 0.00	NT
Ampicillin	MIC	24.80 ± 0.07	24.80 ± 0.10	24.80 ± 0.02	37.20 ± 0.07	74.40 ± 0.10	24.80 ± 0.00	37.20 ± 0.07	24.80 ± 0.30	24.80 ± 0.20
	MBC	37.20 ± 0.00	37.20 ± 0.07	37.20 ± 0.07	74.40 ± 0.10	124 ± 0.70	49.20 ± 0.07	49.20 ± 0.07	37.20 ± 0.07	37.20 ± 0.07
Streptomycin	MIC	17.20 ± 0.07	4.30 ± 0.10	8.60 ± 0.10	25.80 ± 0.10	17.20 ± 0.00	17.20 ± 0.07	17.20 ± 0.00	4.30 ± 0.10	4.30 ± 0.01
	MBC	34.40 ± 0.10	8.60 ± 0.00	17.20 ± 0.00	51.60 ± 0.20	34.40 ± 0.00	34.40 ± 0.10	34.40 ± 0.10	8.60 ± 0.10	8.60 ± 0.10

S. a. – Staphylococcus aureus (ATCC 6538); B. c. – Bacillus cereus (clinical isolate); M. f. – Micrococcus flavus (ATCC 10240); L. m. – Listeria monocytogenes (NCTC 7973).  
Ps. aer. – Pseudomonas aeruginosa (ATCC 27853); S. typh. – Salmonella typhimurium (ATCC 13311); E. coli – Escherichia coli (ATCC 35210); En. f. – Enterococcus faecalis (human isolate); En. cl. – Enterobacter cloacae (human isolate).

Cpd. no.	Fungal yeast									
	A. o.	A. ver.	A. fl.	A. n.	A. fum.	T. v.	P. o.	P. f.	C. a.	
1a	MIC	3.37±0.10	NT	5.05±0.02	5.05±0.02	5.05±0.02	2.52±0.20	3.37±0.10	3.37±0.02	3.37±0.10
	MFC	6.74±0.10	NT	6.74±0.30	6.74±0.30	6.74±0.20	3.37±0.10	5.05±0.20	6.74±0.20	6.74±0.20
1b	MIC	1.45±0.20								
	MFC	5.80±0.30								
Ketoconazole	MIC	15.70±0.20	21±0.00	NT	26.20±0.07	26.20±0.07	475±1.70	380±1.70	38±0.00	37.60±0.00
	MFC	38±0.10	285±1.60	285±1.70	38±0.20	38±0.00	570±1.70	380±1.70	95±0.30	94±0.30
Bifonazole	MIC	48±0.00	48±0.20	48±0.20	48±0.20	48±0.00	64±0.00	48±0.00	64±0.20	32.20±0.07
	MFC	80±1.60	64±0.30	64±0.00	64±0.20	64±0.30	80±0.03	64±0.03	80±1.00	48.30±0.10

A. o. – Aspergillus ochraceus (ATCC 12066); A. v. – Aspergillus versicolor (ATCC 11730); A. fl. – Aspergillus flavus (ATCC 9643); A. n. – Aspergillus niger (ATCC 6275); A. fum. – Aspergillus fumigatus (human isolate); T. v. – Trichoderma viride (IAM 5061); P. o. – Penicillium ochrochloron (ATCC 9112); P. f. – Penicillium funiculosum (ATCC 36839); C. a. – Candida albicans (human isolate).

2d displayed The lowest antibacterial activity, and had no activity against En. cloacae. Also, all derivatives had potent activity against S. aureus and L. monocytogenes compared to streptomycin (except 2 g) (Table 1 and Fig. 2). In the case of 2a-h, structures 2e, 2f and 2 h just increased the activity in comparison structure 2a, while structures 2d and 2 g showed the opposite effect (Table 1 and Fig. 2) (Liaras et al., 2014)

On the other hand, the antifungal activity of derivatives was tested in comparison to ketoconazole and bifonazole as reference drugs. Structure 1a had the best activity. In the case of A. Ochraceus structures 1b had the best activity (Table 1 and Fig. 2) (Liaras et al., 2014)

A series of structures containing thiazole scaffold was reported by Rostom and co-workers and evaluated their in vitro antibacte-

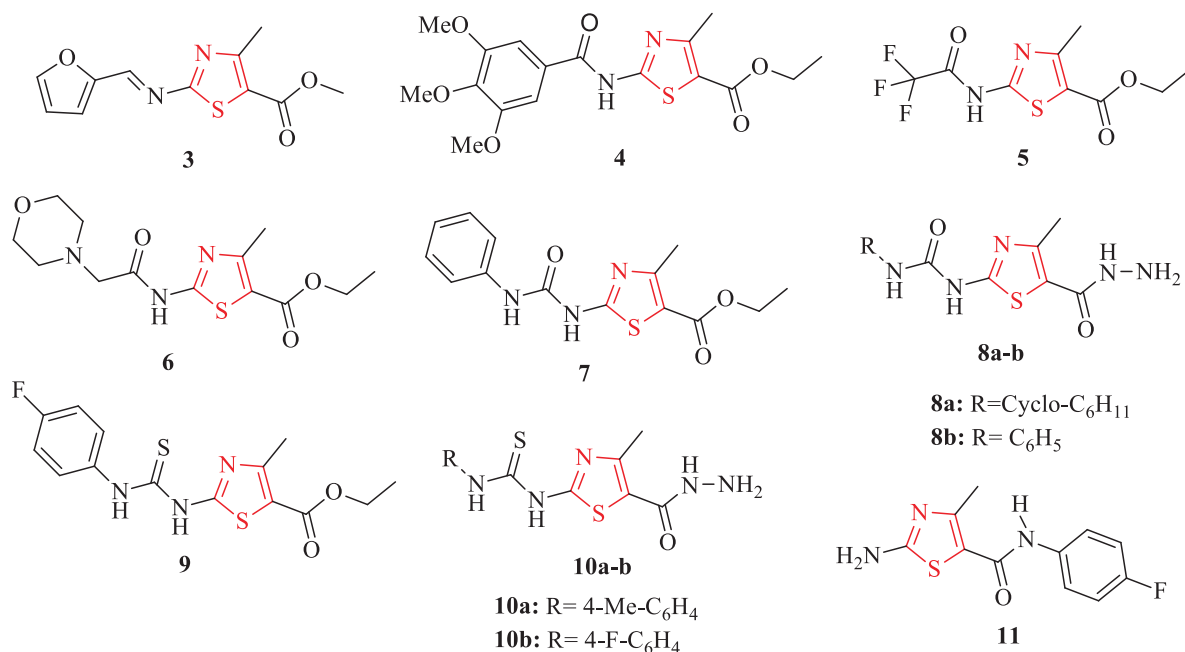


**Fig. 3.** Chemical structures of 3–7, 8a–b, 9, 10a–b, and 11 (Rostom et al., 2014)

**Table 2**  
MIC ( $\mu\text{g/mL}$ ) and MBC ( $\mu\text{g/mL}$ ) of the structures 3–7, 8a-b, 9, 10a-b, and 11 (Rostom et al., 2014)

College	Gram positive bacteria				Gram negative bacteria				Fungus	
	S. a.		B. s.		E. coli		P. a.		C. a.	
	MIC	MBC	MIC	MBC	MIC	MBC	MIC	MBC	MIC	MBC
<b>3</b>	50	100	100	200	25	50	–	NT		
<b>4</b>	6.25	6.25	25	50	12.5	12.5	50	100		
<b>5</b>									100	100
<b>6</b>									100	100
<b>7</b>	25	25	50	50	25	25	50	100	25	25
<b>8a</b>									50	100
<b>8b</b>	12.5	12.5	25	25	12.5	12.5	50	100	25	25
<b>9</b>	12.5	12.5	25	25	25	25	100	100	25	50
<b>10a</b>									100	100
<b>10b</b>	6.25	6.25	12.5	12.5	12.5	12.5	50	50	12.5	12.5
<b>11</b>	12.5	25	25	50	50	100	–	NT	100	100
<b>Ampicillin</b>	6.25	–	12.5	–	6.25	–	12.5	–		
<b>Trihydrate</b>										
<b>Gentamycin</b>	3.12	–	12.5	–	3.12	–	12.5	–		
<b>Clotrimazole</b>									6.25	–
<b>Amphotericin-B</b>									1.56	–

S. a. - *S. aureus* ATCC 6538; B. s. - *B. subtilis* ATCC 6633; E. coli. - *E. coli* ATCC 25922; P. a. - *P. aeruginosa* ATCC 27853. NT = not tested. (-): totally inactive ( $\text{MIC} \geq 200 \mu\text{g/mL}$ ). C. a. - *C. albicans* ATCC 10231 (-): totally inactive ( $\text{MIC} \geq 200 \mu\text{g/mL}$ ).

rial activity. Nineteen structures against gram (+) bacteria had good antibacterial activity. Among these derivatives, five structures (4, 7, 8b, 9, and 10b) had significant activities with broad-spectrum, and structure 10b (with 27% yield) had the best result compared to other ones (Fig. 3 and Table 2). Structures 4 and 10b showed equipotent activity to ampicillin as a reference drug against *S. aureus* ATCC 6538, while structures 8b, 9, and 11 exhibited half the potency of ampicillin (Fig. 3 and Table 2). In the case of *B. subtilis*, structure 10b showed equipotent activity to gentamicin sulfate and ampicillin, while structures 4, 8b, 9, and 11 had half the potency of ampicillin (Fig. 3 and Table 2). In addition, structures 4, 8b, and 10b showed good activity compared to ampicillin and gentamicin sulfate against *E. Coli*. Also, structures 3, 7, and 9 displayed moderate activity against the same organism compared to gentamicin sulfate and ampicillin (Fig. 3 and Table 2) (Rostom et al., 2014)

According to antifungal activity results, structures 5, 6, 7, 8a, 8b, 9, 10a, 10b, and 11 had significant growth inhibitory activity against *C. Albicans* compared to amphotericin B and clotrimazole as reference drugs (Fig. 3 and Table 2) (Rostom et al., 2014)

Prakash et al. synthesized twenty-seven structures containing thiazole scaffold. The antimicrobial activity of derivatives was tested against 4g-negative and positive bacteria and 2 fungal strains. (Table 3). Structures 16c and 17c displayed higher antibacterial activity compared to chloramphenicol as a reference drug, especially against *Staphylococcus aureus* (Fig. 4 and Table 3). In general, structures 12, 13b, 14a, 14b, 15, 16b, and 17b had moderate antibacterial activity, while structures 13a, 13c, 14c, 16a, and 17a showed good activity (Table 3 and Fig. 4) (Prakash et al., 2014)

Antifungal activity evaluations showed structures 17a and 17c had excellent activity, especially against *A. niger* greater than the reference drug (Table 3 and Fig. 4) (Prakash et al., 2014)

A novel series of derivatives containing thiazole were synthesized by Desai and co-workers. In this study, prepared twelve analogues and investigated their antimicrobial activities against 4 bacteria and 3 fungal strains. Structures 18a, 18b, and 18 h showed good antibacterial activity against *S. pyogenes* in comparison to chloramphenicol as a reference drug (Fig. 5 and Table 4). Whereas structures 18a and 18 g displayed good activity against *S. Aureus*

(Fig. 5 and Table 4). Also, structures 18b and 18 h showed very good activity against *S. aureus*, *E. coli*, and *P. Aeruginosa* (Fig. 5 and Table 4). Whereas structures 18c and 18i had excellent activity against *S. aureus* and *P. Aeruginosa* (Fig. 5 and Table 4) (Desai et al., 2015)

According to antifungal studies, structure 18f showed the most potent activity against *C. albicans* MTCC 227 and *A. niger* MTCC 282 in comparison to ketoconazole as a reference drug (Fig. 5 and Table 4). Among all derivatives, structures 18d and 18e had good activity against *A. clavatus*. Moreover, structure 18e exhibited good activity against *A. niger* (Fig. 5 and Table 4) (Desai et al., 2015)

Basha and co-workers synthesized a series of aroyl-4-heteroaryl pyrazoles and pyrroles containing thiazole scaffold and evaluated their antimicrobial activity against 4g-negative and positive bacteria and 2 fungal strains (Fig. 6 and Table 5). Structures 20c, 20d, 20f, 21d, and 21f were active against all bacteria strains, especially *Bacillus subtilis* in comparison to chloramphenicol as a reference drug (Fig. 6 and Table 5). Whereas structures 20d and 20f showed marginally higher activity against all tested concentrations (12.5, 25, 50, and 100  $\mu\text{g/well}$ ) toward the reference drug (Table 4). Structures 20a, 21a, and 21c displayed moderate activity, while 20b, 20e, 21b, and 21e exhibited the least activity. In addition, derivatives 20 and 21 (aromatized structures) showed higher activity than derivatives 19 (non-aromatized structures) (Fig. 6 and Table 5) (Basha et al., 2015)

On the other hand, Structures 20c, 20d, and 20f displayed excellent antifungal activity toward ketoconazole as a reference drug against *Aspergillus niger* at 100  $\mu\text{g}$  (Fig. 6 and Table 5). In the case of *Aspergillus niger* at 100  $\mu\text{g}$ , structures 19a, 19b, 21b, and 21e demonstrated the least activity (Fig. 6 and Table 5) (Basha et al., 2015)

El-Kady et al. reported some structures containing thiazole scaffold and evaluated their antimicrobial activity against 2g-negative and positive and 1 fungal strain (Fig. 7 and Table 6). Among all derivatives, structures 22, 23a, 24a, and 25a had a wide spectrum of antimicrobial activity against *Staphylococcus aureus* NCINB 50080 and *E. coli* ATCC 1177 compared to ciprofloxacin as a reference drug, and structures 26, 27, 23b, 24b, 25b, and 25c effective

**Table 3**  
In vitro antimicrobial activity of the structures 12, 13a-c, 14a-c, 15, 16a-c, and 17a-c (Prakash et al., 2014)

Cpd. no.		Zone of inhibition (mm)					
		Gram-positive bacteria		Gram-negative bacteria		Aspergillus niger	Penicillium chrysogenum
		S. a.	B. s.	P. a.	K. p.		
<b>12</b>	25 µg/well	15 ± 2	15 ± 2	8 ± 2	16 ± 2		
	50 µg/well	17 ± 1	16 ± 2	9 ± 2	17 ± 1		
	100 µg/well	19 ± 1	19 ± 2	12 ± 1	20 ± 2		
<b>13a</b>	25 µg/well	22 ± 2	21 ± 2	12 ± 2	23 ± 1		
	50 µg/well	25 ± 1	22 ± 2	15 ± 2	25 ± 1		
	100 µg/well	26 ± 3	24 ± 3	17 ± 1	28 ± 2		
<b>13b</b>	25 µg/well	11 ± 2	10 ± 1	-	11 ± 1		
	50 µg/well	13 ± 3	12 ± 2	6 ± 2	13 ± 1		
	100 µg/well	15 ± 3	14 ± 3	8 ± 2	16 ± 2		
<b>13c</b>	25 µg/well	24 ± 1	22 ± 1	14 ± 1	26 ± 2		
	50 µg/well	26 ± 2	25 ± 1	16 ± 1	28 ± 2		
	100 µg/well	29 ± 1	26 ± 2	18 ± 1	31 ± 1		
<b>14a</b>	25 µg/well	18 ± 3	18 ± 1	10 ± 1	19 ± 1		
	50 µg/well	20 ± 2	20 ± 2	12 ± 2	20 ± 1		
	100 µg/well	23 ± 2	22 ± 2	14 ± 1	24 ± 2		
<b>14b</b>	25 µg/well	10 ± 3	9 ± 2	-	10 ± 2		
	50 µg/well	12 ± 2	10 ± 1	-	12 ± 2		
	100 µg/well	14 ± 2	13 ± 2	7 ± 1	14 ± 1		
<b>14c</b>	25 µg/well	21 ± 1	19 ± 1	11 ± 2	20 ± 2		
	50 µg/well	23 ± 2	21 ± 1	13 ± 1	22 ± 2		
	100 µg/well	25 ± 2	23 ± 2	15 ± 2	26 ± 1		
<b>15</b>	25 µg/well	17 ± 2	16 ± 2	9 ± 1	17 ± 1		
	50 µg/well	18 ± 3	18 ± 1	10 ± 1	19 ± 2		
	100 µg/well	21 ± 3	21 ± 1	13 ± 2	22 ± 1		
<b>16a</b>	25 µg/well	29 ± 3	25 ± 2	17 ± 1	30 ± 3		
	50 µg/well	31 ± 2	26 ± 3	18 ± 1	32 ± 2		
	100 µg/well	32 ± 2	28 ± 2	21 ± 3	35 ± 2		
<b>16b</b>	25 µg/well	14 ± 3	14 ± 1	7 ± 2	14 ± 2		
	50 µg/well	15 ± 2	15 ± 3	8 ± 1	15 ± 2		
	100 µg/well	18 ± 1	18 ± 1	11 ± 2	18 ± 1		
<b>16c</b>	25 µg/well	34 ± 2	29 ± 2	20 ± 2	35 ± 2		
	50 µg/well	36 ± 2	32 ± 1	22 ± 2	37 ± 3		
	100 µg/well	38 ± 3	35 ± 2	25 ± 2	41 ± 1		
<b>17a</b>	25 µg/well	27 ± 2	24 ± 2	15 ± 2	28 ± 1	32 ± 1	27 ± 1
	50 µg/well	28 ± 1	26 ± 2	17 ± 2	29 ± 1	34 ± 2	29 ± 2
	100 µg/well	30 ± 2	27 ± 1	20 ± 2	33 ± 2	37 ± 2	31 ± 1
<b>17b</b>	25 µg/well	12 ± 2	12 ± 2	6 ± 1	13 ± 1		
	50 µg/well	14 ± 2	13 ± 2	7 ± 1	14 ± 2		
	100 µg/well	17 ± 2	16 ± 2	10 ± 1	17 ± 1		
<b>17c</b>	25 µg/well	32 ± 1	27 ± 1	18 ± 2	32 ± 2	33 ± 2	29 ± 2
	50 µg/well	33 ± 3	29 ± 2	19 ± 2	34 ± 2	36 ± 1	30 ± 1
	100 µg/well	35 ± 2	30 ± 3	23 ± 2	38 ± 1	39 ± 3	32 ± 2
<b>Chloramphenicol</b>	25 µg/well	30 ± 3	32 ± 3	25 ± 2	38 ± 1		
	50 µg/well	33 ± 1	34 ± 3	27 ± 3	40 ± 2		
	100 µg/well	35 ± 2	38 ± 1	30 ± 1	42 ± 3		
<b>Ketoconazole</b>	25 µg/well					31 ± 3	35 ± 1
	50 µg/well					33 ± 2	36 ± 2
	100 µg/well					36 ± 2	38 ± 3

S. a. - Staphylococcus aureus; B. s. - Bacillus subtilis; P. a. -Pseudomonas aeruginosa; K. p. - Klebsiella pneumoniae, (-) No activity.

against E. coli ATCC 1177 (Fig. 7 and Table 6). In addition, 28 and 29 were effective against Staphylococcus aureus NCINB 50080 (Fig. 7 and Table 6) (El-Kady et al., 2016)

Antifungal activity evaluation showed structure 30 had remarkable activity toward AMB20 as a reference drug (Fig. 7 and Table 6) (El-Kady et al., 2016)

A series of ethyl 2-(2-(4-substituted)acetamido)-4-substituted-thiazole-5-carboxylates (Fig. 8) were synthesized by Pawar and co-workers and their in vitro antimicrobial activities were tested against 3 bacteria (Table 7). In comparison, levofloxacin was used as a reference drug. The result of antibacterial activity revealed

that structures 31a, 31b, 31c, 31d, and 32 had the most active and potent antimicrobial activity against B. subtilis, E. Coli, and S. aureus toward the reference drug (Fig. 8 and Table 7). Moreover, the same structures had potent antifungal activity against C. albicans, A. flavus, and A. niger as fungal strains which were chosen for the investigation of antifungal activity compared to miconazole and fluconazole as reference drugs (Fig. 8 and Table 7) (Pawar et al., 2016)

A novel series of 6-(5-Methyl-1H-1,2,3-triazol-4-yl)-5-[(2-(thiazol-2-yl)hydrazono)methyl]imidazo[2,1-b]thiazole derivatives (Fig. 9) were synthesized by Abdel-Wahab et al. All derivatives

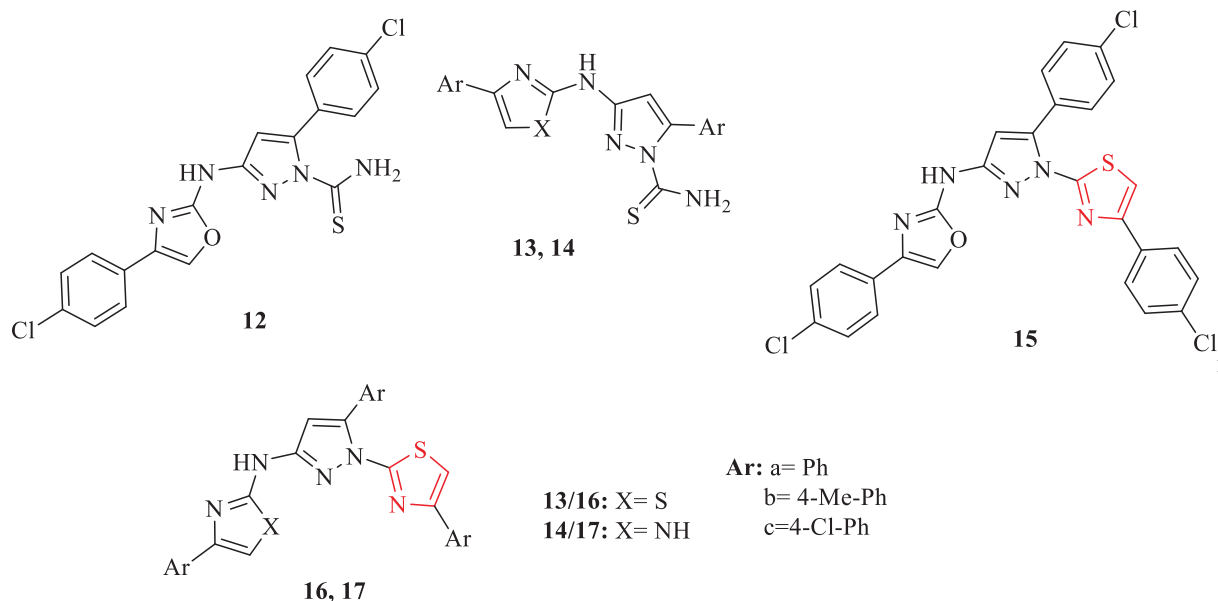


Fig. 4. Chemical structures 12, 13a-c, 14a-c, 15, 16a-c, and 17a-c (Prakash et al., 2014)

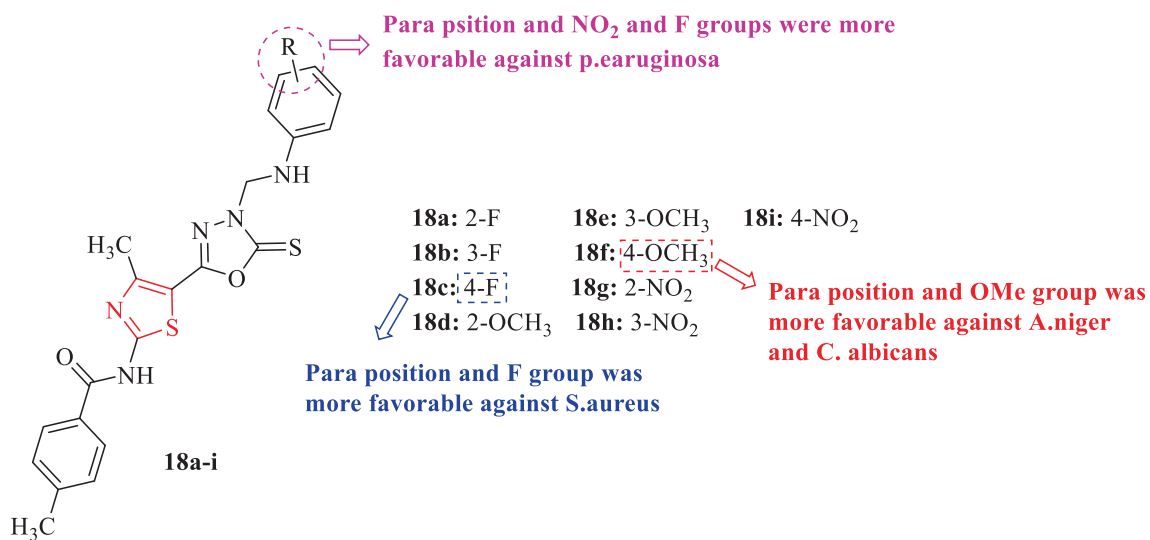


Fig. 5. Chemical structures 18a-i (Desai et al., 2015)

Table 4

MIC ( $\mu\text{g/mL}$ ) of the structures 18a-i (C = Chloramphenicol and K = Ketoconazole) (Desai et al., 2015)

Cpd. no.	MIC ( $\mu\text{g/mL}$ )						
	E. coli MTCC 443	S. aureus MTCC 96	P. aeruginosa MTCC 1688	S. pyogenes MTCC 442	A. niger MTCC 282	A. clavatus MTCC 1323	C. albicans MTCC 227
18a		100		100			
18b	50	50	50	100			
18c		12.5	12.5				
18d						100	
18e					100	100	
18f					25		25
18g		100					
18h	50	50	50				
18i		25	12.5				
C	50	50	50	50	50	50	50
K							

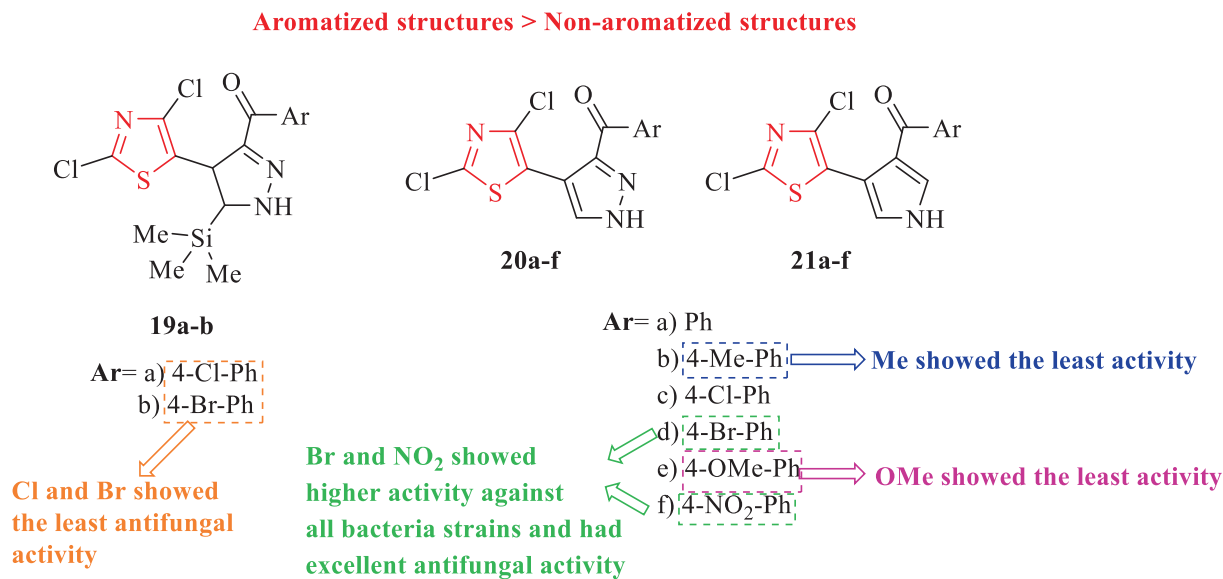


Fig. 6. Chemical structures of 19a-b, 20a-f, and 21a-f (Basha et al., 2015)

and vancomycin (As a reference drug) were tested against 6 bacteria and 2 fungal strains (Fig. 9). According to antibacterial studies, structure 33 exhibited significant antibacterial activity against all bacteria toward the reference drug. Whereas structures 34 and 35 demonstrated good activities against *Staphylococcus aureus* (Fig. 9). In addition, the same structures had good antifungal activities against *Saccharomyces cerevisia* and *Candida albicans* NRRL Y-477 toward the reference drug (Fig. 9) (Abdel-Wahab et al., 2017)

Liao et al. synthesized a novel series of 2-substituted phenoxy-N-(4-substituted phenyl-5-(1H-1,2,4-triazol-1-yl)thiazol-2-yl)acetamide derivatives (Fig. 10). All derivatives were tested against 2 bacteria and three fungal strains (Table 8). Bismertiazol and hymexazol were used as antibacterial and antifungal reference drugs, respectively. Antibacterial studies showed four structures (36a, 36b, 36c, and 36d) had potent inhibition effects against Xoo and exhibited potent inhibition effects against Xac toward the reference drug (Fig. 10 and Table 8). In addition, EC<sub>50</sub> values of the same structures were good, which seem to be more potent than bismertiazole. In addition, Structures 36b, 36c, and 36d (R<sub>1</sub> = OMe) had better activity compared to structures 36 h, 36i, and 36j (R<sub>1</sub> = 4-Cl) against xoo (Fig. 10 and Table 8). Whereas structures 36 h, 36i and 36j (R<sub>1</sub> = 4-Cl) had better activity compared to structures 36e, 36f and 36 g (3,4-di-Cl) (Fig. 10 and Table 8) (Liao et al., 2017)

According to antifungal activity studies, structure 36j displayed high activity against *G. zeae* toward the reference drug (Fig. 10 and Table 8) (Liao et al., 2017)

Shankerrao et al. synthesized a novel series of imidazothiazoles of benzofuran. The antimicrobial activities of structures were tested against 4 bacteria and 2 fungal strains with respect to ampicillin and fluconazole as antibacterial and antifungal reference drugs, respectively (Fig. 11 and Table 9). Among all derivatives, structures 37e and 37d displayed the best result against *E. coli* and *S. Aureus* (Fig. 11 and Table 9). In addition, structures 38b and 37a had moderate activity against *E. coli* and *Klbesilla pneumonia*, while the same structures had an excellent effect against

*S. aureus* and *P. aeruginosa* (Fig. 11 and Table 9) (Shankerrao et al., 2017)

According to antifungal activity studies, three structures (37a, 37b, and 38c) had excellent activity against *A. niger* and *Trichoderma Viridae* compared to other structures and the reference drug (Fig. 11 and Table 9). Whereas two structures (37c and 38a) had moderate activity against *A. niger* and *Trichoderma Viridae* (Fig. 11 and Table 9) (Shankerrao et al., 2017)

A novel series of 2-(benzo[d]thiazol-2-yl)phenyl-4-nitrophenyl alkyl/aryl substituted phosphoramidates were reported by Reddy et al. The derivatives were tested against 3 bacteria and 2 fungal strains in comparison to ampicillin and antibiotic as antimicrobial and antifungal reference drugs, respectively (Fig. 12 and Table 10). Among the derivatives, structures 39c, 39d, and 39 h had the best inhibition activity against *Escherichia coli*, *Streptococcus aureus* ATCC-25923, and *Bacillus subtilis* ATCC-1789 toward the reference drug (Fig. 12 and Table 10). In addition, structure 39e demonstrated good activity against *Bacillus subtilis* (Fig. 12 and Table 10) (Reddy et al., 2018)

On the other hand, antifungal activity studies against 2 fungal strains at two concentrations, 50 and 100 µg/mL showed structures 39b, 39c, and 39 g had the best activity against *C. albicans* and *A. niger* at 100 µg/mL toward the reference drug (Fig. 12 and Table 10). In addition, structure 39a exhibited good activity against *C. albicans* and *A. niger* (Fig. 12 and Table 10). Whereas structures 39d and 39 h showed good activity against *C. Albicans* (Fig. 12 and Table 10). Moreover, structure 39f displayed good activity against *A. niger* (Fig. 12 and Table 10) (Reddy et al., 2018)

Ansari and Khan synthesized some of the structures containing thiazole scaffold. The derivatives were tested against 10g-negative and positive bacteria in comparison to ofloxacin as a reference drug. Structures 40a, 40c, and 40b had a higher activity with respect to other ones (Fig. 13 and Table 11). Structure 40c had the best activity against *P. vulgaris*, *E. coli*, and *P. Aeruginosa* (Fig. 13 and Table 11). Structure 40b had the highest activity against *K. pneumonia* and structure 40d displayed the highest activity against *B. bronchiseptica*. Moreover, structures 40a and

**Table 5**  
In vitro antimicrobial activity of the structures 19a-b, 20b-f, and 21a-f (Basha et al., 2015)

Cpd. no.	concentrations	Zone of Inhibition (mm)				
		Gram-Positive bacteria		Gram-Negative bacteria		Aspergillus niger
		Staphylococcus aureus	Bacillus subtilis	Pseudomonas aeruginosa	Klebsiella pneumoniae	
<b>19a</b>	100 µg/well					8 ± 2
<b>19b</b>	100 µg/well					9 ± 3
<b>20b</b>	12.5 µg/well	13 ± 3	12 ± 3	9 ± 3	14 ± 3	
	25 µg/well	15 ± 2	14 ± 2	11 ± 1	16 ± 2	
	50 µg/well	18 ± 3	16 ± 1	14 ± 1	18 ± 3	
<b>20c</b>	100 µg/well	22 ± 2	19 ± 1	15 ± 3	19 ± 1	10 ± 3
	12.5 µg/well	24 ± 1	28 ± 1	16 ± 2	24 ± 2	
	25 µg/well	26 ± 1	30 ± 2	18 ± 1	26 ± 3	
<b>20d</b>	50 µg/well	28 ± 2	32 ± 3	20 ± 2	28 ± 2	
	100 µg/well	30 ± 3	35 ± 2	23 ± 3	31 ± 1	34 ± 2
	12.5 µg/well	26 ± 1	31 ± 2	18 ± 2	27 ± 1	
<b>20e</b>	25 µg/well	27 ± 3	33 ± 4	19 ± 1	29 ± 3	
	50 µg/well	30 ± 1	36 ± 2	22 ± 3	32 ± 2	
	100 µg/well	32 ± 3	41 ± 1	24 ± 3	33 ± 2	36 ± 2
<b>20f</b>	12.5 µg/well	11 ± 2	11 ± 2	-	-	
	25 µg/well	13 ± 1	12 ± 2	-	-	
	50 µg/well	14 ± 3	15 ± 3	10 ± 3	-	
<b>21a</b>	100 µg/well	17 ± 3	16 ± 1	12 ± 2	10 ± 2	9 ± 1
	12.5 µg/well	27 ± 1	32 ± 2	17 ± 2	27 ± 1	
	25 µg/well	29 ± 3	35 ± 4	20 ± 1	30 ± 3	
<b>21b</b>	50 µg/well	31 ± 1	38 ± 2	22 ± 3	33 ± 2	
	100 µg/well	33 ± 3	42 ± 1	25 ± 3	34 ± 2	36 ± 2
	12.5 µg/well	15 ± 2	14 ± 3	11 ± 2	16 ± 2	
<b>21c</b>	25 µg/well	17 ± 1	16 ± 2	14 ± 3	17 ± 1	
	50 µg/well	19 ± 2	17 ± 2	15 ± 1	20 ± 3	
	100 µg/well	23 ± 1	21 ± 2	17 ± 3	22 ± 1	
<b>21d</b>	12.5 µg/well	9 ± 2	10 ± 3	-	-	
	25 µg/well	11 ± 1	12 ± 2	-	-	
	50 µg/well	12 ± 2	14 ± 2	-	-	
<b>21e</b>	100 µg/well	14 ± 1	15 ± 1	10 ± 3	-	
	12.5 µg/well	21 ± 2	20 ± 3	14 ± 2	20 ± 1	
	25 µg/well	23 ± 2	22 ± 2	15 ± 1	22 ± 2	
<b>21f</b>	50 µg/well	24 ± 1	25 ± 1	16 ± 2	23 ± 1	
	100 µg/well	27 ± 3	27 ± 1	19 ± 3	25 ± 2	
	12.5 µg/well	23 ± 2	27 ± 2	15 ± 2	22 ± 2	
<b>chloramphenicol</b>	25 µg/well	25 ± 1	28 ± 3	16 ± 2	23 ± 1	
	50 µg/well	26 ± 3	31 ± 1	18 ± 1	26 ± 3	
	100 µg/well	28 ± 4	34 ± 2	21 ± 5	29 ± 2	
<b>Ketoconazole</b>	12.5 µg/well	8 ± 2	9 ± 1	-	-	
	25 µg/well	10 ± 1	10 ± 3	-	-	
	50 µg/well	12 ± 1	12 ± 2	-	-	
<b>chloramphenicol</b>	100 µg/well	13 ± 1	14 ± 3	9 ± 3	-	
	12.5 µg/well	24 ± 2	29 ± 2	15 ± 2	24 ± 2	
	25 µg/well	27 ± 1	30 ± 3	17 ± 2	25 ± 1	
<b>Ketoconazole</b>	50 µg/well	28 ± 3	32 ± 1	18 ± 1	27 ± 3	
	100 µg/well	29 ± 4	34 ± 2	21 ± 5	28 ± 2	
	12.5 µg/well	28 ± 1	30 ± 1	23 ± 1	36 ± 2	
<b>Ketoconazole</b>	25 µg/well	30 ± 3	32 ± 3	25 ± 2	38 ± 1	
	50 µg/well	33 ± 1	34 ± 2	27 ± 3	40 ± 2	
	100 µg/well	35 ± 2	38 ± 1	30 ± 2	42 ± 3	
<b>Ketoconazole</b>	100 µg/well					36 ± 1

40b showed good activity against *E. coli* and *P. Aeruginosa* (Fig. 13 and Table 11) (Ansari and Khan, 2017)

All 25 derivatives were tested against 5 fungal strains with respect to Ketoconazole as a reference drug. According to the results obtained, structures 40a and 40b had higher activity against *Penicillium citrinum* toward the reference drug (Fig. 13 and Table 11) (Ansari and Khan, 2017).

In 2019, a series of novel benzothiazole linked to acetohydrazide, carboxamide, and sulfonamide scaffolds (Fig. 14 and Table 12) were reported by Fadda and co-workers. Four bacteria were used in the antimicrobial activity evaluation (Table 12). Chloramphenicol and cephalothin were chosen as reference drugs.

Structures 41a and 41b had broad-spectrum antibacterial activity against all organisms (Fig. 14 and Table 12). The same structures showed equipotent activity to chloramphenicol in inhibiting the growth *B. subtilis*. Whereas their activities were fifty percent lower than chloramphenicol against *Bacillus thuringiensis*. In the case of 45, 46, 47a-d, and 48, all structures showed good to moderate activity against gram-positive bacteria (Fig. 14. and Table 12). Structures 43 and 44 showed weak growth inhibitory with respect to the reference drugs against *B. subtilis* and *B. Thuringiensis* (Fig. 14 and Table 12). Structures 41a and 41b displayed good to

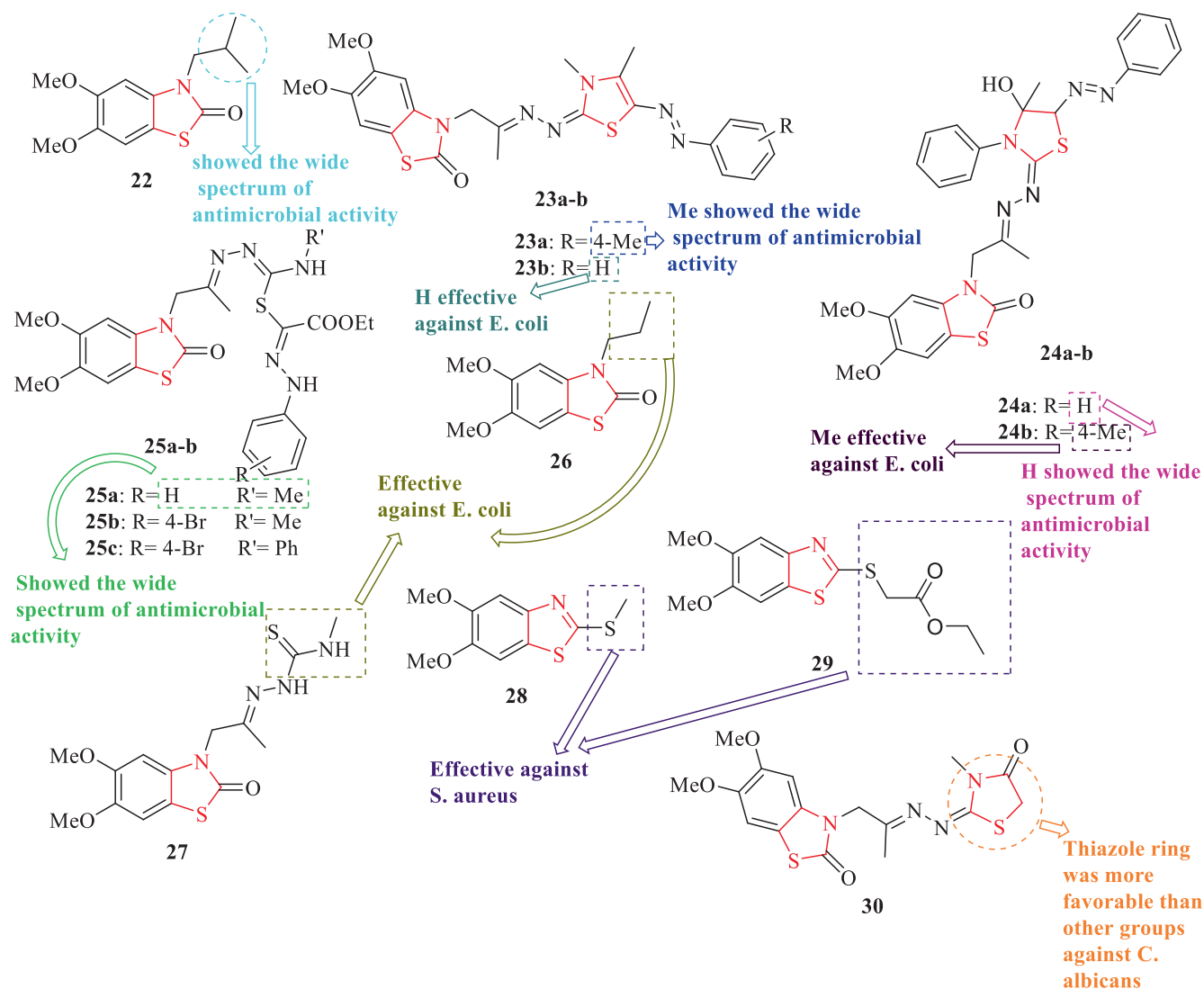


Fig. 7. Chemical structures of 22, 23a-b, 24a-b, 25a-c, 26, 27, 28, 29, and 30 (El-Kady et al., 2016)

Table 6

Inhibition zones (mm) of the structures 22, 23a-b, 24a-b, 25a-c, 26, 27, 28, 29, and 30 (El-Kady et al., 2016)

Cpd. no.	Inhibition zones (mm)		
	E. coli ATCC 1177	S. aureus NCINB 50,080	C. albicans ATCC10231
22	11	9	
23a	10	10	
23b	10		
24a	10	9	
24b	10		
25a	10	8	
25b	9		
25c	10		
26	10		
27	8		
28		10	
29		10	
30			19
Ciprofloxacin AMB20	20	21	20

moderate growth inhibitory against *B. subtilis* and *B. thuringiensis* toward the reference drugs (Fig. 14 and Table 12) (Fadda et al., 2019)

According to antifungal activity studies, all derivatives were tested against *F. oxysporum* and *B. fabae*. Cycloheximide served as a reference drug. structures 41b and 42 exhibited moderate activity against *B. fabae* and *F. Oxysporum* (Fig. 14 and Table 12). Moreover, structure 41a had the best inhibition compared to other structures (Fig. 14 and Table 12) (Fadda et al., 2019)

Deshineni et al. synthesized a new series of ethyl-2-(3-((2-(4-(4-aryl)thiazol-2-yl)hydrazono)methyl)-4-hydroxy/isobutoxyphenyl)-4-methylthiazole-5-carboxylates by one-pot multi-component approach (Fig. 15). In this investigation, 4 bacteria and 2 fungal strains were used. Levofloxacin and miconazole were used as antibacterial and antifungal reference drugs. The result showed structures 49a, 49c, 50b, and 50c had a wide spectrum of antimicrobial activity against *Staphylococcus aureus*, *Bacillus subtilis*, *Escherichia coli*, and *Azotobacter* with respect to the reference drug (Fig. 15 and Table 13). Further, Structures 49a and 50a dis-

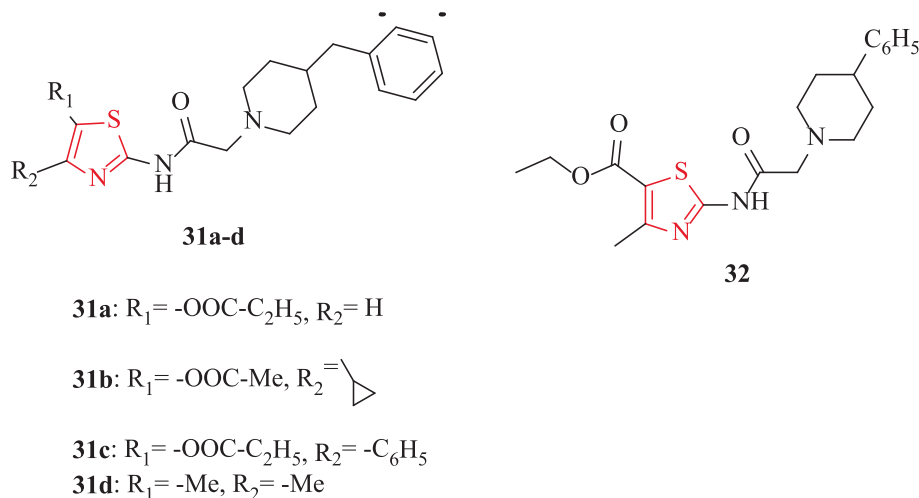


Fig. 8. Chemical structures of 31a-d and 32 (Pawar et al., 2016)

Table 7  
Antimicrobial activity (MIC values ( $\mu\text{g/mL}$ ) of the structures 31a-d and 32 (Pawar et al., 2016)

Cpd. no.	MIC values ( $\mu\text{g/mL}$ )					
	B. subtilis	E. coli	S. aureus	C. Albicans	A. Flavus	A. Niger
31a	29	29	28	25	12.5	12.5
31b	29	29	28	25	12.5	12.5
31c	25	29	28	50	25	25
31d	28	29	30	25	12.5	12.5
32	28	29	30	25	12.5	25
Levofloxacin	29	29	28			
Fluconazole				40	25	25
Miconazole				12.5	12.5	12.5

played good activity against *S. aureus*, *B. subtilis*, *E. coli*, and *Azotobacter* (Fig. 15 and Table 13) (Deshineni et al., 2020)

Antifungal activity of all derivatives demonstrated structures 49b, 49c, 50b, and 50c had good activity against *A. niger* MTCC 282 and *C. albicans* MTCC 227 toward the reference drug (Fig. 15 and Table 13) (Deshineni et al., 2020)

Althagafi et al. synthesized a novel series of thiazole derivatives. As reference drugs, ampicillin and gentamicin were used. According to the results, structures 51, 53a, and 54 exhibited more potent activity against *Staphylococcus aureus* compared to ampicillin with preliminary antimicrobial activity values of  $24.3 \pm 0.63$ ,  $23.8 \pm 0.72$ , and  $24.1 \pm 1.20$   $\mu\text{g/mL}$ , respectively (Fig. 16 and Table 14). Structures 55 and 56 displayed more potent activity against *Salmonella typhimurium* compared to gentamicin (Fig. 16 and Table 14) (Althagafi et al., 2019)

Among all derivatives tested against two fungal strains, structures 51, 52, 53a, 53b, 53c, 53d, 53e, 54, and 57 exhibited higher activity against *Aspergillus niger* compared to amphotericin B as an antifungal reference drug (Fig. 16 and Table 14) (Althagafi et al., 2019)

A new series of N-(4-(4-bromophenyl)thiazol-2-yl)-2-chloroacetamides were synthesized by Sharma and co-workers. The derivatives were tested against 3 bacteria and 2 fungal strains. As antibacterial and antifungal reference drugs, norfloxacin and fluconazole were used, respectively. Among the derivatives, structures 58, 59, and 60 had the best antimicrobial activity (Fig. 17). The antimicrobial activity results showed structure 60 had remark-

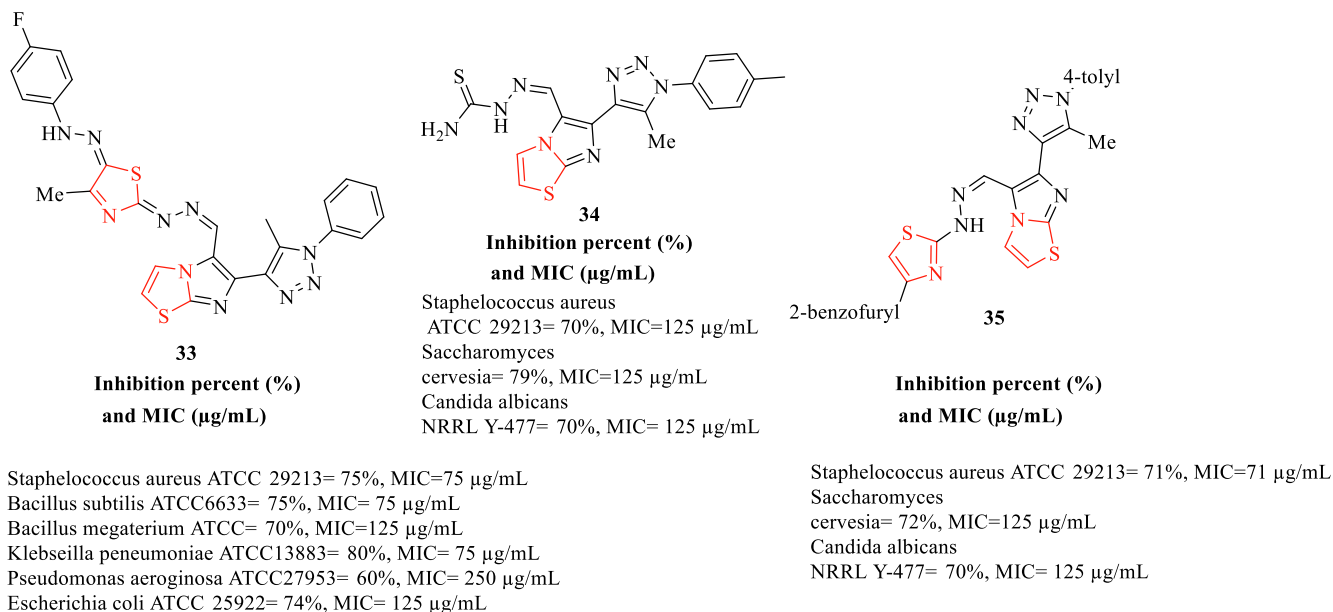
able activity against *S. Aureus* (Fig. 17). Structure 58 had high activity against *E. Coli* and structure 59 had potent activity against *B. Subtilis* and *E.coli* (Fig. 17) (Sharma et al., 2019a)

Antifungal activity results were found to structures 59 and 60 had high activity against 2 fungal strains (Fig. 17) (Sharma et al., 2019a)

A novel series of 4-(4-Bromophenyl)thiazol-2-amines were synthesized by Sharma et al. All derivatives were tested against 3 bacteria and norfloxacin was used as a reference drug. Among all derivatives, structures 61, 62, 63, and 64 showed good antimicrobial activity toward the reference drug (Fig. 18). In vitro antimicrobial results showed structure 61 had good potential against *E. Coli* and *S. Aureus* (Fig. 18). Moreover, structure 63 had good potential against *B. Subtilis* (Fig. 18) (Sharma et al., 2019b)

All derivatives were tested against 2 fungal strains in comparison to fluconazole as a reference drug. Antifungal activity results showed structure 64 had remarkable activity against *C. Albicans* and structure 62 had the highest potent against *A. niger* (Fig. 18) (Sharma et al., 2019b)

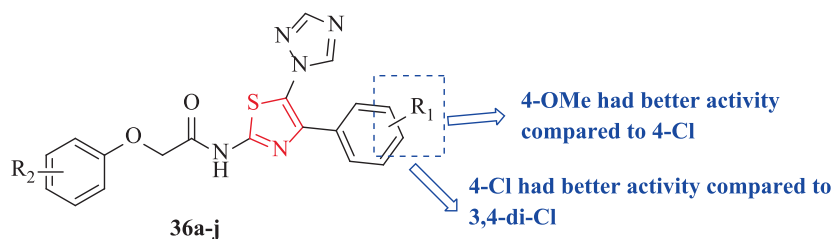
Sirakanyan et al. synthesized a novel series of derivatives containing thiazole scaffold which evaluated 11 derivatives against 6 bacteria with respect to ampicillin and streptomycin as reference drugs. Among all eleven derivatives synthesized, structures 65d, 65c, and 65f had lower activity against *Pseudomonas aeruginosa* toward streptomycin (Fig. 19 and Table 15). Structures 65f had lowest MIC against *Bacillus cereus* toward ampicillin (Fig. 19 and Table 15). Whereas structures 65b and 65c exhibited moderated



#### Vancomycine

Staphelococcus aureus ATCC 29213= 97%, MIC=75  $\mu\text{g/mL}$   
Bacillus subtilis ATCC6633= 94%, MIC= 75  $\mu\text{g/mL}$   
Bacillus megaterium ATCC= 87%, MIC=75  $\mu\text{g/mL}$   
Klebseilla peneumoniae ATCC13883= 80%, MIC= 75  $\mu\text{g/mL}$   
Pseudomonas aeruginosa ATCC27953= no activity, MIC= 75  $\mu\text{g/mL}$   
Escherichia coli ATCC 25922= 88%, MIC= 75  $\mu\text{g/mL}$   
Saccharomyces cervesia= 90%, MIC=75  $\mu\text{g/mL}$   
Candida albicans NRRL Y-477= 97%, MIC= 75  $\mu\text{g/mL}$

Fig. 9. Chemical structures of 33–35 and inhibition and MIC values of the structures 33–35 (Abdel-Wahab et al., 2017)



**36a**=  $R_1 = \text{H}$ ,  $R_2 = 4\text{-Cl}$   
**36b**=  $R_1 = 4\text{-OMe}$ ,  $R_2 = 4\text{-Cl}$   
**36c**=  $R_1 = 4\text{-OMe}$ ,  $R_2 = 2,4\text{-di-Cl}$   
**36d**=  $R_1 = 4\text{-OMe}$ ,  $R_2 = 4\text{-F}$   
**36e**=  $R_1 = 3,4\text{-di-Cl}$ ,  $R_2 = \text{H}$   
**36f**=  $R_1 = 3,4\text{-di-Cl}$ ,  $R_2 = 4\text{-Cl}$   
**36g**=  $R_1 = 3,4\text{-di-Cl}$ ,  $R_2 = 2,4\text{-di-Cl}$   
**36h**=  $R_1 = 4\text{-Cl}$ ,  $R_2 = 4\text{-Cl}$   
**36i**=  $R_1 = 4\text{-Cl}$ ,  $R_2 = 2,4\text{-di-Cl}$   
**36j**=  $R_1 = 4\text{-Cl}$ ,  $R_2 = 4\text{-F}$

Fig. 10. Chemical structures 36a-j (Liao et al., 2017)

activity against the same organism (Fig. 19 and Table 15). Structure 65f showed good activity against *Listeria monocytogenes* toward the reference drugs (Fig. 19 and Table 15) (Sirakanyan et al., 2021)

All derivatives tested against six fungal strains toward ketoconazole and bifonazole as reference drugs. according to the results, structures 65a, 65c, and 65e had high activity against

**Table 8**  
Antimicrobial activity of the structures 36a-j (Liao et al., 2017)

Cdp. no.	Average values of inhibition rate (%)				G. zeae
	Xanthomonas oryzae pv. oryzae		Xanthomonas axonopodis pv. citri		
	200 µg/mL	100 µg/mL	200 µg/mL	100 µg/mL	
36a	100.0 ± 1.8	98.2 ± 2.2	80.2 ± 1.2	64.1 ± 1.8	
36b	95.2 ± 1.5	78.1 ± 2.1	80.2 ± 2.1	57.4 ± 1.6	
36c	100.0 ± 3.0	99.0 ± 1.2	55.2 ± 2.6	31.3 ± 3.1	
36d	90.3 ± 2.2	77.6 ± 1.4	66.1 ± 0.8	46.8 ± 1.6	
36e	75.0 ± 2.0	67.4 ± 4.1			
36f	31.2 ± 1.8	26.6 ± 1.3			
36g	33.9 ± 1.7	21.3 ± 1.5			
36h	86.8 ± 1.7	61.3 ± 2.1			
36i	37.0 ± 1.5	28.9 ± 1.1			
36j	81.7 ± 1.8	60.8 ± 1.4			50.53 ± 1.72
Bismertiazol	72.4 ± 3.1	54.2 ± 1.2	77.5 ± 1.4	50.0 ± 2.2	
Hymexazol					52.23 ± 2.86

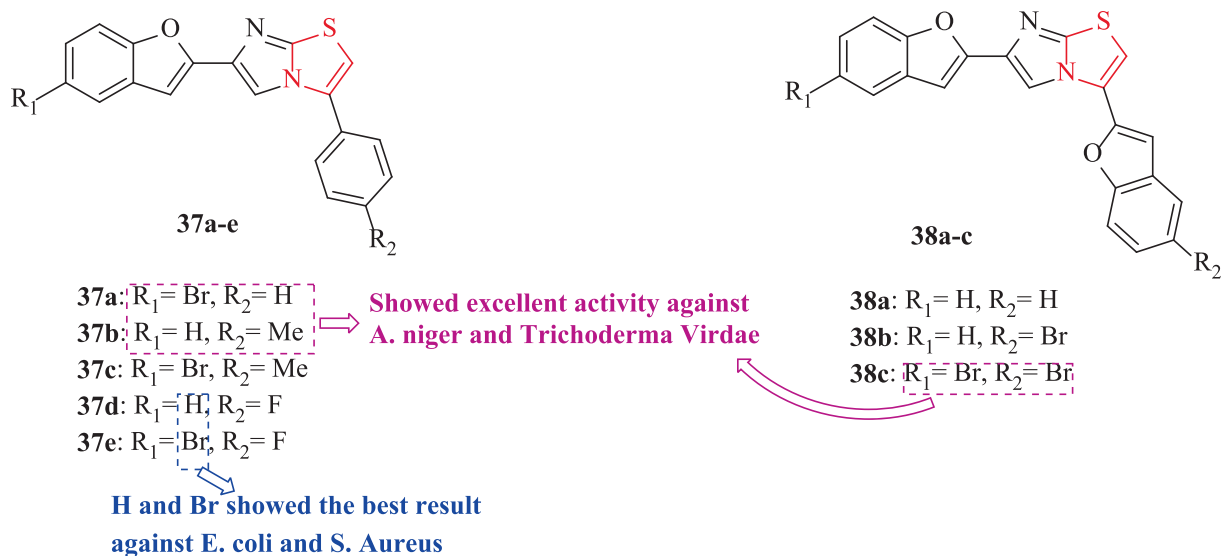


**Fig. 11.** Chemical structures of 37a-e and 38a-c (Shankerrao et al., 2017)

**Table 9**  
Antimicrobial activity (IZ) of the structures 37a-e and 38a-c (Shankerrao et al., 2017)

Cpd. no.	Zone of inhibition (mm)											
	S. aureus		K. pneumonia		P. aeruginosa		E. Coli		A. Niger		T. viridae	
	50 µL	100 µL	50 µL	100 µL	50 µL	100 µL	50 µL	100 µL	50 µL	100 µL	50 µL	100 µL
37a	20	27	16	22	18	25	15	18	19	22	15	19
37b									22	26	24	26
37c									14	20	23	25
37d	14	17					18	20				
37e	18	22					16	20				
38a									14	16	13	18
38b	23	28	13	18	18	24	12	16	23	26	21	25
38c									28	34	28	30
Ampicillin	24	30	28	32	20	28	28	31				
Fulconozol												

Aspergillus versicolor compared to ketoconazole (Fig. 19 and Table 15). Moreover, structure 65a had significant activity against

P. verrucosum var. Cyclopium and P. Funiculosum toward ketoconazole (Fig. 19 and Table 15) (Sirakanyan et al., 2021)

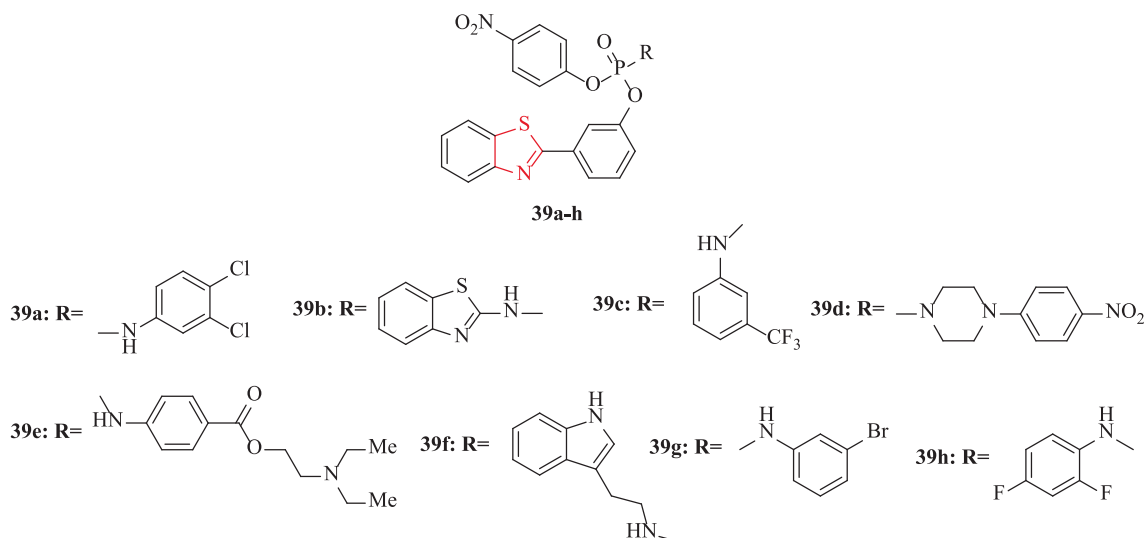


Fig. 12. Chemical structures 39a-h (Reddy et al., 2018)

Table 10

Zone of inhibition of the structures 39a-h (Reddy et al., 2018)

Cpd. no.	Zone of inhibition (mm)									
	Streptococcus aureus (ATCC-25923)		Bacillus subtilis (ATCC-1789)		Escherichia coli (ATCC-9637)		Aspergillus niger (MTCC-1881)		Candida albicans (ATCC-2091)	
	50 µg/mL	100 µg/mL	50 µg/mL	100 µg/mL	50 µg/mL	100 µg/mL	50 µg/mL	100 µg/mL	50 µg/mL	100 µg/mL
39a							10.7	20.2	9.4	18.7
39b							11.5	21.2	10.8	21.4
39c	14.5	21.7	12.4	22.1	11.8	24.2	12.9	19.8	11.5	20.7
39d	11.0	20.7	12.2	21.7	12.4	20.3			10.3	19.7
39e			10.5	19.6						
39f							10.8	19.3		
39g							12.1	18.6	9.7	19.7
39h	10.8	21.9	10.2	22.4	11.4	22.6			10.4	19.3
Ampicillin	15.9	22.0	17.5	24.0	16.9	23.0				
Fulconozol							15.7	22.5	16.5	24.0

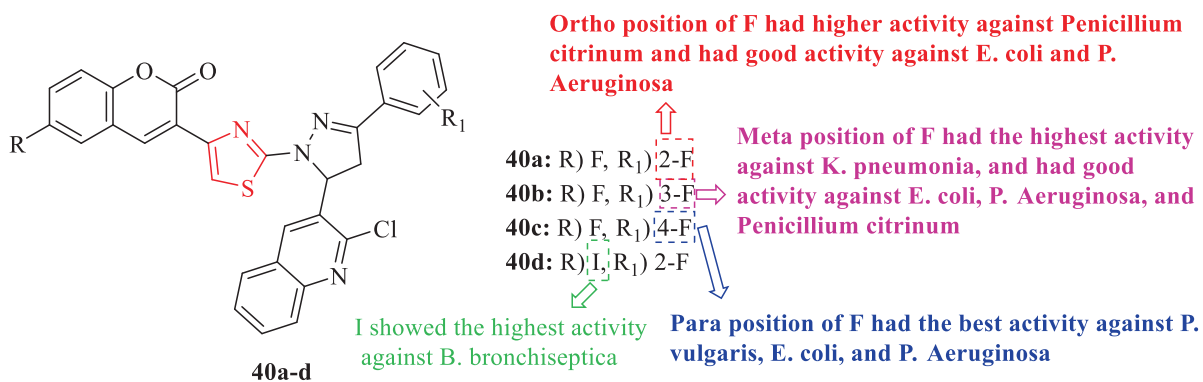


Fig. 13. Chemical structures 40a-d (Ansari and Khan, 2017)

In 2020, a series of novel thiazolyl-1,2,3-triazolyl-alcohol derivatives synthesized by Jagadale et al. In this study, were used 2 bacteria. Streptomycin was used as a reference drug. Among all

derivatives, structures 66b, 66f and 76i showed good antibacterial activity against *S. albus* toward the reference drug (Fig. 20 and Table 16) (Jagadale et al., 2020)

**Table 11**  
Zone of inhibition (mm) and MIC ( $\mu\text{g/mL}$ ) of the structures 40a-d (Ansari and Khan, 2017)

Cpd. no.	Zone of inhibition (mm) and MIC ( $\mu\text{g/mL}$ )					
	E. coli	P. aeruginosa	K. pneumonia	B. bronchiseptica	P. vulgaris	P. citrinum
40a	27.50 $\pm$ 0.33 (50)	30.19 $\pm$ 0.32 (50)				30.94 $\pm$ 0.32 (50)
40b	26.67 $\pm$ 0.31 (50)	29.0 $\pm$ 0.41 (50)	31.30 $\pm$ 0.32 (50)			29.90 $\pm$ 0.31 (50)
40c	28.71 $\pm$ 0.30 (50)	30.28 $\pm$ 0.41 (50)			29.74 $\pm$ 0.28 (50)	
40d				29.84 $\pm$ 0.31 (50)		
Ofloxacin	31.61 $\pm$ 0.41 (12.5)	34.23 $\pm$ 0.14 (12.5)	31.55 $\pm$ 0.19 (12.5)	34.80 $\pm$ 0.24 (25)	32.0 $\pm$ 0.3 (12.5)	
Ketoconazole						28.68 $\pm$ 0.31 (25)

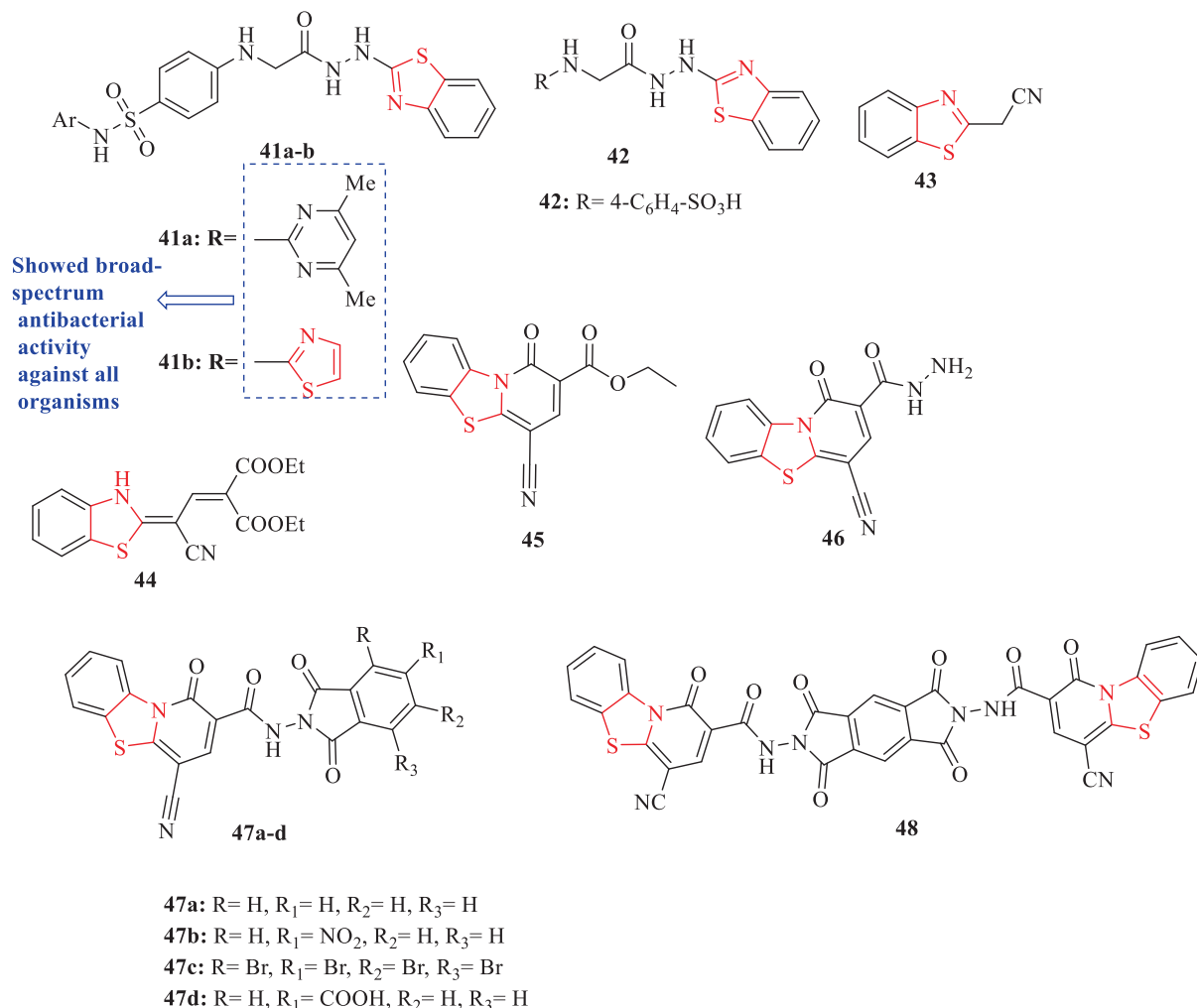


**Fig. 14.** Chemical structures 41a-b, 42-46, 47a-d, and 48 (Fadda et al., 2019)

Antifungal activity studies which were tested against 4 fungal strains showed structures 66a, 66c, 66d, 66e, 66f, 66g, 66h, and 66i had remarkable activity against *A. niger* compared to ravuconazole as a reference drug (Fig. 20 and Table 16) (Jagadale et al., 2020)

Patel and co-workers reported 4-thiazolidinone fused pyrimidines. Ten derivatives were tested against 4 bacteria with respect to ciprofloxacin as a reference drug. Among all derivatives, structures 67c and 67d (2 and 3-CH<sub>3</sub>) and 67a (3-NO<sub>2</sub>) had good activity against *P.aeruginosa* MTCC 741 and *E.coli* MTCC 442 toward the reference drug (Fig. 21 and Table 17). In addition, structures 67b

(2-Cl) and 67d (3-CH<sub>3</sub>) showed good activity against *S.aureus* MTCC 96 and *S.pyogenus* MTCC 443 with respect to the reference drug (Fig. 21 and Table 17) (Patel et al., 2020)

All derivatives were tested against 3 fungal strains. In between, structures 67c, 67d, and 67e had low activity to some extent against *C. Albicans* (Fig. 21 and Table 17) (Patel et al., 2020)

Shinde et al. evaluated the antibacterial activity of a series of 2-(4-(benzo[d]thiazol-5-ylsulfonyl) piperazine-1-yl)-N-substituted acetamides against 4 bacteria with respect to ciprofloxacin as a reference drug. Among all derivatives, structures 68a, 68c, 68e, 68g,

**Table 12**  
Antimicrobial activity (MIC and IZ) of the structures 41a-b, 42-46, 47a-d, and 48 (Fadda et al., 2019)

Cpd. no.	Minimal inhibitory concentration (MIC in µg/mL) and inhibition zone (mm)					
	Bacteria				Fungi	
	B. subtilis	B. thuringiensis	E. coli	P. aeruginosa	F. oxysporum	B. fabae
41a	3.125 (45)	6.25 (40)	12.5 (21)	50.0 (16)	12.5 (30)	12.5 (32)
41b	3.125 (44)	6.25 (45)	12.5 (26)	50.0 (18)	25.0 (30)	25.0 (33)
42					50.0 (20)	50.0 (21)
43	50.0 (24)	50.0 (26)				
44	50.0 (20)	50.0 (25)				
45	50.0 (25)	50.0 (22)				
46	25.0 (24)	50.0 (26)				
47a	12.5 (33)	50.0 (17)				
47b	12.5 (33)	12.5 (34)				
47c	12.5 (35)	50.0 (17)				
47d	12.5 (36)	25.0 (27)				
48	12.5 (35)	25.0 (26)				
Chloramphenicol	3.125 (44)	3.125 (44)	6.25 (37)	6.25 (38)		
Cephalothin	6.25 (36)	6.25 (37)	6.25 (38)	6.25 (37)		
Cycloheximide					3.125 (43)	3.125 (42)

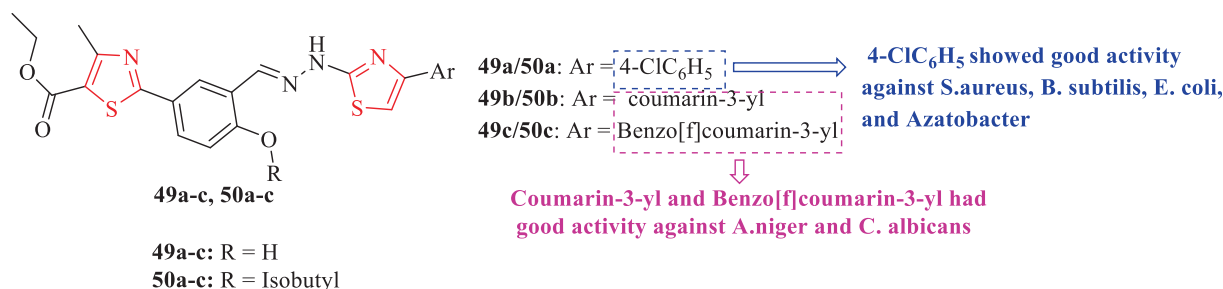


**Fig. 15.** Chemical structures 49a-c and 50a-c (Deshineni et al., 2020)

**Table 13**  
Antimicrobial activity (MIC (µg/mL)) of the structures 49a-c and 50a-c (Deshineni et al., 2020)

Cpd. no.	MIC (µg/mL)					
	Staphylococcus aureus	Bacillus subtilis	Escherichia coli	Azotobacter	Candida albicans	Aspergillus niger
49a	35	30	25	20		
49b	15	20	20	25	12.5	12.5
49c	15	25	20	25	12.5	12.5
50a	25	25	20	15		
50b	15	15	20	20	12.5	25
50c	20	20	20	25	12.5	12.5
Levofloxacin	15	20	16	18		
Miconazole					12.5	12.5

and 68 k showed moderate activity against *E. coli* and *P. aeruginosa* toward the reference drug (Fig. 22 and Table 18). In addition, structures 68b, 68 h, 68i, 68d, and 68j displayed superior activity against *S. aureus* and *B. subtilis* toward the reference drug (Fig. 22 and Table 18) (Shinde et al., 2020)

All derivatives and clotrimazole (As reference drug) were tested against *Aspergillus fumigatus* and *C. Albicans* and results showed structures 68b, 68f, 68 g, and 68j had good activity against *C. Albicans* (Fig. 22 and Table 18). Moreover, structure 68d had good

activity against *A. fumigatus* (Fig. 22 and Table 18) (Shinde et al., 2020)

A series of novel bis(azolyl)sulfonamidoacetamides were synthesized by Sankar P et al. Chloramphenicol as a reference drug and all derivatives were tested against 4 bacteria. Among all derivatives, structures 72a, 72c, and 74c showed low minimal inhibitory concentrations (MICs) against *Bacillus subtilis*, equal to the reference drug (Fig. 23 and Table 19). In general, derivatives 71 and 72 demonstrated greater activity compared to derivatives 69,

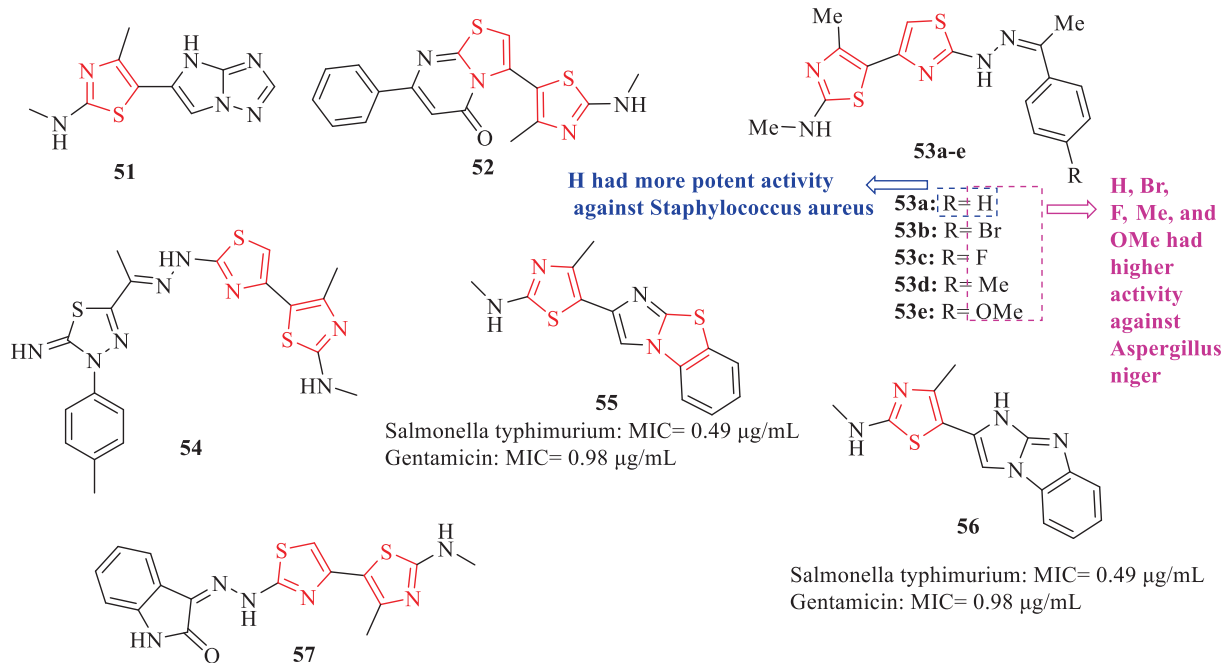


Fig. 16. Chemical structures of 41–52, 53a–e, and 54–57 (Althagafi et al., 2019)

Table 14

Preliminary antimicrobial activity of the structures 51–52, 53a–e, 54 and 57 (Althagafi et al., 2019)

Cpd. no.	Preliminary antimicrobial activity <i>Aspergillus niger</i>
51	25.4 ± 1.20
52	24.3 ± 1.20
53a	25.0 ± 0.72
53b	21.8 ± 0.43
53c	25.2 ± 2.10
53d	24.1 ± 0.85
53e	26.3 ± 0.63
54	25.2 ± 2.10
57	26.3 ± 0.63
Amphotericin B	23.3 ± 0.58

70, 73, and 74 (Fig. 23). In addition, derivatives 73 and 74 exhibited more activity compared to derivatives 69 and 70 (Fig. 23) (Ss et al., 2021)

All derivatives were tested against *Aspergillus niger* and *Penicillium chrysogenum* except 69a, 69b, 70a, and 70b (Fig. 23). Structures 72c and 74c had low MICs against *Aspergillus niger*, but had equal MICs compared to ketoconazole as a reference drug (Fig. 23). In general, derivatives 73 and 74 exhibited greater activity compared to derivatives 69, 70, 71, and 72 (Fig. 23). Whereas derivatives 71 and 72 displayed higher activity compared to 69 and 70 (Fig. 23) (Ss et al., 2021)

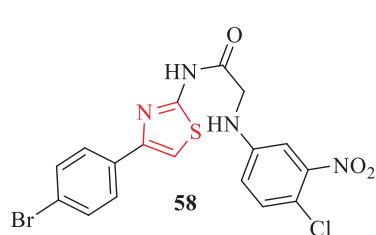
Khidre and Radini. evaluated the antibacterial activity of a novel series of structures containing thiazole scaffold against 4 bacteria with respect to ampicillin as a reference drug. Among all derivatives, structure 75 showed good antimicrobial activity against *B. subtilis*, *S. aureus*, *P. aeruginosa*, and *E. coli* toward the reference drug (Fig. 24 and Table 20). Moreover, structure 76 showed great

activity against *P. aeruginosa* and *E. coli* (Fig. 24 and Table 20) (Khidre and Radini, 2021)

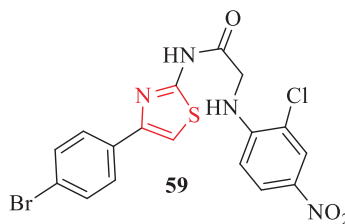
Derivatives were tested against 2 fungal strains and as a reference drug, clotrimazole was used. According to the results, structure 75 exhibited the most activity against *C. albicans* and *Aspergillus flavus* toward the reference drug (Fig. 24 and Table 20). Generally, structure 75 had the best biological activity compared to other structures due to existing bromine at the para position of the phenyl ring (Fig. 24 and Table 20) (Khidre and Radini, 2021)

Shabaan et al. synthesized a novel series of 1,3,4-thiadiazines and 1,3-thiazoles derivatives. Some derivatives were tested against 2 bacterial and 2 fungal strains with respect to neomycin and cyclohexamide as antibacterial and antifungal reference drugs, respectively. Structures 77, 78b, 79a, 80, and 78a had lower MIC against *S. aureus*, while structures 81 and 82 showed higher MIC values (Fig. 25 and Table 21). In addition, structures 78a, 78b, and 77 demonstrated moderate activity against *E. coli*, while structures 80 and 79a exhibited higher MIC values (Fig. 25 and Table 21). Structures 81 and 82 had higher MIC and MBC values against *S. aureus* and *E. coli* (Fig. 25 and Table 21). Moreover, structures 78a showed the most potent activity against *S. aureus* and *E. coli* toward the reference drug (Fig. 25 and Table 21). Structure 77 displayed significant activity against *S. aureus*, Whereas two structures (78b and 79b) exhibited moderate activity (Fig. 25 and Table 21). Also, structures 79a, 82, and 81 had low activities against *S. aureus* (Fig. 25 and Table 21). In contrast, Structures 83 and 84 displayed no activity against *S. aureus* (Fig. 25). Structures 81 had potent activity against *E. coli*, while structures 82, 77, 80, and 79b showed low activities toward the reference drug (Fig. 25 and Table 21) (Shabaan et al., 2021)

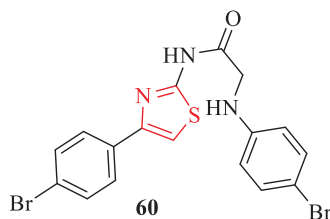
On the other hand, five structures (78b, 81, 77, 80, and 79b) displayed remarkable activity against *A. niger* toward the reference drug (Fig. 25 and Table 21). Whereas structures 82, 83, and 79a displayed moderately active against *A. niger* (Fig. 25 and Table 21).



*Escherichia coli* (MTCC443), MIC= 26.7  $\mu$ M  
Norfloxacin, MIC= 4.7  $\mu$ M

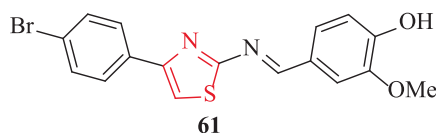


*B. Subtilis*, MIC= 26.7 $\mu$ M;Norfloxacin, MIC= 4.7  $\mu$ M  
*E. Coli*, MIC= 26.7  $\mu$ M;Norfloxacin, MIC= 4.7  $\mu$ M  
*Candida albicans* (MTCC227), MIC= 13.4  $\mu$ M;Fluconazole, MIC= 5.0  $\mu$ M  
*Aspergillus niger* (MTCC281), MIC= 26.7  $\mu$ M;Fluconazole, MIC= 5.0  $\mu$ M

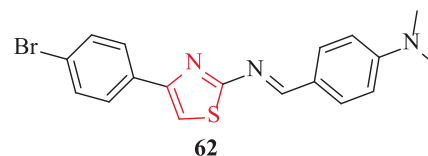


*S. aureus*, MIC= 13.4 $\mu$ M; Norfloxacin, MIC= 4.7  $\mu$ M  
*Candida albicans* (MTCC227), MIC= 26.8  $\mu$ M  
*Aspergillus niger* (MTCC281), MIC= 13.4  $\mu$ M

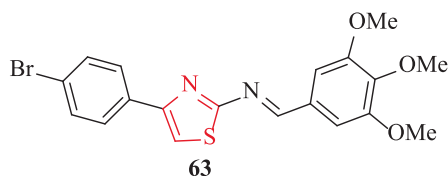
**Fig. 17.** Antimicrobial activity of the structures 58–60 (Sharma et al., 2019a)



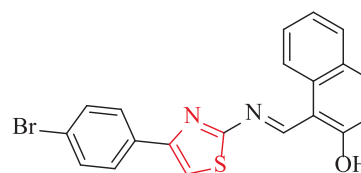
*Escherichia coli* (MTCC443): MIC= 16.1  $\mu$ M;Norfloxacin MIC= 4.7  $\mu$ M  
*Staphylococcus aureus* (MTCC3160); MIC= 16.1; Norfloxacin MIC= 4.7  $\mu$ M



*Aspergillus niger* (MTCC281): MIC= 16.2  $\mu$ M;Fluconazole MIC= 5.0  $\mu$ M

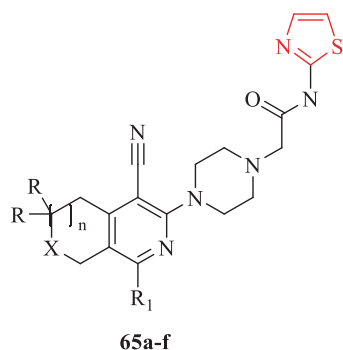


*Bacillus subtilis* (MTCC441): MIC= 28.8; Norfloxacin MIC= 4.7  $\mu$ M



*Candida albicans* (MTCC227): MIC= 15.3  $\mu$ M

**Fig. 18.** Antimicrobial activity of the structures 61–64 (Sharma et al., 2019b)



**65a:** X = CH<sub>2</sub>, n = 0, R = H, R<sub>1</sub> = Bu<sup>t</sup>  
**65b:** X = CH<sub>2</sub>, n = 0, R = H, R<sub>1</sub> = Ph  
**65c:** X = CH<sub>2</sub>, n = 0, R = H, R<sub>1</sub> = 2-furyl  
**65d:** X = O, n = 1, R = R<sub>1</sub> = Me  
**65e:** X = O, n = 1, R = Me, R<sub>1</sub> = i-Pr  
**65f:** X = O, n = 1, R = Me, R<sub>1</sub> = 2-furyl

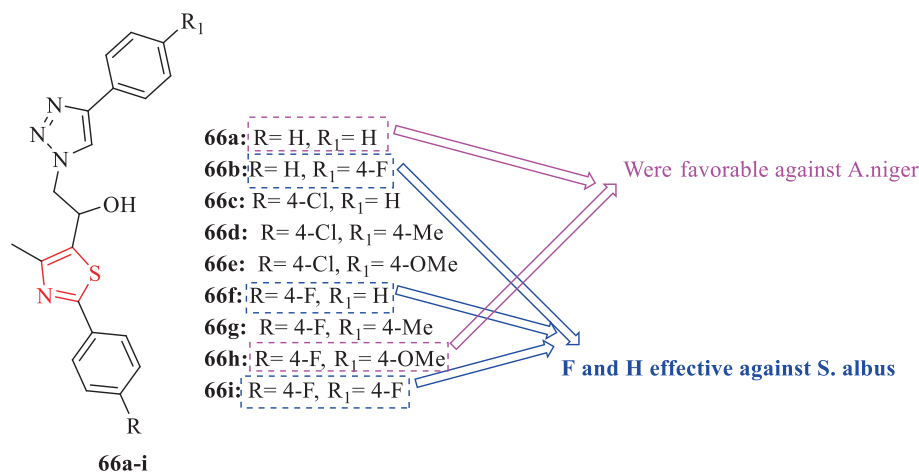
Had significant activity against *P. verrucosum*  
var. *Cyclopium* and *P. Funiculosum*, and  
*Aspergillus versicolor*

Had lower activity against *P. aeruginosa*.  
Had lowest MIC against *B. cereus*.  
Had good activity against *L. monocytogenes*

**Fig. 19.** Chemical structures 65a-f (Sirakanyan et al., 2021)

**Table 15**  
Antimicrobial activity of the structures 65a-f (Sirakanyan et al., 2021)

Cpd. no.		Bacterial strains			Fungal strains		
		<i>Pseudomonas aeruginosa</i>	<i>Bacillus cereus</i>	<i>Listeria monocytogenes</i>	<i>Aspergillus versicolor</i>	<i>Penicillium funiculosum</i>	<i>Penicillium verrucosum</i> var. <i>cyclopium</i>
65a	MIC				0.17 ± 0.001	0.17 ± 0.001	0.17 ± 0.001
	MFC				0.23 ± 0.001	0.23 ± 0.002	0.23 ± 0.002
65b	MIC		0.47 ± 0.002				
	MBC		0.94 ± 0.01				
65c	MIC		0.23 ± 0.002	0.35 ± 0.003	0.23 ± 0.002		
	MBC		0.47 ± 0.003	0.47 ± 0.003	0.47 ± 0.003		
	MFC						
65d	MIC		0.23 ± 0.002				
	MBC		0.47 ± 0.003				
65e	MIC				0.23 ± 0.001		
	MFC				0.47 ± 0.004		
65f	MIC	0.23 ± 0.001	0.06 ± 0.001	0.23 ± 0.002			
	MBC	0.47 ± 0.003	0.11 ± 0.001	0.47 ± 0.006			
Streptomycin	MIC	0.05 ± 0.001	0.025 ± 0.0003	0.15 ± 0.001			
	MBC	0.1 ± 0.002	0.05 ± 0.001	0.3 ± 0.002			
Ampicillin	MIC	0.2 ± 0.002	0.1 ± 0.002	0.15 ± 0.001			
	MBC	-	0.15 ± 0.002	0.3 ± 0.003			
Bifon-Azole	MIC				0.1 ± 0.001	0.2 ± 0.002	0.1 ± 0.001
	MFC				0.2 ± 0.002	0.25 ± 0.002	0.2 ± 0.002
Ketoco-nazole	MIC				0.2 ± 0.002	0.2 ± 0.001	0.2 ± 0.002
	MFC				0.5 ± 0.004	0.5 ± 0.002	0.3 ± 0.01

**Fig. 20.** Chemical structures 66a-i (Jagadale et al., 2020)**Table 16**  
Antimicrobial activity (MIC (µg/mL)) of the structures 66a-i (Jagadale et al., 2020)

Cpd. no.	MIC (µg/mL)	
	<i>A.niger</i>	<i>S.albus</i>
66a	31.25	
66b		62.5
66c	62.5	
66d	62.5	
66e	62.5	
66f	62.5	62.5
66g	62.5	
66h	31.25	
66i	62.5	62.5
Streptomycin		7.81
Fluconazole	7.81	
Ravuconazole	31.25	

Structures 78b and 77 had remarkable activities against *C. albicans* (Fig. 25 and Table 21). Whereas two structures (82 and 79b) displayed moderate activity (Shabaan et al., 2021)

A new series of 4-(6-substituted quinolin-4-yl)-N-arylthiazol-2-amines were synthesized by Thakare et al. All derivatives were tested against 4 bacteria. As a reference drug, streptomycin was used. Structure 85f had moderated activity against *E. Coli* (Fig. 26 and Table 22). Furthermore, structures 85a, 85e, 85f, and 85g displayed moderate activity against *S. albus*, while structures 85b and 85d had good activity (Fig. 26 and Table 22) (Thakare et al., 2021)

The antifungal activities of derivatives were evaluated against 2 fungal strains with respect to ravuconazole and fluconazole as the reference drugs. According to the results, structures 85h, 85i, 85j, 85k, 85l, 85m, 85n, 86a and 86b were found to have moderate to good activity against *A. niger* toward ravuconazole (Fig. 26 and Table 22). Moreover, structure 86a showed good activity against

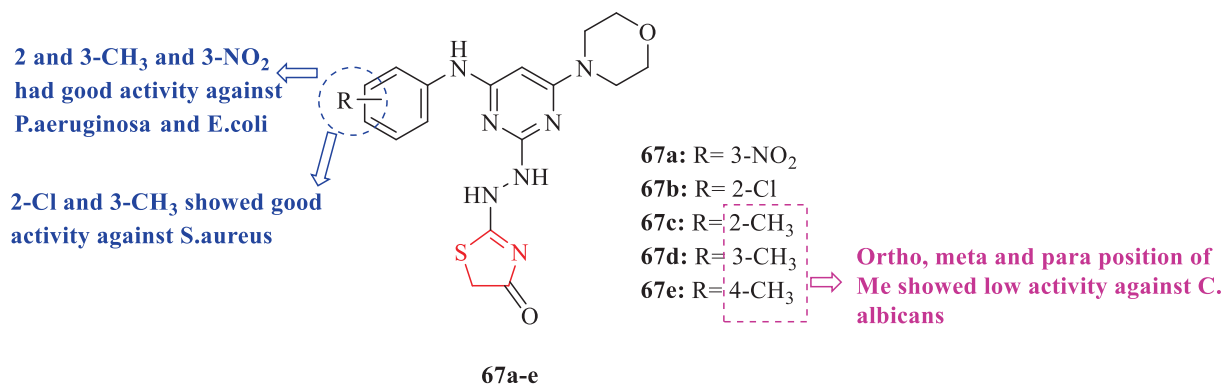


Fig. 21. Chemical structures 67a-e (Patel et al., 2020)

Table 17

Antimicrobial activity (MIC (μg/mL)) of the structures 67a-e (Patel et al., 2020)

Cpd. no.	MIC (μg/mL)				
	<i>S.aureus</i> MTCC 96	<i>S.pyogenus</i> MTCC 443	<i>P.aeruginosa</i> MTCC 741	<i>E.coli</i> MTCC 442	<i>C.albicans</i> MTCC 227
<b>67a</b>			62.5	100	
<b>67b</b>	100	250			
<b>67c</b>			100	100	250
<b>67d</b>	100	100	100	125	250
<b>67e</b>					250
<b>Ciprofloxacin</b>	50	50	25	25	
<b>Nystatin</b>					100

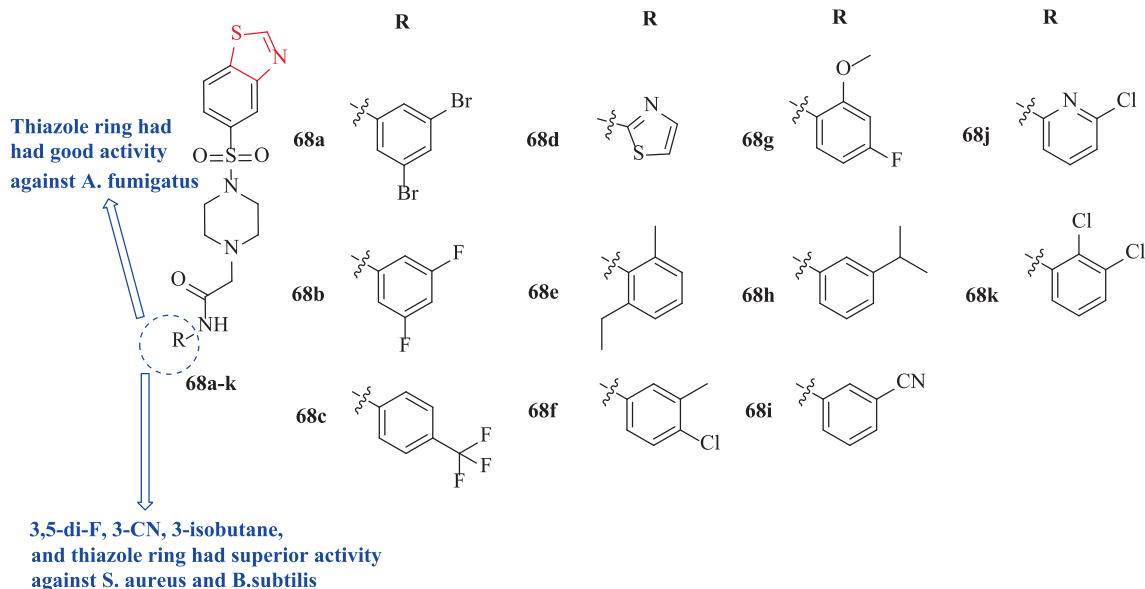


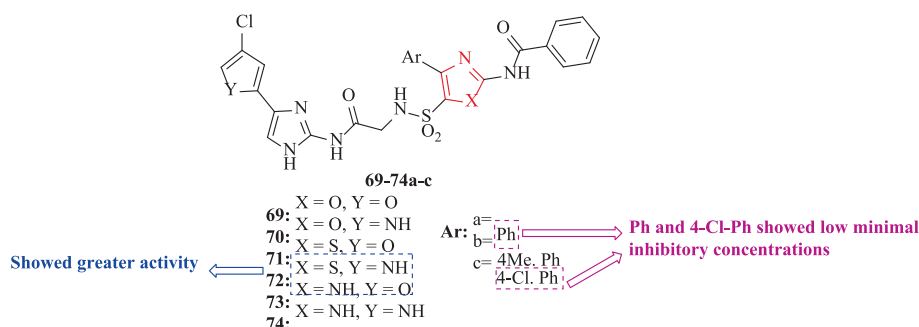
Fig. 22. Chemical structures 68a-k (Shinde et al., 2020)

*A. candida* and comparable activity against *A. niger* (Fig. 26 and Table 22). Structure 85b showed moderate activity against *A. candida* (Fig. 26 and Table 22). The structure 85c had good activity against *A. candida* and *A. niger* (Fig. 26 and Table 22) (Thakare et al., 2021)

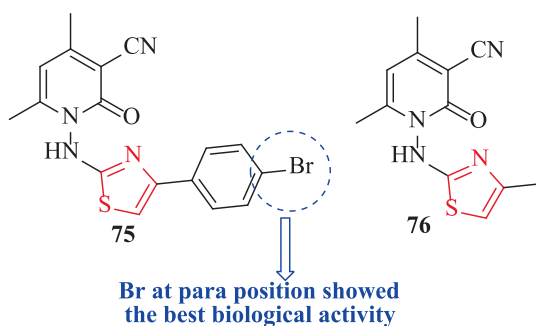
In 2022, El-Hagrassey and co-workers synthesized a novel series of derivatives containing thiazole. Ampicillin as a reference drug and the novel derivatives were tested against 4 bacteria. According to antibacterial activity studies, structure 90 displayed the highest activity against both gram-negative and positive bacte-

**Table 18**  
Antimicrobial activity (MIC ( $\mu\text{g/mL}$ )) of the structures 68a-k (Shinde et al., 2020)

Cpd. no.	MIC ( $\mu\text{g/mL}$ )					
	S.aureus	B.Subtilis	E.coli	P.aeruginosa	C.albicans	A. fumigatus
68a			18			
68b	21	17			17	
68c			22	13		
68d	26	13				21
68e			26			
68f					19	
68 g				22	15	
68 h	18	18				
68i		22				
68j	17	10			22	
68 k			25			
Ciprofloxacin	19	20	36	34		
Clotrimazole					25	25

**Fig. 23.** Chemical structures 69a-c-74a-c (Ss et al., 2021)**Table 19**  
Antimicrobial activity (MIC (MBC/MFC)  $\mu\text{g/well}$ ) of the structures 72a, 72c and 74c (Ss et al., 2021)

Cpd. no.	MIC (MBC/MFC) $\mu\text{g/well}$	
	Bacillus subtilis	Aspergillus niger
72a	6.25 (12.5)	
72c	6.25 (12.5)	6.25 (12.5)
74c	6.25 (12.5)	6.25 (12.5)
Fluconazole	6.25	
Ravuconazole		6.25

**Fig. 24.** Chemical structures 75–76 (Khidre and Radini, 2021)

ria, Whereas structure 89 had a weak effect on E. coli and P. Aeruginosa (Fig. 27 and Table 23). Also, structures 87a, 87b, 87c, and 88 did not show an effect on E. coli and structures 87a, 87b, and 88

had no effect on S.aureus (Fig. 27). Structures 87b and 88 did not show effect on P. aeruginosa and B. Subtilis (Fig. 27) (El-Hagrassey et al., 2022)

On the other hand, derivatives were tested against C. Albicans for investigation of antifungal activity. As a reference drug, clotrimazole was used. Structure 90 had the highest activity against C. albicans (Fig. 27 and Table 23). In addition, structures 87b and 88 had no effect on C. albicans (Fig. 27). Whereas structure 89 showed good activity against C. albicans (Fig. 27 and Table 23) (El-Hagrassey et al., 2022)

A novel series of 2,3-Dihydropyrido[2,3-d]pyrimidine-4-ones and Pyrrolo[2,1-b][1,3]benzothiazoles synthesized by Al-Mutairi et al. Cefotaxime as reference drug and all derivatives were tested against 6 bacteria (Fig. 28 and Table 13). The antibacterial evaluations of all derivatives exhibited 4 structures (91a, 91b, 92a, and 92d) that had higher activity toward the reference drug (Fig. 28 and Table 13). Structure 91a had an equipotent activity with respect to the reference drug against Chlamydia pneumonia and Bacillus subtilis, and structure 92a had equipotent activity against Chlamydia pneumonia and Bacillus subtilis, while had more activity against Staphylococcus aureus (Fig. 28 and Table 13). Moreover, structure 92d because of the presence of pyrrolobenzothiazole with p-fluorophenyl substituent exhibited significant activity against all bacteria compared to the reference drug (Fig. 28 and Table 13). In general, structures 92b, 92c, and 92e had good inhibition activity against all bacterial strains (Fig. 28 and Table 13) (Al-Mutairi et al., 2022)

All derivatives were tested against 3 fungal strains. As a reference drug, fluconazole was used for the investigation of antifungal activity. According to studies, structures 91a, 91b, 92a, and 92d had high activity (Fig. 28 and Table 24). Structure 92d showed equipo-

**Table 20**  
Antimicrobial activity (MIC ( $\mu\text{g/mL}$ )) of the structures 75 and 76 (Khidre and Radini, 2021)

Cpd. no.	MIC ( $\mu\text{g/mL}$ )					
	E. coli	P. aeruginosa	S. aureus	B. subtilis	C. albicans	A. flavus
75	93.7 $\pm$ 0.95	62.5 $\pm$ 2.00	46.9 $\pm$ 0.84	62.5 $\pm$ 0.50	7.8 $\pm$ 0.17	5.8 $\pm$ 0.65
76	93.7 $\pm$ 0.95	93.7 $\pm$ 0.95	20	25	12.5	12.5
Ampicillin	125 $\pm$ 0.58	125 $\pm$ 3.51	187.5 $\pm$ 0.06	125 $\pm$ 1.73		
Clotrimazole					5.8 $\pm$ 0.06	3.9 $\pm$ 0.06

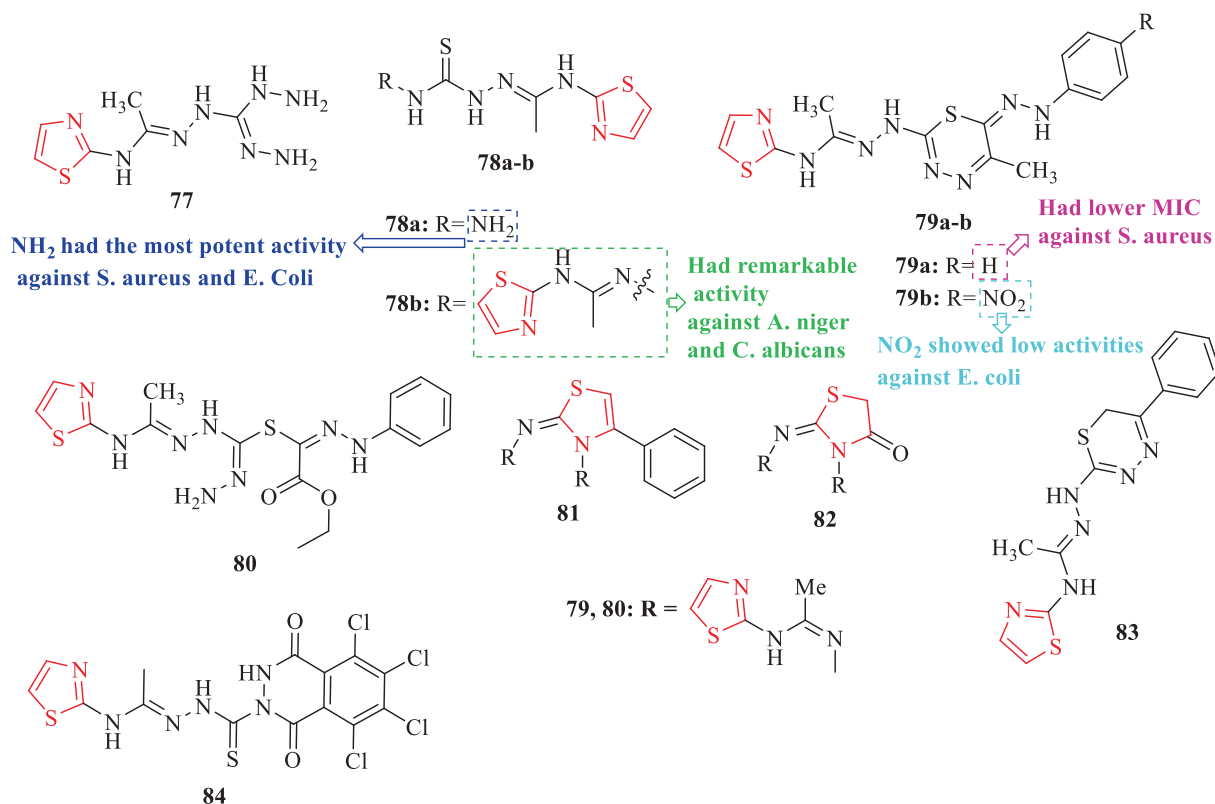


**Fig. 25.** Chemical structures 77–84 (Shabaan et al., 2021)

**Table 21**  
Antimicrobial activity of the structures 77, 78a-b, 79a-b, and 80–84 (Shabaan et al., 2021)

Cpd. no.	Staphylococcus aureus				Escherichia coli			
	MIC ( $\mu\text{g/ml}$ )	MBC ( $\mu\text{g/ml}$ )	MIC ( $\mu\text{g/ml}$ )	MBC ( $\mu\text{g/ml}$ )	S. aureus	E. coli	C. albicans	A. niger
77	39.06	39.06	156.25	312.50	32	23	31	30
78a	39.06	78.13	156.25	156.25	29	27		36
78b	78.13	31.5	156.25	625.00	29	27	32	36
79a	39.06	78.13	625.00	625.00	22	0		25
79b	19.06	39.06			25	21	24	35
80	9.77	19.06	625.00	1250.00	23	22		35
81	312.00	625	312.50	625.00	15	32		35
82	312.00	625			22	14	24	25
83								28
84					16			
Neomycin					37	30	39	0
Cyclohe-xamide					0	0	0	39

tent activity against *Aspergillus flavus* while had more high activity against *Ganoderma lucidum* and *Candida albicans* toward the reference drug (Fig. 28 and Table 24). Structure 92a showed signif-

icant activity against *Ganoderma lucidum* and *Aspergillus flavus* and had more potent activity against *Candida albicans* compared to the reference drug (Fig. 28 and Table 24). Also, structures 91a

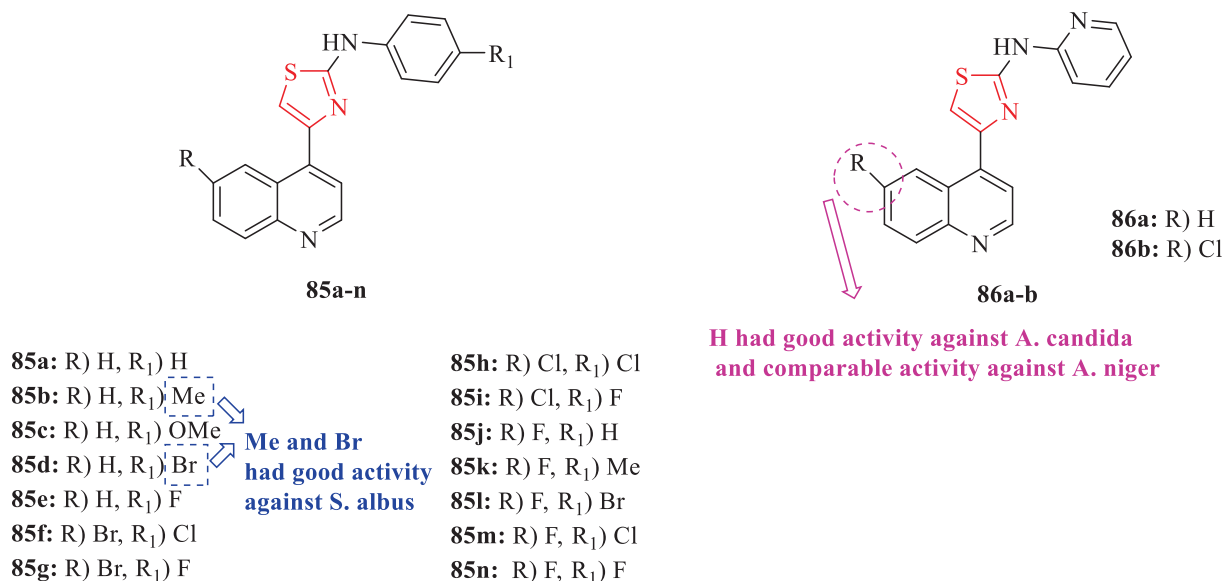


Fig. 26. Chemical structures 85a-n and 86a-b (Thakare et al., 2021)

Table 22  
Antimicrobial activity (MIC (μg/mL)) of the structures 85a-n and 86a-b (Thakare et al., 2021)

Cpd. no.	MIC (μg/mL)			
	E. coli	S. albus	A. Candida	A. niger
<b>85a</b>		125		
<b>85b</b>		62.5	125	
<b>85c</b>			62.5	62.5
<b>85d</b>		62.5		
<b>85e</b>		125		
<b>85f</b>	250	125		
<b>85g</b>		125		
<b>85h</b>				62.5
<b>85i</b>				125
<b>85j</b>				125
<b>85k</b>				125
<b>85l</b>				62.5
<b>85m</b>				125
<b>85n</b>				125
<b>86a</b>			31.25	31.25
<b>86b</b>				250
<b>Streptomycin</b>	7.81	7.81		
<b>Fluconazole</b>			7.81	7.81
<b>Ravuconazole</b>			7.81	31.25

and 91b had good activity against *Aspergillus Flavus*, *Candida Albicans*, and *Ganoderma Lucidum* (Fig. 28 and Table 24) (Al-Mutairi et al., 2022)

Othman et al. synthesized and investigated the antimicrobial activity of a series of thiazole, thiophene, and thieno[2,3-d]pyrimidines against 4 bacteria and 2 fungal strains. As antibacterial and antifungal reference drugs, ampicillin and clotrimazole were used, respectively. Structure 93 against *S. aureus* and *B. Subtilis* had potent activity (Fig. 29 and Table 25). Structures 94, 95, and 96 showed weak sensitivity against *P. aeruginosa* and *E. Coli* (Fig. 29 and Table 25). In addition, structures 98 and 99 against *P. aeruginosa* exhibited moderate potency, while structures 97 and 93 had potent activity (Fig. 29 and Table 25). Moreover, structures 98 and 97 displayed less sensitivity against *E. coli* toward the reference drug (Fig. 29 and Table 25) (Othman et al., 2022)

Four structures (98, 99, 96, and 93) against *A. fumigatus* RCMB showed potent antifungal activity. Further, structures 95 and 93 showed remarkable antifungal activity against *C. albicans* toward the reference drug (Fig. 29 and Table 25) (Othman et al., 2022)

A novel series of structures containing thiazole scaffold were synthesized by Kartsev and co-workers and evaluated their antibacterial activity against 6 bacteria, using a microdilution

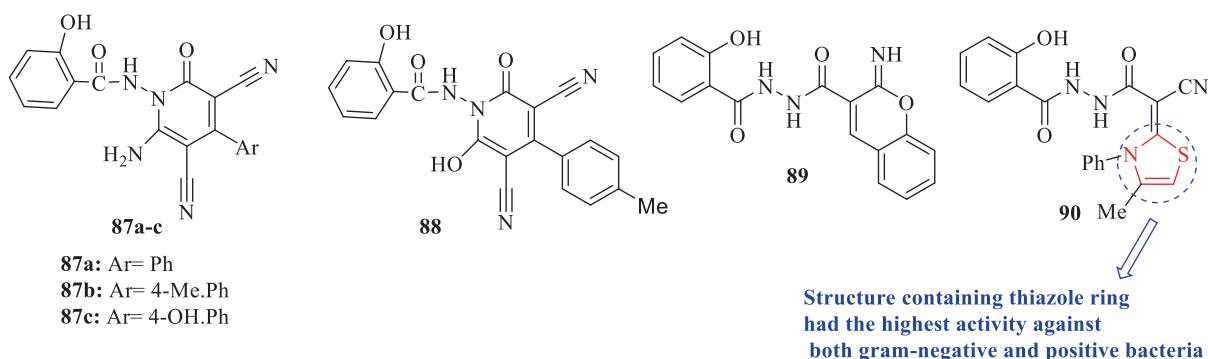


Fig. 27. Chemical structure 87a-c and 88–90 (El-Hagrassey et al., 2022)



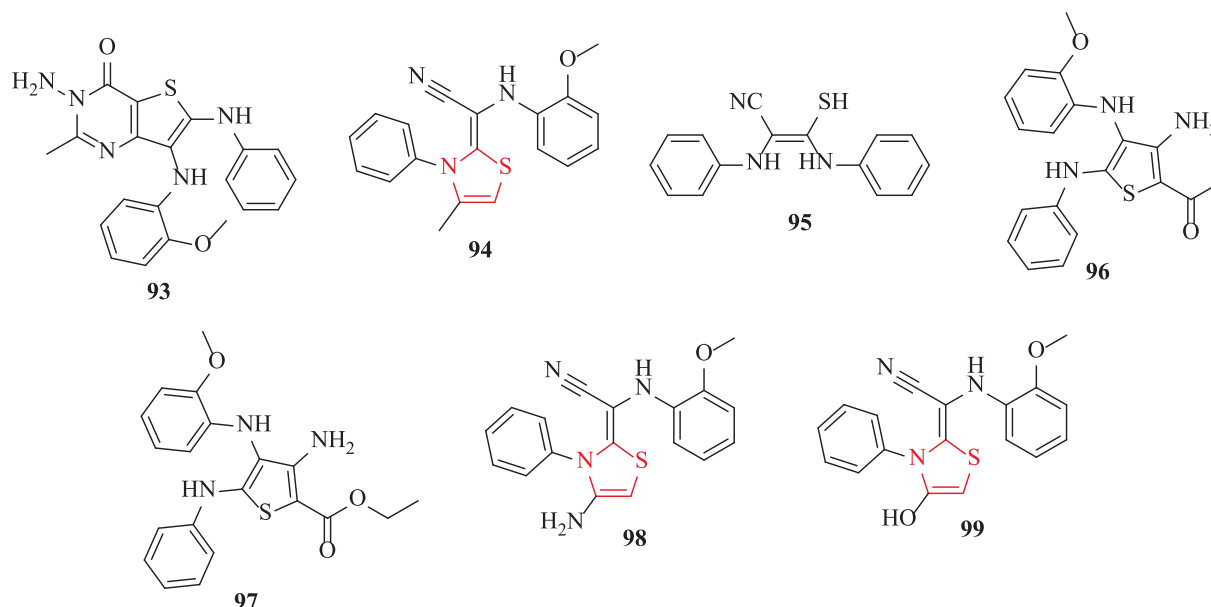


Fig. 29. Chemical structures 93–99 (Othman et al., 2022)

Table 25

Mean diameter of inhibition zones (Mean  $\pm$  SEM (mm)) MIC (Mean  $\pm$  SEM ( $\mu\text{g/mL}$ )) of the structures 93–99 (Othman et al., 2022)

Cpd. no.	Mean diameter of inhibition zones (Mean $\pm$ SEM (mm)) MIC (Mean $\pm$ SEM ( $\mu\text{g/mL}$ ))					
	S. aureus 25,923	B. Subtilis 6633	P. aeruginosa	E. coli RCMB 010,052	A. fumigatus RCMP 02,568	C. Albicans ATCC10231
93	27.1 $\pm$ 0.11 (0.03 $\pm$ 0.18)	25.1 $\pm$ 0.15 (0.05 $\pm$ 0.13)	19.7 $\pm$ 0.14 (0.98 $\pm$ 0.55)		22.2 $\pm$ 0.17 (0.49 $\pm$ 0.32)	21.4 $\pm$ 0.50 (0.98 $\pm$ 0.25)
94			14.3 $\pm$ 0.25 (1.25 $\pm$ 0.07)	12.1 $\pm$ 0.25 (250 $\pm$ 0.62)		
95			16.7 $\pm$ 0.13 (31.25 $\pm$ 0.46)	15.2 $\pm$ 0.44 (62.5 $\pm$ 0.26)		22.1 $\pm$ 0.02 (0.49 $\pm$ 0.38)
96			12.7 $\pm$ 0.16 (250 $\pm$ 0.01)	9.9 $\pm$ 0.25 (500 $\pm$ 0.04)	21.6 $\pm$ 0.15 (0.49 $\pm$ 0.32)	
97			8.9 $\pm$ 0.23 (0.50 $\pm$ 0.15)	22.3 $\pm$ 0.17 (0.49 $\pm$ 0.28)		
98			18.7 $\pm$ 0.45 (7.81 $\pm$ 0.41)	21.8 $\pm$ 0.01 (0.49 $\pm$ 0.12)	20.2 $\pm$ 0.10 (1.95 $\pm$ 0.52)	
99			17.3 $\pm$ 0.43 (15.62 $\pm$ 0.31)		19.5 $\pm$ 0.12 (0.98 $\pm$ 0.05)	
Ampicillin	27.7 $\pm$ 0.82 (0.03 $\pm$ 0.53)	25.4 $\pm$ 0.18 (0.05 $\pm$ 0.22)	20.3 $\pm$ 0.31 (1.95 $\pm$ 0.11)	26.8 $\pm$ 0.15 (0.03 $\pm$ 0.48)		
Clotrimazole					23.7 $\pm$ 0.10 (0.12 $\pm$ 0.28)	22.8 $\pm$ 0.17 (0.49 $\pm$ 0.45)

A series of coumarin thiazoles were synthesized by Yang et al and their antimicrobial activities were evaluated against 9 bacteria. As antibacterial reference drugs, norfloxacin and ciprofloxacin were used. Structure 104d against *S. aureus* displayed equivalent antibacterial activity toward norfloxacin (Fig. 31 and Table 27). Structures 104a–b against *E. coli* ATCC 25922 showed the same MIC with respect to norfloxacin (Fig. 31 and Table 27). Structures 104b and 104c against most tested strains showed poor bioactivities (Fig. 31). In addition, structures 109b–d exhibited 2 to 8 times antibacterial potency against MRSA toward the reference drugs (Fig. 31 and Table 27). Structure 109a against *E. coli* ATCC 25,922 showed almost 2 times inhibition potency toward norfloxacin

(Fig. 31 and Table 27). Structure 109c against *A. baumannii* showed high activity with respect to ciprofloxacin with the same MIC value and 8-fold more active than norfloxacin (Fig. 31 and Table 27). In the case of 107a–g, structure 107a against MRSA, *Enterococcus faecalis*, and *Staphylococcus aureus* showed the best antibacterial efficacy (Fig. 31 and Table 27). The same structure against MRSA was 8 times superior to ciprofloxacin and norfloxacin (Fig. 31 and Table 27). Structure 107b against MRSA, *S. aureus*, *A. baumannii*, and *E. faecalis* showed good activity which was 4 times higher than or equivalent to norfloxacin (Fig. 31 and Table 27). Structures 107c–g exhibited no bioactivity or remarkably declined inhibitory activity (Fig. 31). Further, structures 104 and 106a showed no sen-

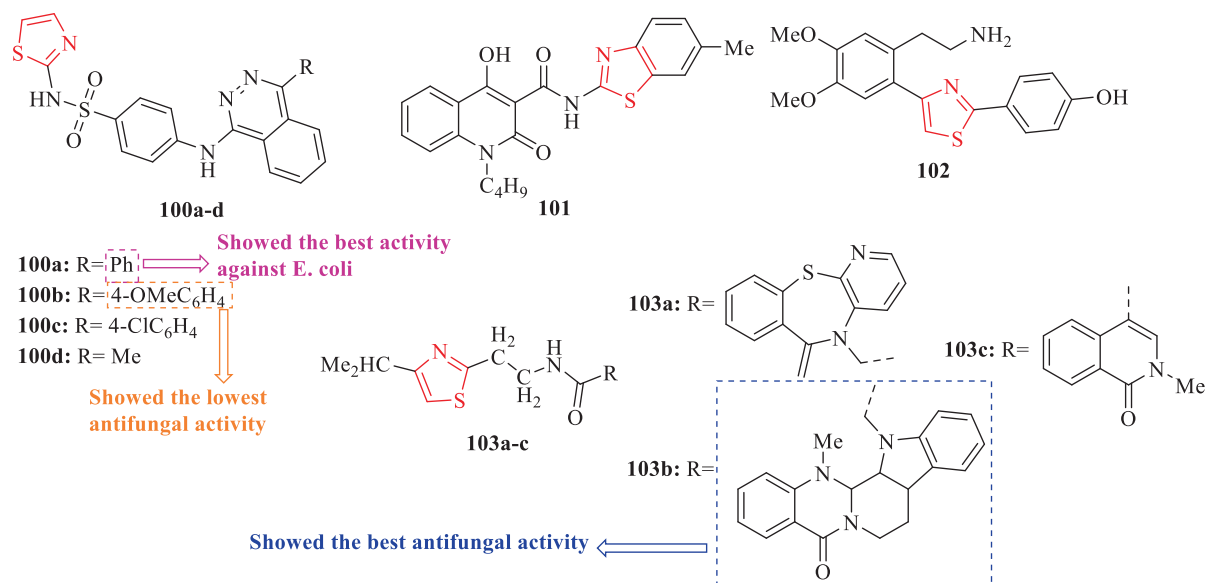


Fig. 30. The structures of heteroaryl (aryl) thiazole derivatives 100a-d, 101–102, and 103a-c (Kartsev et al., 2022)

Table 26

Antimicrobial activity of the structures 100a, 100c, 100d, 101–102, and 103a-c (Kartsev et al., 2022)

Cdp. no.	MIC/MBC in mg/mL										
	B.c.	E.c.	S.T.	MRSA	P.a.	E. c.	A.n.	A.v.	P.f.	T.v.	P.v.c.
100a	MIC	0.17 ± 0.00		0.94 ± 0.00	0.23 ± 0.00	0.94 ± 0.00					
	MBC	0.23 ± 0.00		1.88 ± 0.00	0.47 ± 0.00	1.88 ± 0.00					
100c	MIC									0.17 ± 0.00	
	MFC									0.23 ± 0.00	
100d	MIC									0.47 ± 0.00	
	MFC									0.94 ± 0.00	
101	MIC	0.17 ± 0.00	0.17 ± 0.19				0.17 ± 0.00	0.17 ± 0.00	0.17 ± 0.00	0.06 ± 0.00	0.17 ± 0.00
	MBC	0.23 ± 0.00	0.23 ± 0.00								
102	MIC		0.23 ± 0.00	0.47 ± 0.00	0.23 ± 0.00	0.47 ± 0.00	0.23 ± 0.00	0.23 ± 0.00	0.23 ± 0.00	0.11 ± 0.00	0.23 ± 0.00
	MBC		0.47 ± 0.00	0.94 ± 0.00	0.47 ± 0.00	0.94 ± 0.00				0.11 ± 0.00	
103a	MIC									0.23 ± 0.00	
	MFC									0.11 ± 0.00	
103b	MIC						0.23 ± 0.00	0.35 ± 0.08	0.23 ± 0.00	0.17 ± 0.00	0.35 ± 0.08
	MFC						0.47 ± 0.00	0.47 ± 0.00	0.47 ± 0.00	0.23 ± 0.00	0.47 ± 0.00
103c	MIC									0.08 ± 0.00	
	MFC									0.11 ± 0.00	
Streptomycin	MIC	0.02 ± 0.00	0.10 ± 0.00	0.10 ± 0.00	0.10 ± 0.00	0.05 ± 0.00	0.10 ± 0.00				
	MBC	0.05 ± 0.00	0.20 ± 0.00	0.20 ± 0.01	/	0.10 ± 0.00	0.20 ± 0.00				
Ampicillin	MIC	0.10 ± 0.00	0.15 ± 0.00	0.10 ± 0.00	/	0.20 ± 0.00	0.20 ± 0.00				
	MBC	0.15 ± 0.00	0.20 ± 0.00	0.20 ± 0.00	/	/	/				
Bifonazole	MIC						0.15 ± 0.00	0.10 ± 0.00	0.20 ± 0.00	0.15 ± 0.00	0.10 ± 0.00
	MFC						0.20 ± 0.00	0.20 ± 0.00	0.25 ± 0.00	0.20 ± 0.00	0.20 ± 0.00
Ketoconazole	MIC						0.20 ± 0.00	0.20 ± 0.00	0.20 ± 0.00	1.0 ± 0.01	0.20 ± 0.00
	MFC						0.5 ± 0.00	0.5 ± 0.00	0.5 ± 0.00	1.5 ± 0.00	0.03 ± 0.010

sitivity to the tested germs, while structure 108b showed 2-fold bacteriostatic activity toward ciprofloxacin and norfloxacin against MRSA (Fig. 31 and Table 27) (Yang et al., 2022)

Antifungal activity was evaluated against 5 fungal strains. As an antifungal reference drug, fluconazole was used. Structure 107a against *C. tropicalis*, *A. fumigatus*, *C. albicans* ATCC 90023, and *C.*

parapsilosis ATCC 22019 showed the best activity toward the reference drug, while structures 105a, 106, and 107b-c had weak activity against all fungi (Fig. 31). In addition, structures 105b, 107d-g, and 106a-b against *C. albicans* ATCC 90023 demonstrated moderate to good antifungal activity (Fig. 31 and Table 27). Structure 107a against all tested fungi except *C. albicans* showed promising

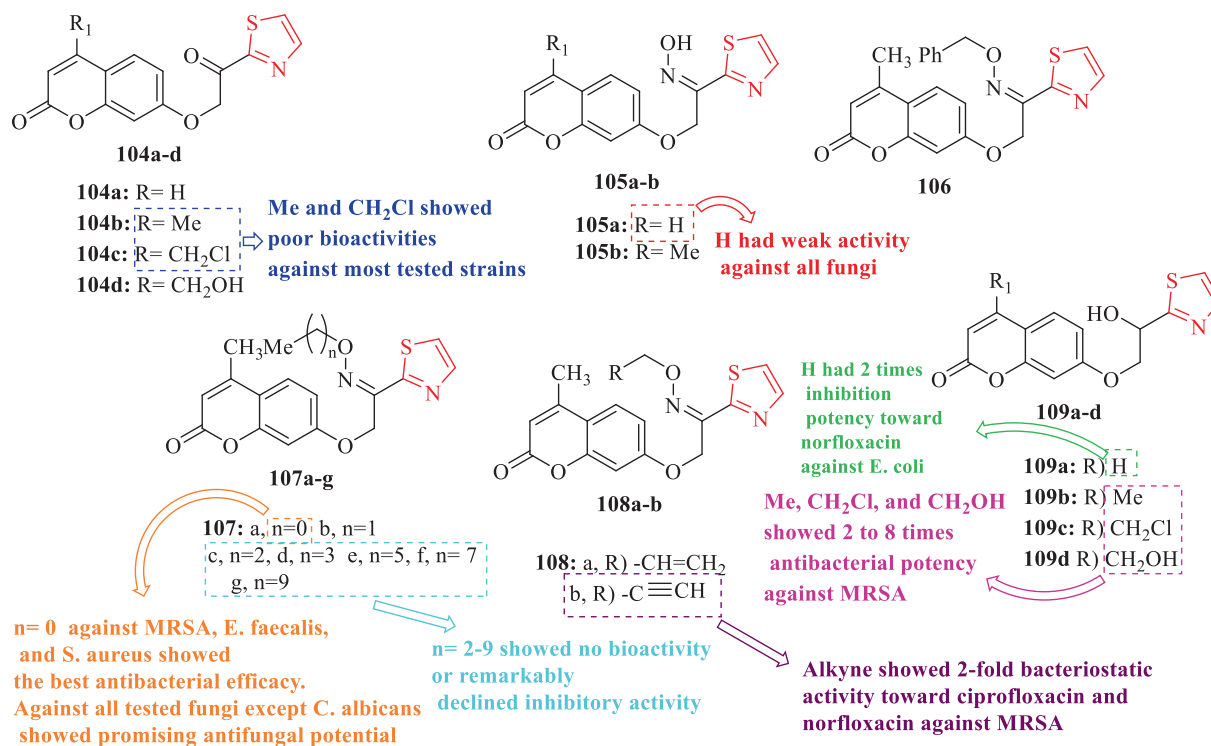


Fig. 31. Chemical structures 104a-d, 105a-b, 106, 107a-g, 108a-b, and 109a-d (Yang et al., 2022)

Table 27

MIC values ( $\mu\text{g/mL}$ ) of the structures 104a, 104b, 104d, 105b, 107a, 107b, 107d-g, 108a-b, and 109a-d (Yang et al., 2022)

Cpd. no.	MIC values ( $\mu\text{g/mL}$ )									
	MRSA	E. f.	S. a.	A. b.	E. c.	C. a.	C. t.	A. f.	C. a.	C. p
104a					8					
104b					8					
104d			8							
105b									256	
107a	1	2	16			64	4	8	64	4
107b	2	4	6	8						
107d									32	
107e									32	
107f									32	
107g									64	
108a									256	
108b									128	
109a					4					
109b	1									
109c				1						
109d	4									
Norfloxacin	8	4	8	8	8					
Ciprofloxacin	8	2	2	1	2					
Fluconazole						1	8	8	256	16

MRSA, methicillin-resistant Staphylococcus aureus (N315); E. f., Enterococcus faecalis; S. a., Staphylococcus aureus; A. b., Acinetobacter baumannii; Escherichia coli ATCC 25922; C. a., Candida albicans; C. t., Candida tropicalis; A. f., Aspergillus fumigatus; C. a. 90023, Candida albicans ATCC 90023, C. p. 22019, Candida parapsilosis ATCC 22019.

antifungal potential and was selected as a potential drug candidate (Fig. 31 and Table 27) (Yang et al., 2022)

### 3. Thiazole derivatives with anti-inflammatory activity

The response to diverse stimuli by organisms is meaning Inflammation. There are a lot of diseases like asthma, psoriasis, and arthritis that deal with inflammation. Therefore, the need for anti-inflammatory drugs is needed more than ever. Non-steroidal

anti-inflammatory drugs (NSAIDs) are one of the most important types of anti-inflammatory drugs., but their long-term use shows remarkable side effects such as nephrotoxicity and adverse cardiovascular events (Petrou et al., 2021)

Deb et al. evaluated in vivo anti-inflammatory activity of a new series of N-(benzo[d]thiazol-2-yl)-2-(substituted)acetamide derivatives and 2-substituted-N-(1,3-thiazole-2-yl)acetamide derivatives, using the carrageenan-induced rat paw edema model. According to the results, four structures (110a-d) were found to

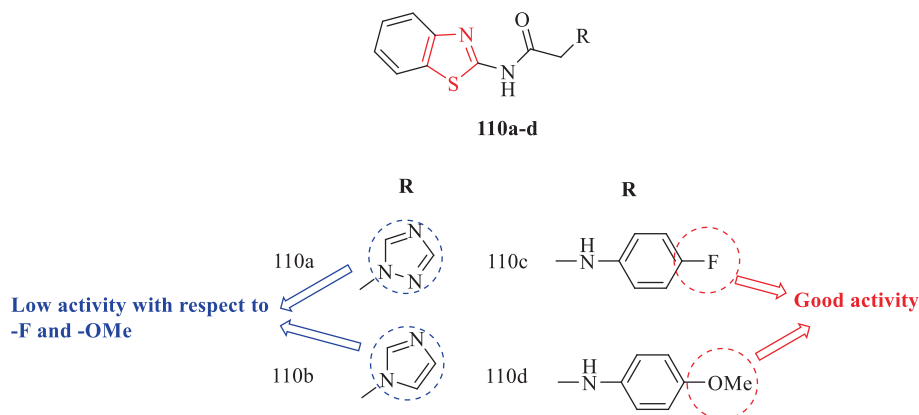


Fig. 32. Chemical structures 110a-d (Deb et al., 2014)

Table 28

Anti-inflammatory activity (volume of paw edema (ml) of the structures 110a-d (Deb et al., 2014)

Cpd. no.	2 h	4 h
<b>110a</b>	0.32 ± 0.019 (65.59)	0.29 ± 0.021 (67.77)
<b>110b</b>	0.29 ± 0.016 (68.81)	0.27 ± 0.070 (70.00)
<b>110c</b>	0.26 ± 0.019 (72.04)	0.23 ± 0.090 (74.44)
<b>110d</b>	0.27 ± 0.023 (70.97)	0.25 ± 0.013 (72.22)
<b>Indomethacin</b>	0.21 ± 0.023 (77.42)	0.19 ± 0.019 (78.89)

have significant activity with respect to other structures (about 84–93 % of the reference) (Fig. 32 and Table 28). Moreover, structures 110d and 110c with 4-methoxyaniline and 4-fluoroaniline substituent exhibited good activity toward structures 110b and

110a with imidazole and triazole scaffold (Fig. 32 and Table 28) (Deb et al., 2014)

A novel series of 1,2,3,4-tetrahydronaphthalen-6-yl-thiazoles and thiazolidinones were synthesized by Haiba and co-workers, but Twenty four structures were chosen for analgesic and anti-inflammatory activity. Anti-inflammatory activity study showed structures 114 and 118 had equipotent activity toward indomethacin as a reference drug with quicker action onset. In addition, six structures (111a, 111b, 113, 117, 119b, and 119c) showed dual analgesic and anti-inflammatory (Fig. 33). Among all derivatives, structure 113 (carrying coumarin-thiazole ring) in comparison with indomethacin exhibited remarkable dual analgesic and anti-inflammatory activity (Fig. 33 and Table 29). According to anti-inflammatory activity at 4 h, eleven structures (113, 118, 114, 111b, 119b, 111c, 112, 115, 116, 117, and 119a) showed the great-

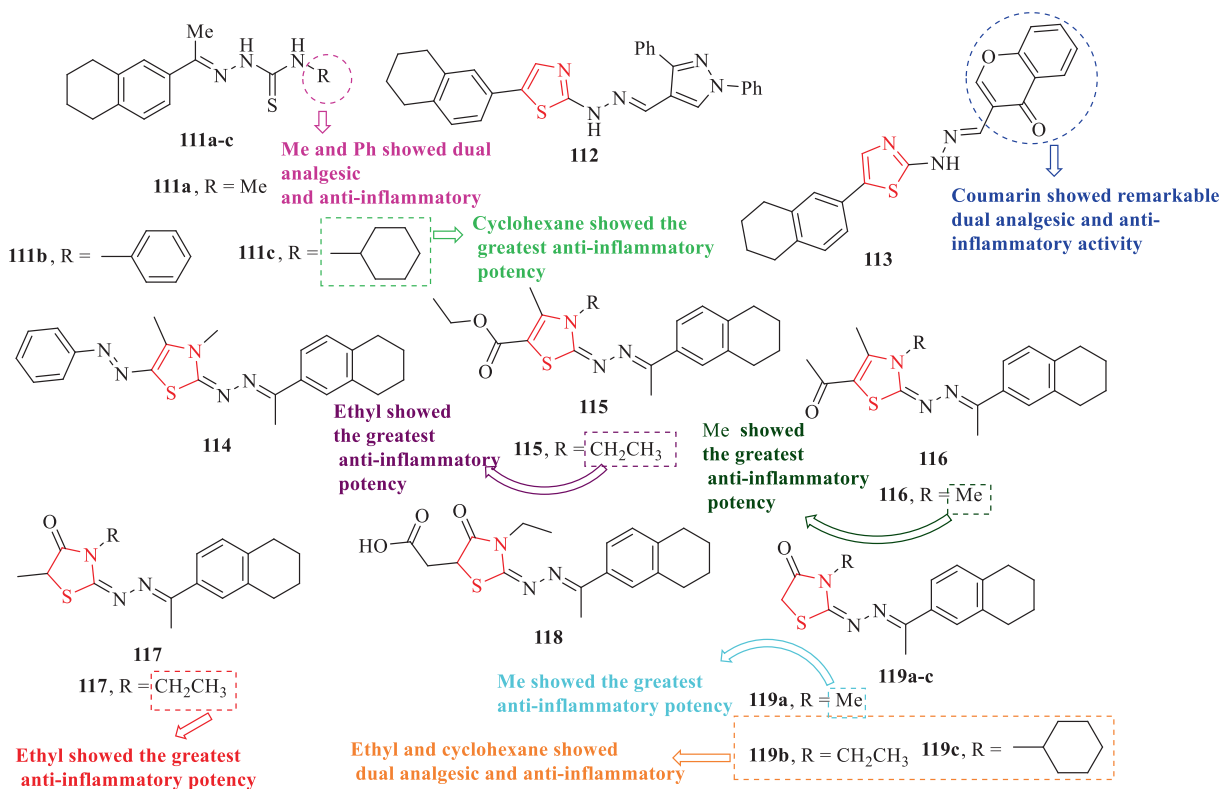


Fig. 33. The structures of 1,2,3,4-tetrahydronaphthalen-6-yl-thiazole and thiazolidinone derivatives (111a-c, 112-118, and 119a-c) (Haiba et al., 2014)

**Table 29**

Anti-inflammatory activity (paw edema volume (mL) of the structures 111b-c, 112-118, and 119a-b (Haiba et al., 2014)

Cpd. no.	1 h	4 h
<b>111b</b>		0.44 ± 0.03)
<b>111c</b>		0.41 ± 0.02
<b>112</b>	0.33 ± 0.01	0.41 ± 0.02
<b>113</b>	0.32 ± 0.00	0.36 ± 0.00
<b>114</b>	0.33 ± 0.01	0.39 ± 0.01
<b>115</b>		0.41 ± 0.01
<b>116</b>		0.41 ± 0.01
<b>117</b>		0.41 ± 0.01
<b>118</b>	0.33 ± 0.01	0.38 ± 0.01
<b>119a</b>		0.41 ± 0.01
<b>119b</b>		0.40 ± 0.02
<b>Indomethacin</b> (0.03 mmol/kg)	0.37 ± 0.01	0.38 ± 0.00

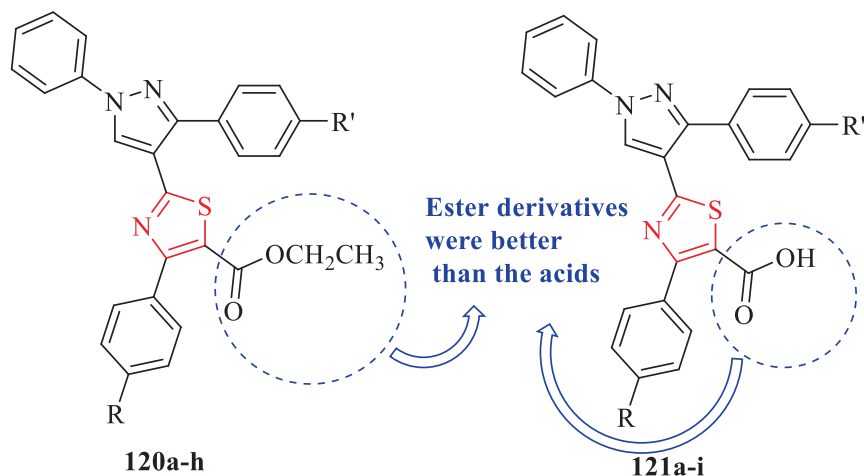
est anti-inflammatory potency (Fig. 33 and Table 29). Remarkable edema inhibition at the 1st h post-administration was observed by four structures (112, 114, 113, 118) (Fig. 33 and Table 29) (Haiba et al., 2014)

In 2015, Khloya et al. evaluated the anti-inflammatory activity of a series of pyrazolylthiazole carboxylates and corresponding acid derivatives. Evaluation of thirty-two derivatives showed structure 120 h had the best activity and structures 121b, and 121i had remarkable anti-inflammatory activity after 3 h (Fig. 34 and Table 30). After three hours of carrageenan injection, eight structures (120a, 120c, 120f, and 121a-e) exhibited remarkable activity (Fig. 34 and Table 30). Nine structures (120d-e, 120 g-h, 121b, 121e-f, 121 h, and 121 g) were found to have significant activity compared to the reference drug after 4 h of carrageenan injection (Fig. 34 and Table 30). In general, the ester derivatives were better than the acids and the results after 4 h of carrageenan injection revealed that all derivatives do not get simply metabolized in the body (Fig. 34 and Table 30) (Khloya et al., 2015)

A novel series of structures thiazole bearing pyrazole were synthesized via a one-pot reaction method by D. Kamble and co-workers. According to in vivo anti-inflammatory activity results, structures 122d and 122e had stronger protection against inflammation by Carrageenan at 180 min, while at 90 min onwards structure 122e showed outstanding protection against inflammation (Fig. 35 and Table 31). In addition, structure 122e at 30, 90, 120, and 150 min exhibited unremarkable differences with respect to diclofenac as a reference drug (Fig. 35 and Table 31). Four structures (122a, 122b, 122c, and 122f) showed considerable differences compared to the control, while its anti-inflammatory activity at 30, 60, and 90 min had non-significant differences compared to the reference drug (Fig. 35 and Table 31). Moreover, structures 122c, 122e, and 120f had strong COX-II inhibitory activity (Fig. 35) (Kamble et al., 2016)

Kumar et al. reported N-[2-(1H-indol-3-yl)ethyl]-2-amino/ami noaryl/alkyl/aryl/heteroarylthiazole-4-carboxamides. The anti-inflammatory activity of all derivatives were evaluated. Among all derivatives, structures 123b (*p*-tolyl), 123d (2-thienyl), 124a (NH<sub>2</sub>), and 124c (*p*-fluoro aminophenyl) displayed significant anti-inflammatory activity at 1 h compared to indomethacin as reference drug (Fig. 36 and Table 32). After 4 h, three structures (123b, 124a, and 124b) stayed active (Fig. 36 and Table 32). Also, five structures (123a, 123c, 123e, 124b, and 124d) showed good activity after 1 h (Fig. 36 and Table 32) (Kumar et al., 2016)

In 2017, a new series of structures containing thiazoles were synthesized by Toma et al. The mentioned derivatives were investigated for their anti-inflammatory activity. Among all derivatives, structures 126b, 126c, and 126d displayed good activity after 1 and 2 h compared to diclofenac as a reference (Fig. 37 and Table 33). Structures 125a, 125b, and 126a showed moderate activity after 1, 2, and 3 h (Fig. 37 and Table 33). In general, it seems that the 4-pyridyl substituent and the carboxylate ester group are effective in anti-inflammatory activity (Fig. 37 and Table 33) (Toma et al., 2017)



**120: R)** a= OCH<sub>3</sub>; b = F; c = Cl; d = H;  
e = OCH<sub>3</sub>; f = OCH<sub>3</sub>; g = F; h = Cl

**120: R')** a= H; b = H; c = H; d = OCH<sub>3</sub>;  
e = OCH<sub>3</sub>; f = Cl; g = Cl; h = Cl

**121: R)** a= OCH<sub>3</sub>; b = F; c = Cl; d = H;  
e = OCH<sub>3</sub>; f = F; g = Cl; h = H; i = OCH<sub>3</sub>

**121: R')** a= H; b = H; c = H; d = OCH<sub>3</sub>;  
e = OCH<sub>3</sub>; f = OCH<sub>3</sub>; g = OCH<sub>3</sub>; h = F; i = Cl

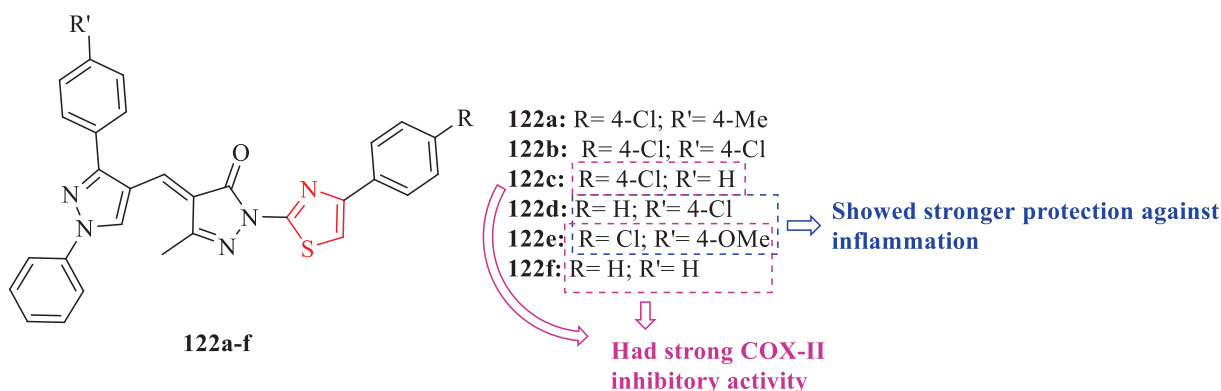
**Fig. 34.** The structures of pyrazolylthiazole carboxylates (120a-h) and corresponding acid derivatives (121a-i) (Khloya et al., 2015)

**Table 30**  
Anti-inflammatory activity of the structures 120a-h, 121a-i (Khloya et al., 2015)

Cpd. no.	Volume of edema <sup>a</sup> (mL) and % AI <sup>b</sup>			
	3 h		4 h	
	Swelling	Inhibition (%)	Swelling	Inhibition (%)
120a	0.24 ± 0.10	86.12		
120b	0.31 ± 0.06	82.08	0.42 ± 0.13	88.29
120c	0.24 ± 0.12	87.23		
120d			0.24 ± 0.08	90.95
120e			0.17 ± 0.04	90.95
120f	0.25 ± 0.08	85.54		
120 g			0.19 ± 0.04	89.89
120 h	0.12 ± 0.04	93.06	0.18 ± 0.07	90.42
121a	0.24 ± 0.05	86.12		
121b	0.18 ± 0.04	89.59	0.17 ± 0.03	90.95
121c	0.20 ± 0.06	88.43		
121d	0.21 ± 0.09	87.86		
121e	0.20 ± 0.06	88.43	0.19 ± 0.06	89.89
121f			0.18 ± 0.04	90.42
121 g			0.20 ± 0.07	89.36
121 h			0.18 ± 0.04	90.42
121i	0.16 ± 0.05	90.75		
Indomethacin	0.15 ± 0.03	91.32	0.16 ± 0.05	91.48

a Values are expressed as mean ± SEM (number of animals = 6) and analyzed by ANOVA.

b Values in parentheses (percentage anti-inflammatory activity, AI %).

**Fig. 35.** Chemical structures 122a-f (Kamble et al., 2016)**Table 31**  
Anti-inflammatory activity (Mea paw volume (ml) ± SEM) of the structures 122a-f (Kamble et al., 2016)

Cpd. no.	30 Min	60 Min	90 Min	180 Min
122a	0.4 ± 0.02	0.41 ± 0.016	0.39 ± 0.01	
122b	0.39 ± 0.021	0.37 ± 0.013	0.39 ± 0.017	
122c	0.41 ± 0.025	0.39 ± 0.036	0.38 ± 0.031	
122d				0.35 ± 0.011
122e			0.34 ± 0.011	0.32 ± 0.006
122f	0.4 ± 0.02	0.41 ± 0.016	0.39 ± 0.01	
Diclofenac	0.36 ± 0.005	0.4 ± 0.004	0.36 ± 0.007	0.29 ± 0.004

Abdelazeem and co-workers evaluated the in vivo anti-inflammatory activity of a series of diphenylthiazole derivatives. According to the stated results, structure 127 had the best activity that was comparable with indomethacin as a reference drug after 1, 3, and 5 h (Fig. 38 and Table 34). Also, structure 128 showed excellent activity compared to the reference drug after 1 h (Fig. 38 and Table 34) (Abdelazeem et al., 2017)

Wang et al. evaluated the anti-inflammatory activity of a new series of new benzo[d]thiazole-hydrazone. Anti-inflammatory activity results demonstrated ten structures (129a, 129b, 129c,

129d, 129e, 129f, 129 g, 129 h, 129i, and 129j) had greater activity (Fig. 39 and Table 35). Moreover, structures 129f and 129 h exhibited the highest docking scores (Fig. 39 and Table 35) (Wang et al., 2017)

Mohareb et al. evaluated the anti-inflammatory activity of new structures of fused thiazole derivatives derived from 2-(2-oxo-2H-chromen-3-yl)thiazol-4(5H)-one (Fig. 40 and Table 36). The evaluation of anti-inflammatory activity showed structures 133, 134b, 136, 137a and 137b compared to other derivatives at 3 graded doses had high activity (Fig. 40 and Table 36). Structures 130a-c,

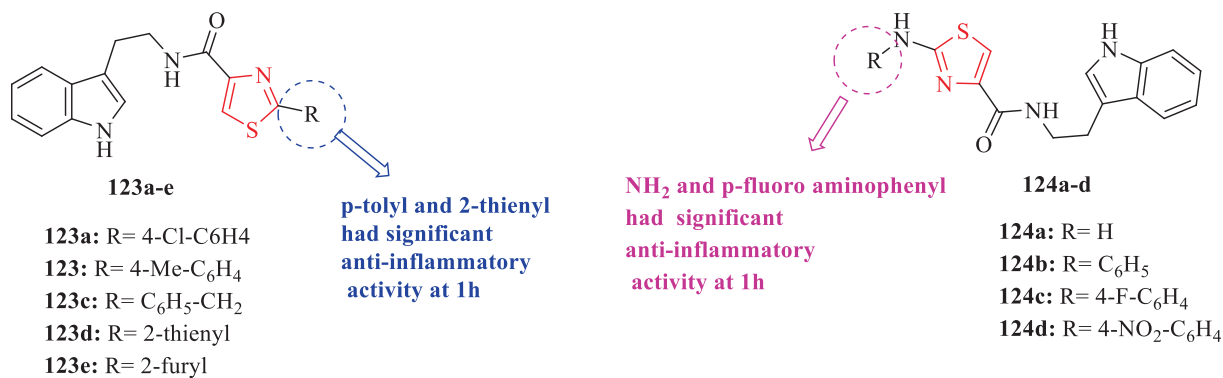


Fig. 36. Chemical structures 123a-e and 124a-d (Kumar et al., 2016)

Table 32

Anti-inflammatory activity (Mean value of oedema volume (% inhibition) of 123a-e and 124a-d (Kumar et al., 2016)

Cpd. no.	1 h	4 h
<b>123a</b>	0.23 ± 0.14 (68)	
<b>123b</b>	0.13 ± 0.06 (81)	0.38 ± 0.15 (70)
<b>123c</b>	0.17 ± 0.12 (76)	
<b>123d</b>	0.13 ± 0.06 (82)	
<b>123e</b>	0.18 ± 0.10 (75)	
<b>124a</b>	0.10 ± 0.02 (86)	0.23 ± 0.09 (82)
<b>124b</b>	0.16 ± 0.04 (77)	0.27 ± 0.01 (78)
<b>124c</b>	0.12 ± 0.01 (83)	
<b>124d</b>	0.24 ± 0.02 (66)	
<b>Indomethacin</b>	0.04 ± 0.02 (94)	0.17 ± 0.03 (86)

131a-c, 132, 133, 134a, 135, 137a, and 137b demonstrated the high antiulcer activity (Fig. 40 and Table 36) (Mohareb et al., 2017)

Abu-Hashem et al. synthesized thiazolopyrimidines, 1,3,5-oxadiazepines, 1,3,5-triazines, and benzodifuranyl derivatives. Among all derivatives containing thiazole scaffold, ten structures (138a-f, 139a-b, and 140a-b) exhibited the highest anti-inflammatory activity compared to diclofenac as a reference drug after 3 h (Fig. 41 and Table 37) (Abu-Hashem et al., 2020)

Kamat and co-workers evaluated the anti-inflammatory activity of a series of pyridine- and thiazole-based hydrazides, using denaturation of the bovine serum albumin method. Among all derivatives, three structures (141f, 141 g, and 141 h) showed good activity toward other structures (Fig. 42 and Table 38). The highest inhibition among all derivatives was achieved for structure 141 h at 5 different concentrations (Fig. 42 and Table 38). In addition,

Table 33

Anti-inflammatory activity (Oedema volume (ml) (average ± SD) %inhibition) of the structures 125a-b and 126a-d (Toma et al., 2017)

Cpd. no.	1 h	2 h	3 h
<b>125a</b>	0.60 ± 0.46 (36.71)	1.26 ± 0.61 (30.35)	1.35 ± 0.64 (34.04)
<b>125b</b>	0.75 ± 0.29 (21.68)	1.13 ± 0.38 (36.99)	1.50 ± 0.43 (26.69)
<b>126a</b>	0.67 ± 0.27 (29.89)	1.16 ± 0.70 (35.80)	1.46 ± 0.71 (28.24)
<b>126b</b>	0.40 ± 0.18 (58.39)	0.89 ± 0.28 (50.28)	
<b>126c</b>	0.38 ± 0.20 (60.84)	0.87 ± 0.40 (51.75)	
<b>126d</b>	0.48 ± 0.32 (50.00)	0.65 ± 0.31 (63.56)	
<b>Diclofenac</b>	0.74 ± 0.21 (2255)	0.98 ± 0.33 (45.48)	1.06 ± 0.36 (47.84)

structures 141a, 141b, 141c, 141d, and 141e had moderate inhibition (Fig. 42 and Table 38) (Kamat et al., 2020)

Maghraby et al. reported and evaluated the anti-inflammatory activity of a series of structures containing thiazole scaffold. According to in vivo anti-inflammatory activity results, three structures (142, 143, and 144) showed significant activity (Fig. 43 and Table 39). Further, structure 144 showed the highest inhibition toward other structures compared to the reference drug after 4 h (Fig. 43 and Table 39) (Maghraby et al., 2020)

Han et al. evaluated the anti-inflammatory activity of a series of new 2-aminobenzothiazole derivatives, using the carrageenan-induced mouse paw edema method. The results of the study showed structures 145, 146, and 147 had the best activity compared to other structures and the same structures showed as potent sEH inhibitors, but structure 147 in rat liver microsomes was unstable (Fig. 44 and Table 40) (Han et al., 2021)

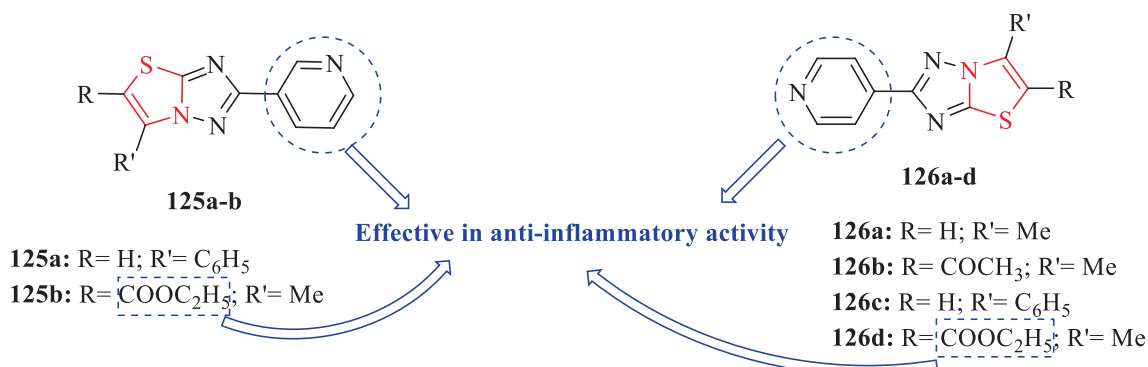


Fig. 37. Chemical structures 125a-b and 126a-d (Toma et al., 2017)

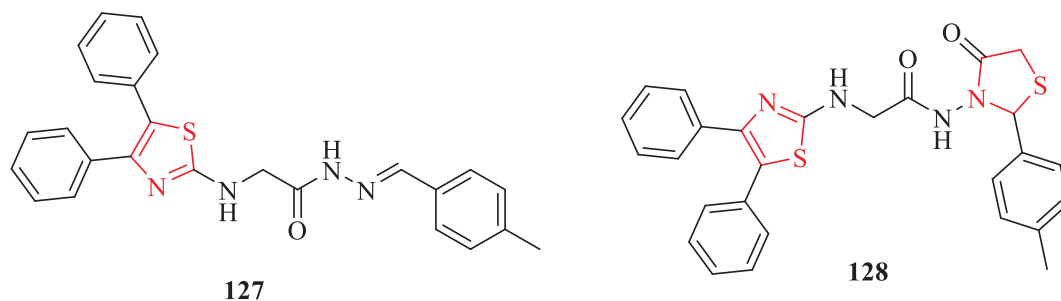


Fig. 38. Chemical structures 127–128 (Abdelazeem et al., 2017)

Table 34

Anti-inflammatory activity (Edema thickness (mm)  $\pm$  SEM (edema inhibition %)) of the structures 127 and 128 (Abdelazeem et al., 2017)

Cpd. no.	1 h	3 h	5 h
127	0.196 $\pm$ 0.012 (71)	0.258 $\pm$ 0.013 (84)	0.630 $\pm$ 0.015 (80)
128	0.117 $\pm$ 0.014 (83)		
Indomethacin	0.113 $\pm$ 0.004 (83)	0.221 $\pm$ 0.005 (86)	0.545 $\pm$ 0.003 (81)

Ankali et al. evaluated the anti-inflammatory activity of a novel series of 1,3-Thiazoles. According to the results, four structures (148a, 148b, 148c, and 148d) exhibited more potent anti-inflammatory activity with Cl, NO<sub>2</sub>, and Br substituting on the phenyl ring compared to diclofenac as reference drugs (Fig. 45 and Table 41). Moreover, structures 148e and 148f with CH<sub>3</sub> and OH substitutes showed moderate activity compared to structures 148a, 148b, and 148d after 5 h (Fig. 45 and Table 41). It seems that structures with electron-withdrawing groups such as Cl and NO<sub>2</sub> on the phenyl ring are greater anti-inflammatory activity toward structures with electron-donating groups (Ankali et al., 2021)

In 2021, a series of thiazole/oxazole substituted benzothiazole derivatives were synthesized by Kumar and Singh. All derivatives were tested against carrageenin at 3 different doses for their anti-inflammatory activity. According to the results, structure 149 with ethyl group at the 3-position of benzothiazole displayed greater activity compared to phenyl butazon as a reference drug

(Fig. 46 and Table 42). In addition, derivatives 150a-h showed moderate anti-inflammatory activity (Fig. 46 and Table 42). Among the derivatives, structure 150e with chlorine at the 4-position of the phenyl azo group exhibited remarkable anti-inflammatory activity (Fig. 46 and Table 42) (Kumar and Singh, 2021)

In 2022, Sukanya et al investigated the inhibition of novel series of thiazole derivatives against two enzymes. The investigation of anti-inflammatory activity exhibited structures 151a and 151b had significant activity compared to other structures (Fig. 47 and Table 43). The same structures had moderated activity against MMP-9 compared to positive control and had remarkable activity against MMP-2 compared to positive control (Fig. 47 and Table 43). It seems that the presence of NO<sub>2</sub> substitute at both phenyls is effective in their anti-inflammatory activity (Sukanya et al., 2022)

Saliyeva and co-workers synthesized a series of derivatives containing thiazole scaffold and evaluated in vivo anti-inflammatory activity in white rats carrageenan-induced edema paw model. Diclofenac sodium was used as a reference drug. All derivatives showed moderate anti-inflammatory activity (Fig. 48 and Table 44). Structures 152a and 152b displayed the best activity compared to the reference drug (Fig. 48 and Table 44). Moreover, structures 152c, 152d, 152e, 152f, 152 g and 152 h exhibited moderate to good activity (Fig. 48 and Table 44) (Saliyeva et al., 2021)

Yamsani and Sundararajan. investigated the anti-inflammatory activity of thirteen series of novel derivatives containing thiazole scaffold, using a carrageenan-induced paw edema method. Almost

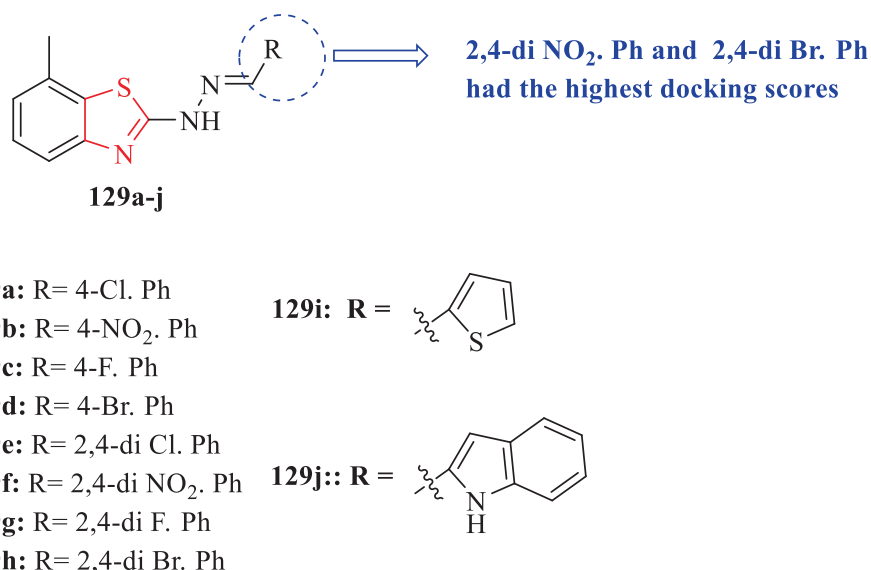


Fig. 39. Chemical structure 129a-j (Wang et al., 2017)

**Table 35**  
Anti-inflammatory activity ( $IC_{50}$   $\mu\text{g/mL}$ ) of the structures 129a-j (Wang et al., 2017)

Cpd. no.	$IC_{50}$ $\mu\text{g mL}^{-1}$
129a	28.74 $\pm$ 1.25
129b	24.07 $\pm$ 1.07
129c	32.15 $\pm$ 0.36
129d	20.07 $\pm$ 0.47
129e	18.17 $\pm$ 0.74
129f	12.74 $\pm$ 0.43
129 g	16.14 $\pm$ 0.45
129 h	10.12 $\pm$ 0.34
129i	28.74 $\pm$ 0.17
129j	30.18 $\pm$ 0.74
Indomethacin	40.04 $\pm$ 0.45

all derivatives demonstrated remarkable activity (Fig. 49). As a reference drug, diclofenac was used. Derivatives substituted at the *para*-position of phenyl ring attached at C-1 of pyrazole, namely 155e, 155f, and 155 g had excellent activity toward the reference drug (Fig. 49 and Table 45). Structure 155a with unsubstituted phenyl at C-1 of pyrazole had a nearly equipotent anti-inflammatory activity toward the reference drug (Fig. 49 and Table 45). In addition, Structures 155b, 155c, and 155d displayed moderated activity (Fig. 49 and Table 45). Also, Structures 153,

**Table 36**  
Anti-inflammatory activity a carrageenin-induced rat hind paw oedema mean value of oedema value (% protection) of the structures 133, 134b, 136, and 137a-b (Mohareb et al., 2017)

Cpd. no.	10 mg/Kg	20 mg/Kg	40 mg/Kg
133	0.09 $\pm$ 0.02 (96)	0.16 $\pm$ 0.08 (93)	0.19 $\pm$ 0.06 (92)
134b	0.39 $\pm$ 0.02 (83)	0.09 $\pm$ 0.01 (96)	0.39 $\pm$ 0.13 (83)
136	0.13 $\pm$ 0.07(94)	0.24 $\pm$ 0.04 (89)	0.07 $\pm$ 0.03 (97)
137a	0.18 $\pm$ 0.03 (92)	0.18 $\pm$ 0.09 (92)	0.09 $\pm$ 0.01 (96)
137b	0.29 $\pm$ 0.11 (87)	0.37 $\pm$ 0.07(84)	0.49 $\pm$ 0.11 (79)
Diclofenac	0.32 $\pm$ 0.09 (86)	0.31 $\pm$ 0.07 (88)	0.09 $\pm$ 0.29 (96)

154a, 154b, 155 h, 155i, and 155j showed low activity (Fig. 49 and Table 45). In general, Structure 155f showed the most potent activity, and structure 153 displayed low activity (Fig. 49 and Table 45) (Yamsani and Sundararajan, 2022)

Abdel-Aziz et al. evaluated COX-1/COX-2 inhibitory as well as anti-inflammatory activity of a series of pyrimidine/thiazole hybrids, using the carrageenin-stimulated paw edema bioanalysis. Structures 156c, 156d, 156 h, 156i, and 156j exhibited potent COX-2 inhibitors (Fig. 50 and Table 46). Also, the same structures had significant COX-2 inhibition over COX-1 inhibition. Structures 156 h, 156i, and 156j compared to celecoxib as a control showed

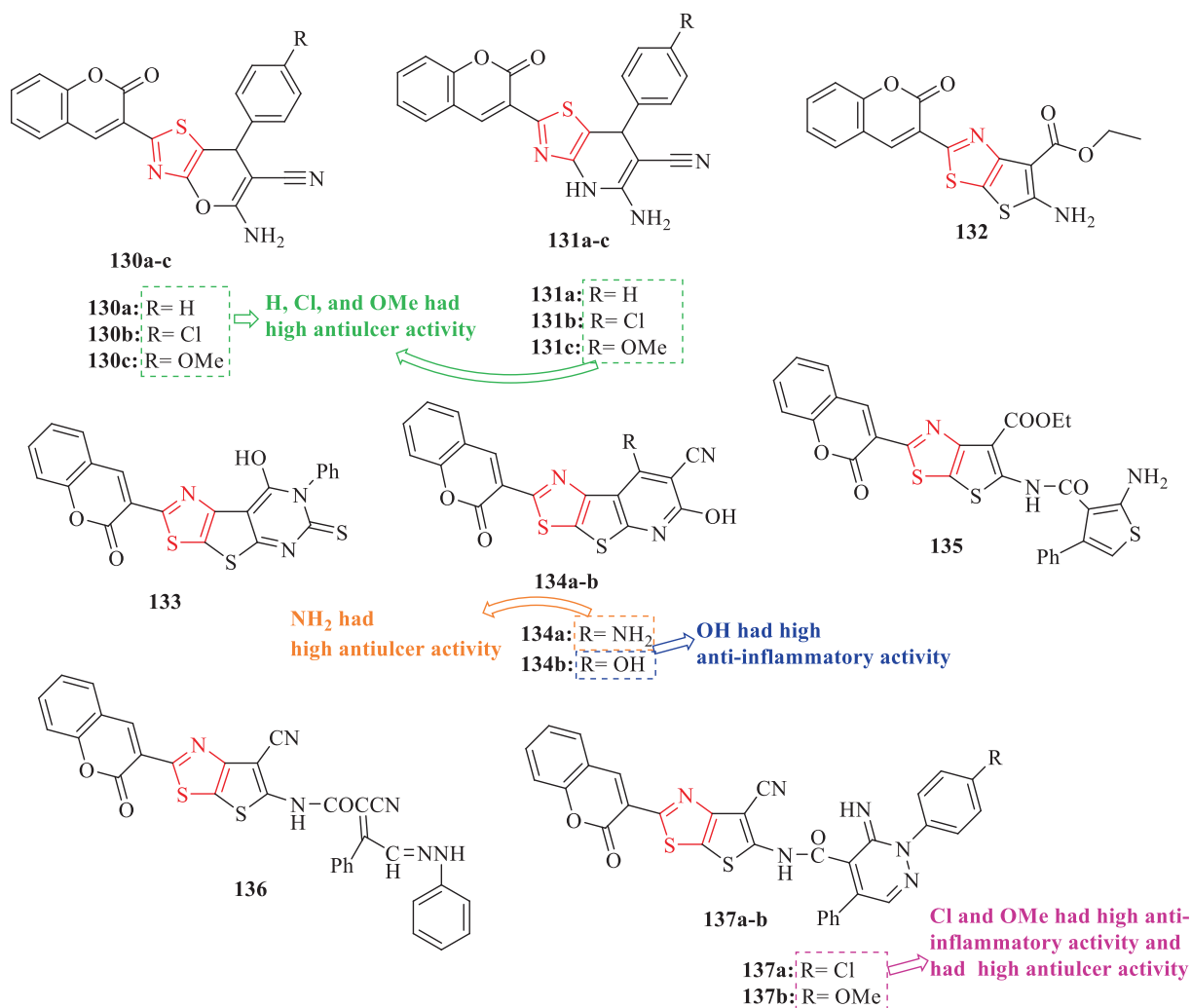


**Fig. 40.** Chemical structures 130a-c, 131a-c, 132-133, 134a-b, 135-136, and 137a-b (Mohareb et al., 2017)

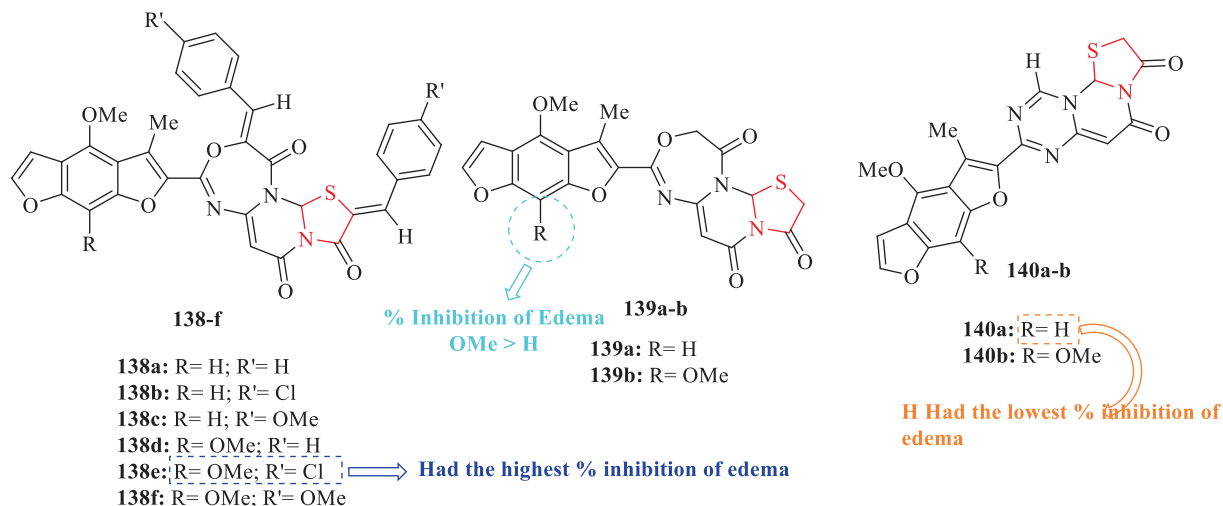


Fig. 41. Chemical structures 138a-f, 139a-b, and 140a-b (Abu-Hashem et al., 2020)

Table 37

Anti-inflammatory activity of the structures 138a-f, 139a-b, and 140a-b (Abu-Hashem et al., 2020)

Cpd. no.	% Change in Paw Height (Mean $\pm$ SEM) 3 h	Anti-Inflammatory Activity (% Inhibition of Edema) 3 h
138a	0.24 $\pm$ 0.01	59
138b	0.20 $\pm$ 0.02	63
138c	0.22 $\pm$ 0.02	61
138d	0.23 $\pm$ 0.02	60
138e	0.19 $\pm$ 0.02	64
138f	0.21 $\pm$ 0.01	62
139a	0.26 $\pm$ 0.01	57
139b	0.25 $\pm$ 0.02	58
140a	0.28 $\pm$ 0.01	55
140b	0.27 $\pm$ 0.02	56
Diclofenac	0.20 $\pm$ 0.01	63

the most strong COX-2-inhibitory activity (Fig. 50 and Table 46). Structures 156b (R = NH<sub>2</sub>) and 156a (R = Ph) showed two times less potent activity against the COX-2 isoform compared to structures 156j and 156i (Fig. 50 and Table 46). Moreover, structures 156e, 156f, and 156g remarkably dwindled COX-2-inhibitory activity and selectivity (Fig. 50 and Table 46) (Abdel-Aziz et al., 2022)

#### 4. Thiazole derivatives with anticancer activity

Cancer is an illness that is caused by cells that grow and multiply too quickly. There are many different ways to try to treat cancer, but the most common is chemotherapy. Cancer is still a serious problem, because most cancer drugs do not have low toxicity to take, and cancer cells are often very resistant to them as well (Ayati et al., 2019)

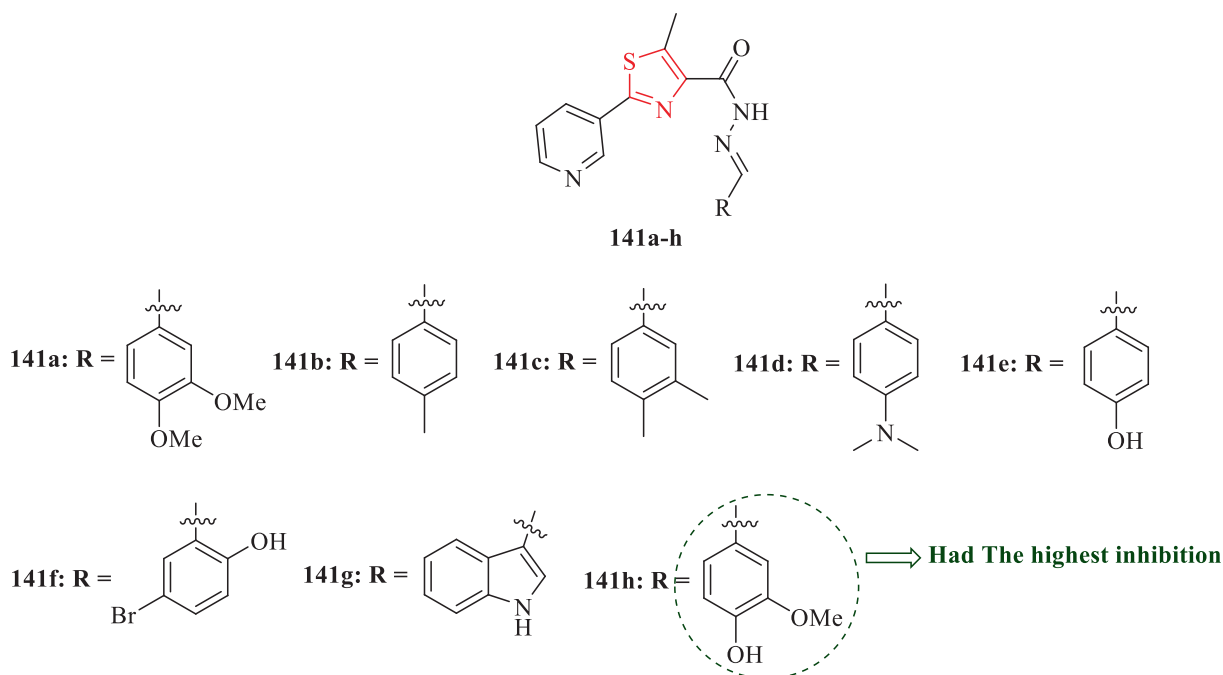
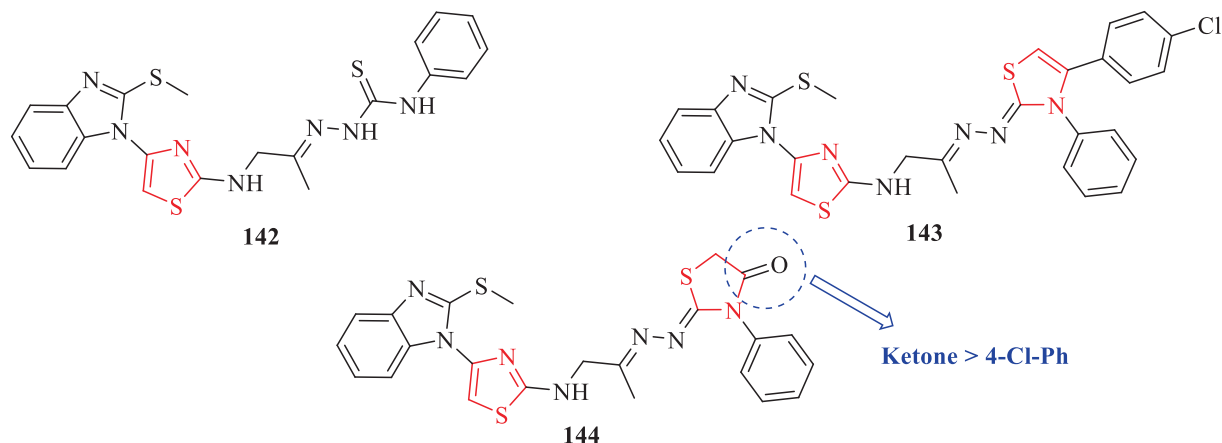


Fig. 42. Chemical structures 141a-h (Kamat et al., 2020)

**Table 38**

Anti-inflammatory activity (Inhibition of protein denaturation (%)) of the structures 141a-h (Kamat et al., 2020)

Cpd. no.	20( $\mu\text{g/mL}$ )	40( $\mu\text{g/mL}$ )	60( $\mu\text{g/mL}$ )	80( $\mu\text{g/mL}$ )	100( $\mu\text{g/mL}$ )	IC <sub>50</sub> ( $\mu\text{g/mL}$ )
<b>141a</b>	22.66 $\pm$ 1.05	30.51 $\pm$ 2.22	42.86 $\pm$ 2.43	52.54 $\pm$ 0.90	69.65 $\pm$ 1.21	76.12
<b>141b</b>	24.46 $\pm$ 1.19	35.06 $\pm$ 0.56	48.94 $\pm$ 1.53	61.43 $\pm$ 1.24	73.82 $\pm$ 1.45	61.29
<b>141c</b>	17.65 $\pm$ 1.34	27.27 $\pm$ 1.52	35.26 $\pm$ 1.42	49.58 $\pm$ 0.98	62.06 $\pm$ 1.57	80.68
<b>141d</b>	19.18 $\pm$ 0.71	27.92 $\pm$ 1.59	37.33 $\pm$ 1.43	49.89 $\pm$ 1.45	65.78 $\pm$ 1.64	80.18
<b>141e</b>	25.49 $\pm$ 0.85	31.18 $\pm$ 1.28	49.24 $\pm$ 1.60	58.12 $\pm$ 0.56	71.07 $\pm$ 0.34	62.74
<b>141f</b>	30.66 $\pm$ 1.04	40.01 $\pm$ 1.33	53.98 $\pm$ 1.78	68.39 $\pm$ 1.00	80.34 $\pm$ 0.95	55.58
<b>141 g</b>	31.42 $\pm$ 0.95	41.00 $\pm$ 1.24	56.72 $\pm$ 2.00	71.47 $\pm$ 0.90	83.46 $\pm$ 2.21	52.89
<b>141 h</b>	32.63 $\pm$ 1.07	41.00 $\pm$ 1.24	59.51 $\pm$ 2.46	78.24 $\pm$ 1.37	87.97 $\pm$ 1.37	46.29
<b>Diclofenac sodium</b>	42.98 $\pm$ 1.28	57.08 $\pm$ 1.6	75.54 $\pm$ 1.26	83.56 $\pm$ 0.96	94.60 $\pm$ 0.90	35.03

**Fig. 43.** Chemical structures of 142–144 (Maghraby et al., 2020)**Table 39**

Anti-inflammatory activity of the structures 142–144 (Maghraby et al., 2020)

Cpd. no.	Thickness of right paw (cm) (Mean $\pm$ S.E.)					
	Zero time	0.5 h	1 h	2 h	3 h	4 h
<b>142</b>	7.33 $\pm$ 0.17	5.67 $\pm$ 0.44	5.00 $\pm$ 0.01	4.67 $\pm$ 0.17	4.83 $\pm$ 0.17	5.50 $\pm$ 0.29
<b>143</b>	7.17 $\pm$ 0.17	6.33 $\pm$ 0.17	5.33 $\pm$ 0.17	5.00 $\pm$ 0.29	4.67 $\pm$ 0.17	5.67 $\pm$ 0.17
<b>144</b>	7.00 $\pm$ 0.01	5.67 $\pm$ 0.17	4.67 $\pm$ 0.17	4.17 $\pm$ 0.17	3.83 $\pm$ 0.17	4.50 $\pm$ 0.29
<b>Indomethacin</b>	7.17 $\pm$ 0.17	5.83 $\pm$ 0.17	5.00 $\pm$ 0.29	4.67 $\pm$ 0.44	4.50 $\pm$ 0.29	4.17 $\pm$ 0.17

In 2014, the anticancer activity of a series of spiro (cyclohexane1,20-thiazolopyridine) derivatives and spiro (cyclohexane-1,20-thiazolidine) derivatives were evaluated against 2 cell lines by Felfel et al. Among all derivatives, structure 157 against both cancer cell lines displayed the most potent activity with respect to LSD as a reference drug (Fig. 51). In addition, structure 158 showed the lowest activity against HepG-2 (Fig. 51) (Felfel et al., 2014)

Altıntop et al. evaluated in vitro cytotoxic effects of a series of nitro-substituted thiazolyl hydrazone derivatives on 2 cell lines, using the MTT method. Cisplatin was used as a reference drug. As a result, structure 159 showed the best activity against NIH/3T3 and MCF-7 compared to other structures, followed by structure 160 (Fig. 52) (Altıntop et al., 2014)

Nofal and co-workers evaluated the cytotoxic activity of a series of benzimidazole-thiazole derivatives against HepG2 and PC12. According to the results, structures 165 and 170 had remarkable activity against two cell lines. When derivatives were tested against HepG2 cells four structures (162, 166, 167, and 169) did not show any cytotoxic effects at two concentrations (10 and

30 mM) (Fig. 53). In PC12 cells at 0.3 mM, three structures (164, 166, and 167) did not display cytotoxicity. In HepC-2 cells, six structures (162, 161, 163, 164, 165, and 168) diminished the viability of the mentioned cells between 20 and 30% at 30 mM (Fig. 53). In addition, structure 168 against the PC12 cell showed the most activity, and structures 165 and 170 against the HepG2 cell line had the most activity (Fig. 53). Moreover, structures 165 and 170 exhibited antitumor activity against HepG2 and PC12 (Fig. 53) (Nofal et al., 2014)

Rostom and co-workers evaluated the in vitro antitumor activity of ethyl 2-amino-4-methylthiazole-5-carboxylate derivatives against sixty subpanel tumor cell lines. According to the non-small cell lung cancer subpanel, structures 171, 173, 174, 175, 177, and 178 showed a changeable rate of sensitivity toward the Hop-92 cell line, especially to structures 175 and 178 (Fig. 54). Structures 171, 174, 175, 176, and 178 were tested against the NCI-H522 cell line within the same subpanel which structures 175, 176, and 178 displayed the highest growth inhibitory (Fig. 54). In the case of the melanoma subpanel of the SK-MEL-2 cell line, structures 172 and 178 exhibited substantial growth inhi-

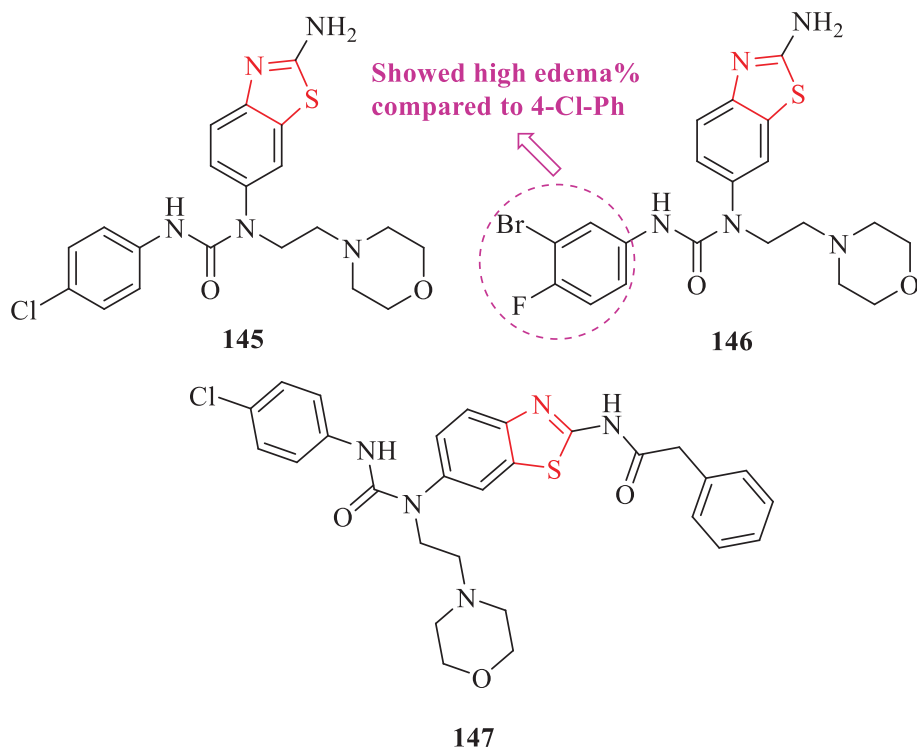


Fig. 44. Chemical structures of 143–145 (Han et al., 2021)

**Table 40**  
Anti-inflammatory activity of the structures 145–147 (Han et al., 2021)

Cpd. no.	In vivo anti-inflammatory							
	1 h		2 h		3 h		4 h	
	Paw thickness (mm)	Edema%	Paw thickness (mm)	Edema%	Paw thickness (mm)	Edema%	Paw thickness (mm)	Edema%
<b>145</b>	3.11 ± 0.17	20.99	3.06 ± 0.09	19.06	3.13 ± 0.21	21.64	3.17 ± 0.12	23.39
<b>146</b>	3.15 ± 0.04	30.86	3.16 ± 0.16	31.49	3.06 ± 0.07	27.39	3.06 ± 0.10	27.12
<b>147</b>	3.33 ± 0.16	21.56	3.22 ± 0.21	17.58	3.19 ± 0.19	16.48	3.30 ± 0.11	20.32
<b>t-AUCB</b>	3.30 ± 0.15	25.01	3.23 ± 0.15	22.61	3.29 ± 0.22	24.98	3.28 ± 0.15	24.71

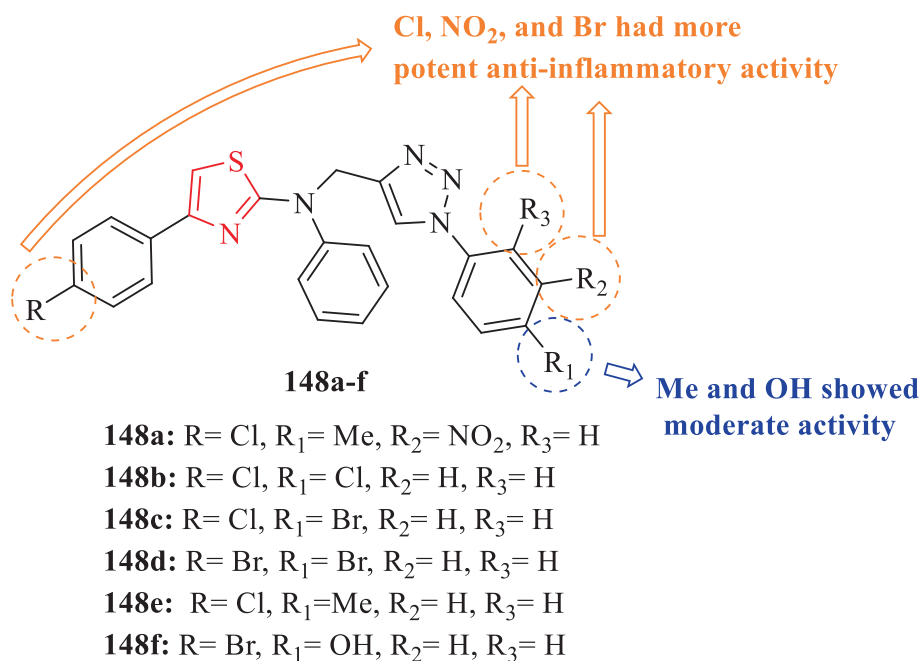
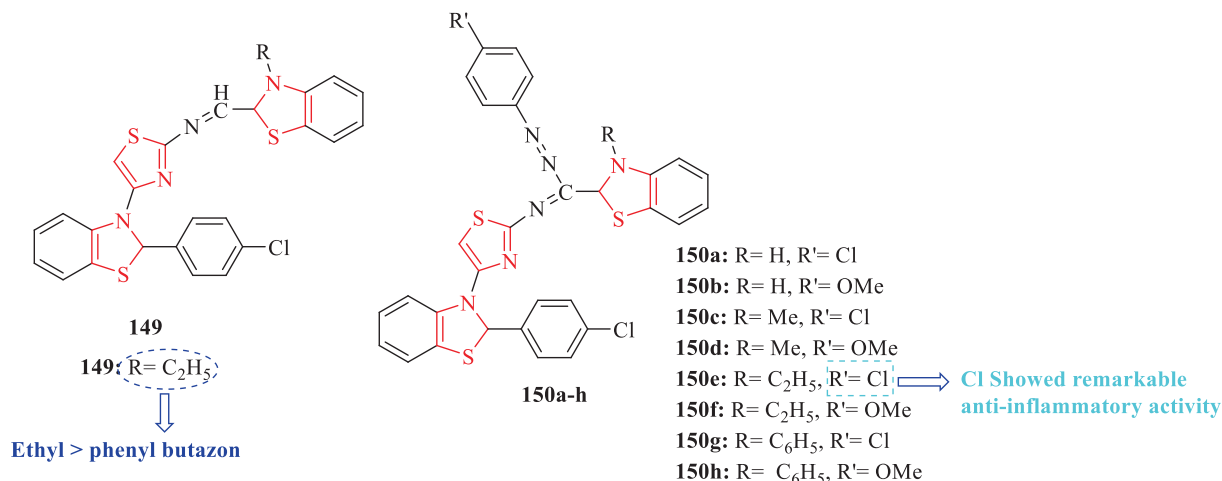


Fig. 45. The structures of 1,3-thiazole derivatives(148a-f) (Ankali et al., 2021)

**Table 41**  
Anti-inflammatory activity of the structures 148a-f (Ankali et al., 2021)

Cpd. no.	Paw edema volume in ml (% of edema inhibition)			
	0.5 h	1 h	3 h	5 h
148a	0.2433 ± 0.1041 (67.26%)	0.2100 ± 0.1305 (68.1%)	0.2167 ± 0.06333 (62.63%)	0.3767 ± 0.008819 (57.07%)
148b	0.1567 ± 0.03844 (78.91%)	0.3033 ± 0.1572 (54.04%)	0.1533 ± 0.09770 (73.56%)	0.3400 ± 0.0200 (61.21%)
148c	0.3533 ± 0.09597 (52.46%)	0.5200 ± 0.1484 (21.21%)	0.6633 ± 0.1241 (-14.36%)	0.5100 ± 0.08737 (41.82%)
148d	0.1000 ± 0.06245 (86.54%)	0.1633 ± 0.05897 (75.25%)	0.2300 ± 0.07211 (60.03%)	0.3633 ± 0.008819 (58.55%)
148e	0.2433 ± 0.09207 (67.26%)	0.1000 ± 0.06245 (84.84%)	0.1167 ± 0.01856 (96.8%)	0.4933 ± 0.2478 (43.72%)
148f	0.067 ± 0.02963 (91.03%)	0.1233 ± 0.03756 (81.31%)	0.1800 ± 0.05033 (91.32%)	0.6367 ± 0.1419 (27.37%)
Diclofenac	0.100 ± 0.06009 (86.54%)	0.123 ± 0.1418 (81.31%)	0.4967 ± 0.07860 (79.20%)	0.4533 ± 0.04702 (48.29%)

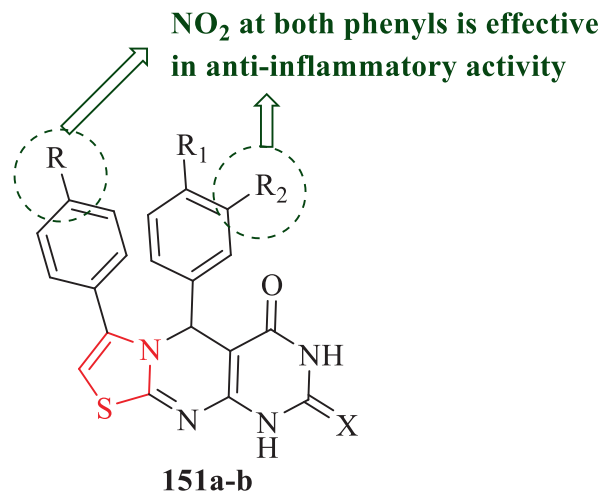


**Fig. 46.** Chemical structures 149 and 150a-h (Kumar and Singh, 2021)

**Table 42**  
Anti-inflammatory activity of the structure 149 and 150e (Kumar and Singh, 2021)

Cpd. no.	Dose (mg/kg p.o.)	Anti-inflammation Activity % of inhibition
149	25	38.5
	50	55.4
	100	69.6
150e	25	34.7
	50	34.7
	100	34.7
Phenyl butazone	25	22.2
	50	35.8
	100	66.5

bitory (Fig. 54). Structures 172 and 174 against the IGROV1 cell line of ovarian cancer showed high growth inhibitory (Fig. 54). Moreover, two structures (171 and 172) against the colon cancer subpanel of the HCC-2998 cell line displayed significant growth inhibitory activity (Fig. 54). Most of the CNS, breast, and prostate cell lines were resistant to the selected derivatives. All structures were effective on inhibit the growth of the renal UO-31 cell line, but their percentages of growth inhibitory were low (Fig. 54). In general, structure 174 against most of the subpanel tumor cell lines had a broad spectrum of anticancer activity, especially against the non-small cell lung cancer Hop-92, melanoma SK-MEL-2, and ovarian cancer IGROV1 cell lines, and structure 172 exhibited substantial growth inhibitory potentials against melanoma SK-MEL-2, colon cancer HCC-2998 and ovarian cancer IGROV1 (Fig. 54) (Rostom et al., 2014)



151a: R = OMe, R<sub>1</sub> = H, R<sub>2</sub> = NO<sub>2</sub>, X = O  
151b: R = NO<sub>2</sub>, R<sub>1</sub> = Cl, R<sub>2</sub> = NO<sub>2</sub>, X = S

**Fig. 47.** Chemical structures 151a-b (Sukanya et al., 2022)

Ali et al. evaluated the anticancer activity of eleven structures out of imidazo[2,1-b]thiazole derivatives against the sixty cell lines. According to the results, structures 181b and 182b against all cell line panels showed the lowest mean percentage growth.

**Table 43**  
Anti-inflammatory activity of the structures 151a-b (Sukanya et al., 2022)

Cpd. no.	Anti-inflammatory activity against MMP-2 (% Inhibition)	Anti-inflammatory activity against MMP-9 (% Inhibition)
151a	90 ± 0.41	45 ± 0.38
151b	85 ± 0.34	35 ± 0.54
Tetra-cycline hydrochloride	99 ± 0.51	95 ± 0.35

Structures 179a and 180–182(a) against CNS SNB-75 and Renal UO-31 cancer cell lines had high growth percentages (Fig. 55). Structure 181a against Non-Small Cell Lung HOP-92 had significant potency (Fig. 55). Furthermore, structures 179b and 180–182(b) against Renal A498, Leukemia MOLT-4, and SR cancer cell lines showed substantial potency (Fig. 55). Structure 182a with rapamycin (NSC S226080) had great correlation levels (Fig. 55). Moreover, structures 179a, 180a, 181a, 181b, 181c, and 182b with rapamycin demonstrated remarkable correlations (Fig. 55). Structure 181c with merbarone had a significant correlation (Fig. 55) (Ali et al., 2014)

Koppireddi et al. evaluated the anti-proliferative activity of twelve novel derivatives containing thiazole scaffold against 4 human cancer cell lines with respect to doxorubicin as a reference drug. Structures 183b, 183c, 183d, 183e, and 183f had moderate antiproliferative activity against A549 and showed substantial activity against HeLa (Fig. 56 and Table 47). Structure 183d against all cell lines showed the best activity at a concentration range of 6.5 ± 0.56–17.4 ± 1.34 μM. Also, it caused considerable cytotoxicity in HeLa cells. Thereby, structure 183d caused caspase-8 and caspase-3 activation which guided to cell death of apoptotic (Fig. 56 and Table 47). According to FACS results, Structure 183d arrests cells in G0/G1 phase (Fig. 56 and Table 47). Generally, structures 183a and 183d against HeLa, A549, and THP1 displayed remarkable antiproliferative activity (Fig. 56 and Table 47) (Koppireddi et al., 2014)

Gali and co-workers evaluated the anticancer activity of a series of coumarinylimidazo[2,1-b]thiazoles against 4 cancer cell lines with respect to doxorubicin as a reference drug. According to the in vitro cytotoxic activity results, all derivatives against all the tested cell lines were active. Structure 184c against HeLa,

**Table 44**  
Anti-inflammatory activity of the structures 152a-h (Saliyeva et al., 2021)

Cpd. no.	Rat hind limb volume increase, 4 h, %	Inflammation inhibition, %
152a	76.5 ± 6.3	40.3
152b	78.5 ± 6.0	38.8
152c	86.5 ± 7.1	33.4
152d	90.5 ± 8.9	33.9
152e	86.7 ± 6.4	31.6
152f	83.8 ± 5.9	33.9
152 g	85.5 ± 6.2	33.3
152 h	89.4 ± 7.0	30.3
Diclofenac sodium	64.8 ± 4.5	48.2

MCF-7, and HepG2 displayed broad spectrum activity (Fig. 57). Structure 187 showed remarkable activity against HeLa and MCF-7 (Fig. 57). In addition, structures 184a, 184b, and 185 exhibited significant activity against HeLa (Fig. 57). Whereas structure 186 showed prominent activity against NCI-H460 (Gali et al., 2014)

In 2015, evaluated the anticancer activity of a series of derivatives containing thiazole scaffold against 2 cancer cell lines with respect to doxorubicin as a reference drug by Gomha and co-workers. According to the results, structures 189 and 190 against HEPG2-1 and HCT-116 showed significant activity (Fig. 58). Structures 188, 192, 193, and 194 against HCT-116 exhibited moderate activity (Fig. 58). In addition, structures 191 and 193 displayed moderate activity against HEPG2-1 (Gomha et al., 2015)

Prabhu et al. reported and evaluated in vitro anticancer activity of a novel 8 derivatives containing thiazole scaffold against human cervical cancer cell line (HeLa) with respect to cisplatin as a reference drug. Structure 195b displayed better activity (Fig. 59 and Table 48). In general, structure 195b showed higher anticancer activity than structures 195e, 195 g, and 195 h (Fig. 59 and Table 48). Moreover, Structures 195d, 195c, 195f, and 195a exhibited less anticancer activity (Fig. 59 and Table 48) (Prabhu et al., 2015)

Tantak et al. investigated the anticancer activity of novel 16 derivatives containing thiazole scaffold against 6 cancer cell lines with respect to doxorubicin as a reference drug. Structure 196a was selective and potent against HEK293T and HeLa cells in the

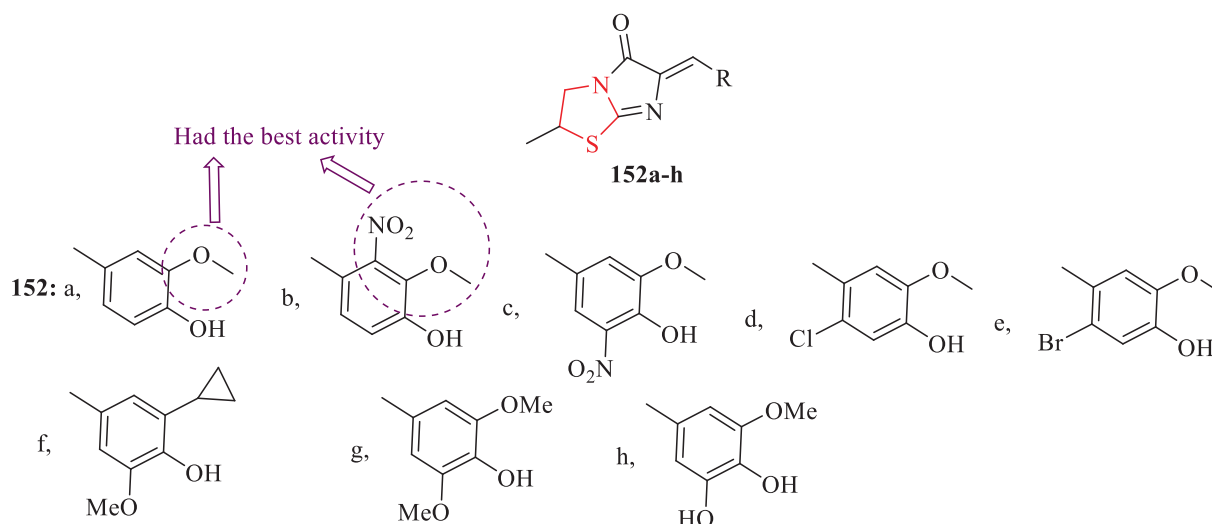


**Fig. 48.** Chemical structures 152a-h (Saliyeva et al., 2021)

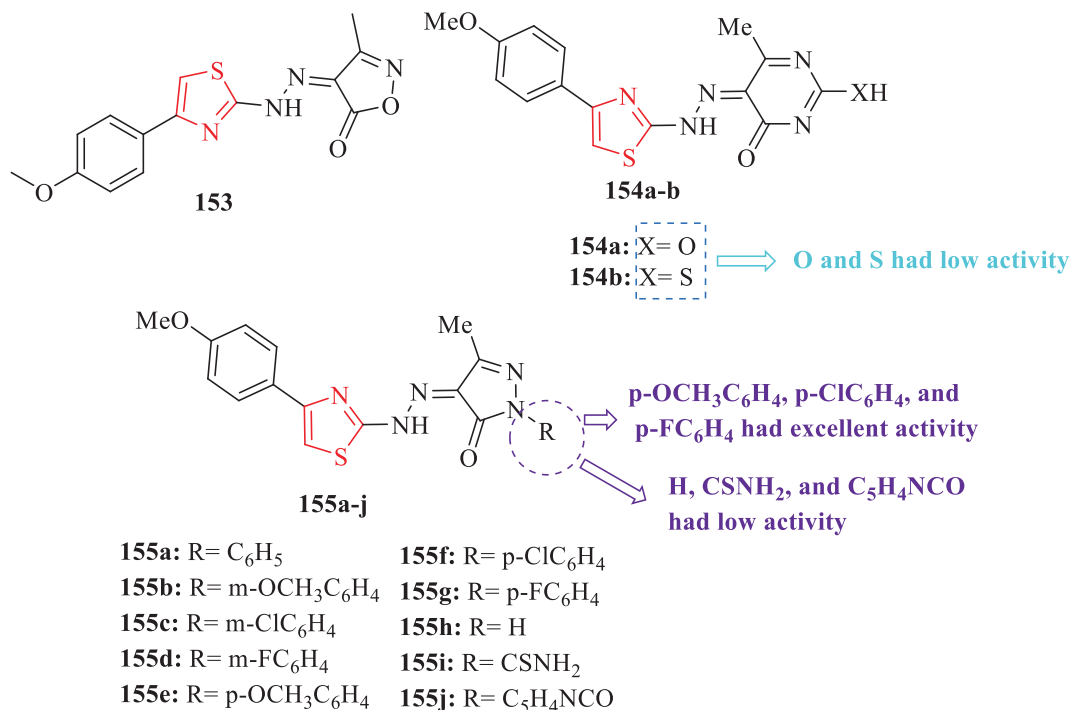


Fig. 49. Chemical structures 153, 154a-b, and 155a-j (Yamsani and Sundararajan, 2022)

Table 45  
Anti-inflammatory activity of the structures 153 and 155a-g (Yamsani and Sundararajan, 2022)

Cpd. no.	Dose (mg/kg)	% Protection			
		30 min	1 h	2 h	3 h
<b>153</b>	10	9 ± 0.41	14 ± 1.85	16 ± 0.59	10 ± 0.20
	20	11 ± 0.99	15 ± 0.42	18 ± 1.14	12 ± 0.6710
<b>155a</b>	10	36 ± 0.87	39 ± 0.95	49 ± 1.64	34 ± 0.40
	20	44 ± 0.58	57 ± 0.14	73 ± 1.23	40 ± 0.76
<b>155b</b>	10	25 ± 0.70	28 ± 1.52	33 ± 0.99	25 ± 0.15
	20	30 ± 2.16	39 ± 0.90	50 ± 0.67	28 ± 0.40
<b>155c</b>	10	29 ± 0.34	30 ± 0.79	35 ± 1.25	26 ± 0.98
	20	33 ± 1.12	43 ± 0.30	55 ± 0.56	31 ± 1.31
<b>155d</b>	10	27 ± 0.78	30 ± 1.63	34 ± 0.41	25 ± 1.14
	20	31 ± 0.95	40 ± 0.81	54 ± 0.43	31 ± 0.87
<b>155e</b>	10	38 ± 1.70	43 ± 0.45	50 ± 0.37	36 ± 0.59
	20	46 ± 0.22	58 ± 0.16	75 ± 1.49	43 ± 0.42
<b>155f</b>	10	40 ± 0.71	46 ± 0.54	53 ± 0.16	38 ± 1.98
	20	49 ± 0.49	60 ± 1.73	76 ± 0.35	45 ± 0.52
<b>155g</b>	10	38 ± 1.15	44 ± 0.60	52 ± 0.89	38 ± 1.16
	20	48 ± 0.37	59 ± 1.94	75 ± 0.72	45 ± 0.45
<b>Tetra- cycline hydrochloride</b>	10	37 ± 1.58	40 ± 0.95	49 ± 0.87	35 ± 1.84
	20	45 ± 0.95	57 ± 1.60	74 ± 0.52	42 ± 0.46

presence of FBS (Fig. 60 and Table 49). Structure 196b had an insignificant effect on HeLa cells but inhibited selectively HEK293T cells compared to structure 196a (Fig. 60 and Table 49). Structure 196c against HeLa had the most potent activity (Fig. 60 and Table 49) (Tantak et al., 2015)

Metwally et al. evaluated the anticancer activity of 5 derivatives containing thiazole scaffold against 2 cancer cell lines. All the derivatives displayed remarkable anticancer activity. Structure 198a against the breast cancer cell line showed the most potent activity, while structure 197 against the liver cancer cell line had the most potent activity (Fig. 61 and Table 50). Also, structure

197 had the best reactivity toward HEPG-2 and MCF-7 (Fig. 61 and Table 50). Structure 198b against HEPG-2 and MCF-7 displayed less potent anticancer activity (Fig. 61 and Table 50) (Metwally et al., 2015)

In 2016, evaluated anticancer activity of 10 derivatives containing thiazole scaffold against 5 human cancer cell lines which were synthesized by Vaddula et al via the one-pot method. Some derivatives displayed moderate activity. Structure 199d against BT-474 and MDA-MB-157 showed significant activity (Fig. 62 and Table 51). Structure 199a against BT-474 exhibited remarkable activity (Fig. 62 and Table 51). Structure 199b against MCF-7 dis-

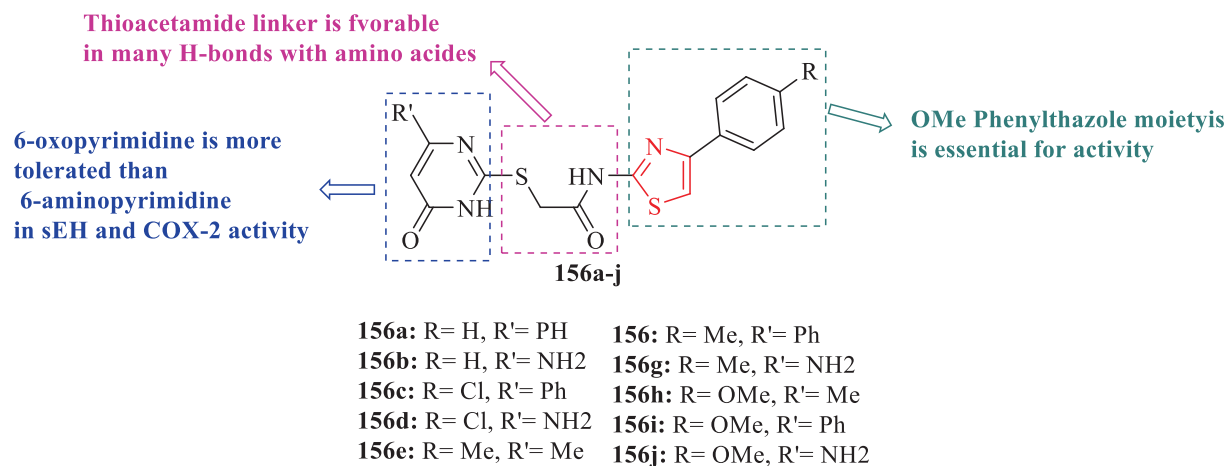


Fig. 50. Chemical structures 156a-j (Abdel-Aziz et al., 2022)

Table 46  
IC<sub>50</sub> values of the structures 156a-j (Abdel-Aziz et al., 2022)

Cpd. no.	COX-1, IC <sub>50</sub> (μM)	COX-2, IC <sub>50</sub> (μM)
156a		2.03
156b		2.33
156c	14.33	1.89
156d	14.53	1.74
156e		3.50
156f		2.93
156 g	13.88	3.09
156 h	14.98	1.43
156i	15.89	1.02
156j	15.31	1.13
Celecoxib	7.32	0.88

played the best activity and structure 199c against BT-474 had the best activity (Fig. 62 and Table 51) (Vaddula et al., 2016)

Karaman and Ulusoy Güzel demirci. evaluated the anticancer activity of a series of derivatives containing thiazole scaffold against sixty different cell panels with respect to cisplatin as a reference drug. Among all derivatives, structures 200a and 200b were

chosen for the investigation of their anticancer activity (Fig. 63 and Table 52). Preliminary results showed structure 200b (R-2,5-dimethoxyphenyl) against prostate cancer cell line DU-145 and two leukemia cell lines K-562 and SR had the lowest growth percentages (Fig. 63 and Table 52). Further, structure 200a exhibited a better antiproliferative activity profile toward structure 200b. Structure 200a against some of the cancer cell lines displayed substantial inhibitory activity, especially against the prostate cancer cell line DU-145 and leukemia cell lines HL-60 (TB) and SR (Fig. 63 and Table 52). Structure 200a against all cancer cell lines except OVCAR-5, NCIH23, and SF-539 exhibited high potent activity (Fig. 63 and Table 52) (Karaman and Ulusoy Güzel demirci, 2016)

Anticancer activity of ten derivatives containing thiazole scaffold was evaluated against 4 cancer cell lines with respect to mitoxantrone as a reference drug by Turan-Zitouni et al. In general, all derivatives against C6 rat glioma cells displayed substantial cytotoxic and anticancer activity. In the case of the A549 cell line, structure 201d showed the most potent cytotoxic agent compared to the reference drug, which was followed by 201c, 201a, and 201b, while structure 201f had the lowest activity (Fig. 64 and Table 53). In the case of the C6 cell line, structure 201d showed the most effective anticancer agent compared to the reference drug, which

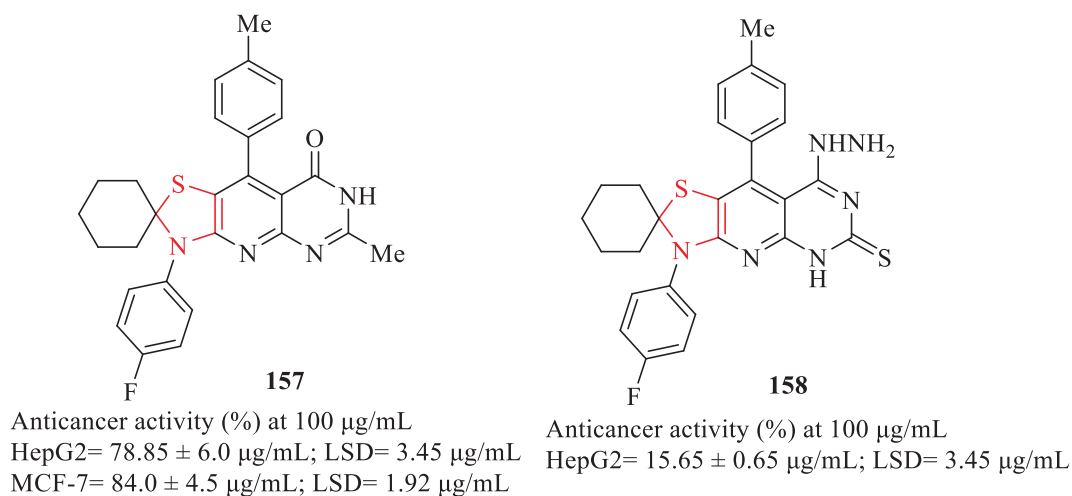


Fig. 51. Anticancer activity of the structures 157 and 158 (Flefel et al., 2014)

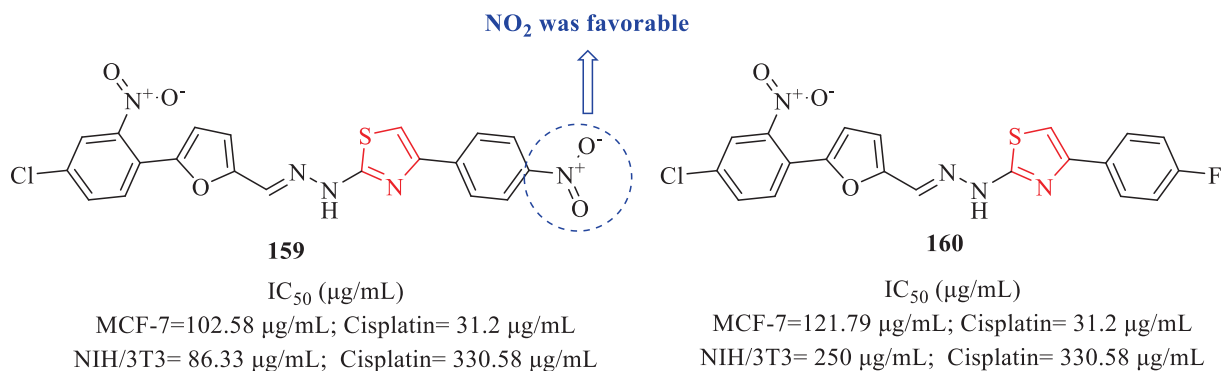


Fig. 52. Anticancer activity of the structures 159 and 160 (Altıntop et al., 2014)

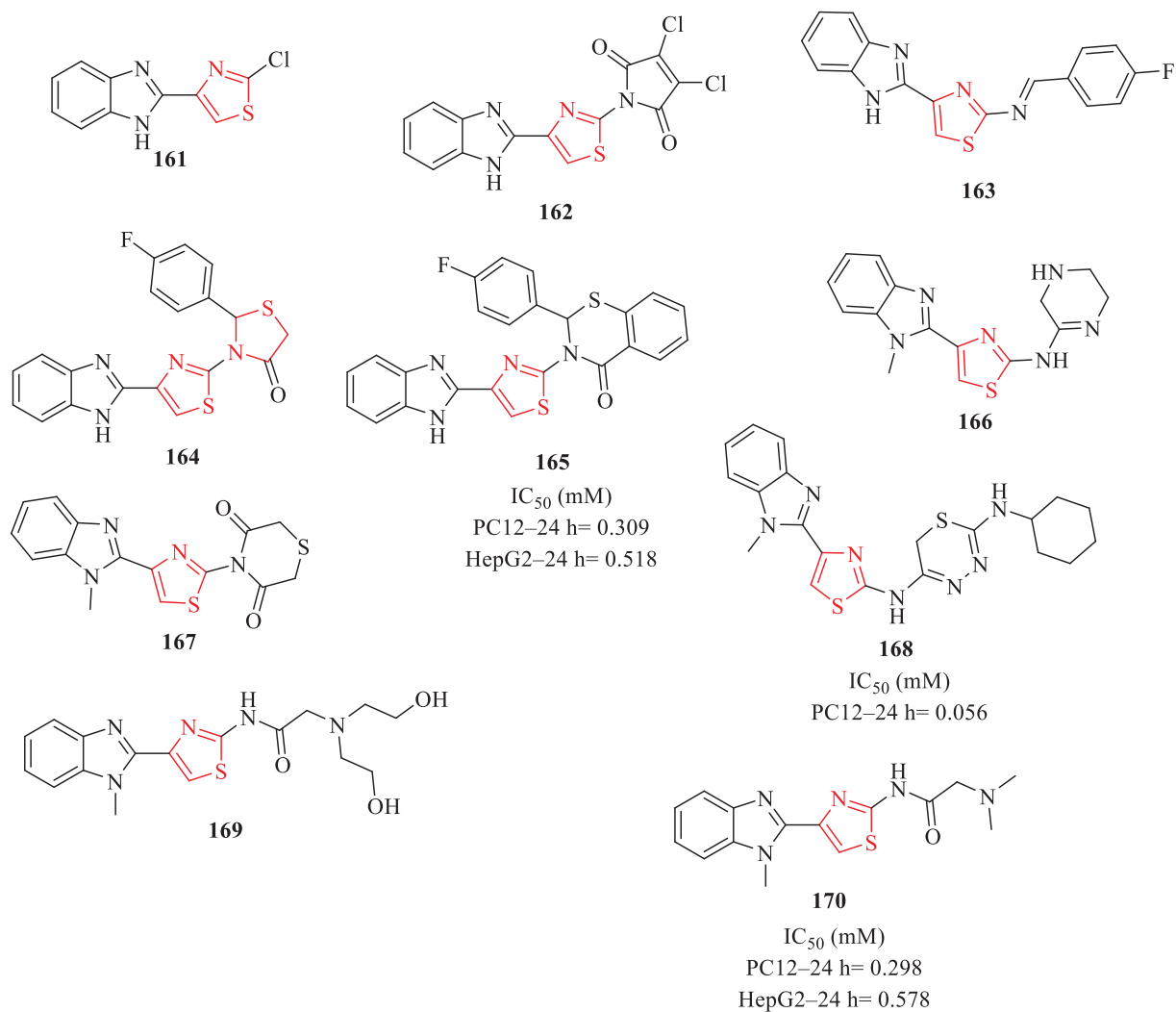


Fig. 53. Chemical structures 161–170 and anticancer activity of the structures 165, 168, and 170 (Nofal et al., 2014)

was followed by structures 201b, 201c, and 201a, while structure 201e had the lowest activity (Fig. 64 and Table 53). In the case of the 5RP7 cell line, structure 201a showed the most potent cytotoxic activity compared to the reference drug, which was followed by 201g and 201c, while structure 201d had the lowest anticancer

activity (Fig. 64 and Table 53). Among all derivatives, structure 201d showed significant antiproliferative effects on C6 and A549 cell lines. Also, structure 201d against C6 and A549 cell lines displayed anticancer activity (Fig. 64 and Table 53) (Turan-Zitouni et al., 2016)

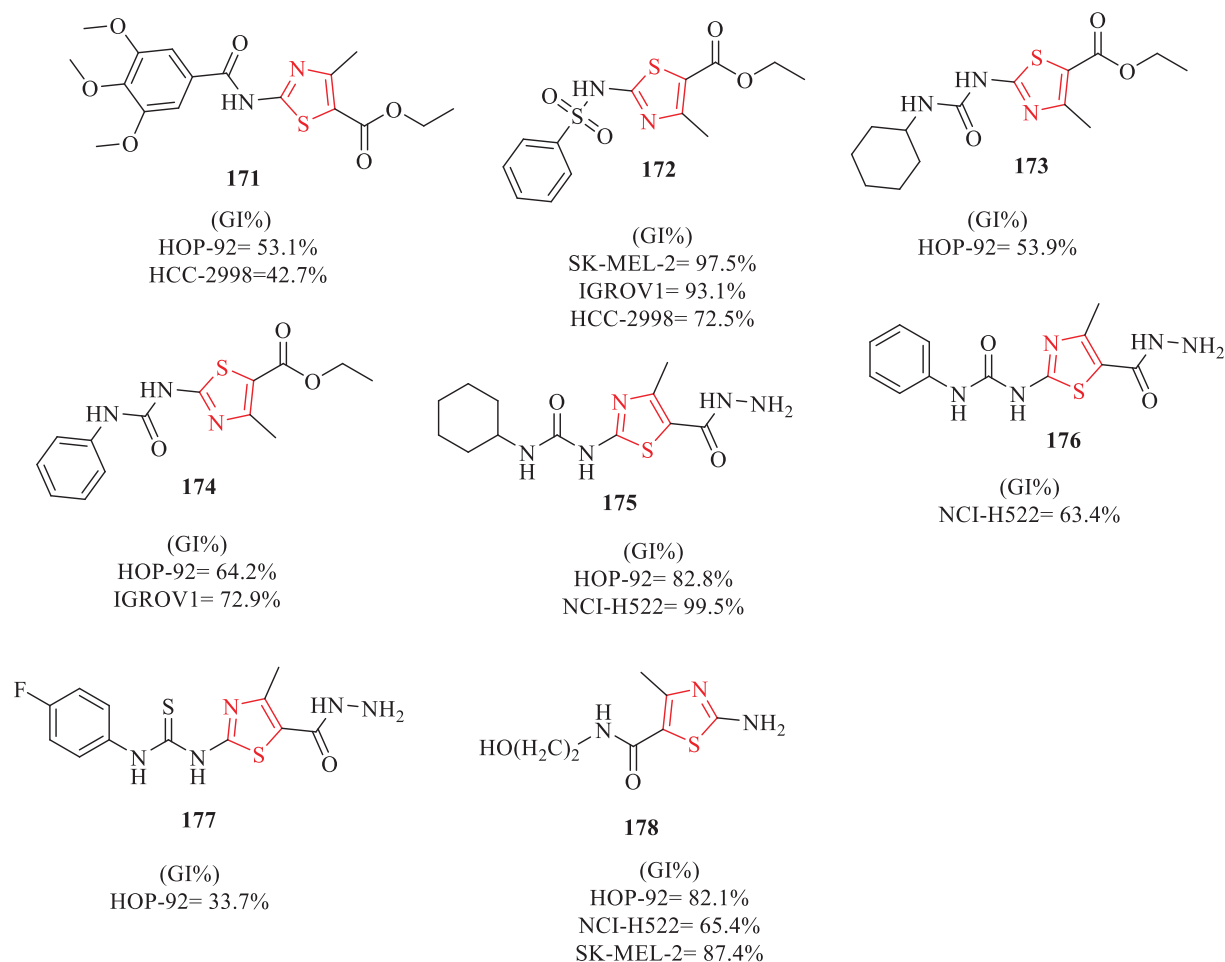


Fig. 54. Chemical structures 171–178 and anticancer activity of the structures 171–178 (GI%= In vitro growth inhibitory percentage) (Rostom et al., 2014)

The anticancer activity of eleven derivatives containing thiazole scaffold was evaluated against 3 cancer cell lines with respect to foretinib as a reference drug by Lei and co-workers. Structures 202a, 202b, 202e, 202f, and 202 h against the HT-29 cell line exhibited remarkable activity (Fig. 65 and Table 54). Structures 202a, 202b, 202d, 202e, 202f, and 202 h displayed substantial anticancer activity against the MKN-45 cells (Fig. 65 and Table 54). Structures 202a, 202b, 202c, 202d, 202e, 202f, 202 g, 202 h, 202i, 202j, and 202 k against H460 showed superior activity (Fig. 65 and Table 54). It seems that the presence of R<sub>2</sub> groups is a substantial effect on anticancer activity, but R<sub>1</sub> groups had little effect on cytotoxicity (Lei et al., 2016)

The anticancer activity of eleven derivatives containing thiazole scaffold was evaluated against 3 cancer cell lines with respect to 5-Fluorouracil as a reference drug by Cai et al. At a concentration of 5 µg/mL, some of the derivatives such as structures 203a and 203b displayed good anticancer activity against A-549 compared to the reference drug (Fig. 66 and Table 55). Among all the mentioned derivatives, just structure 204 showed moderate activity against HCT-8, while other derivatives showed low inhibitor or no inhibition impacts against HCT-8 and Bel7402 (Fig. 66 and Table 55) (Cai et al., 2016)

The anticancer activity of 21 derivatives containing thiazole scaffold was evaluated against 3 cancer cell lines with respect to cisplatin as a reference drug by Shi et al. Most of the mentioned

derivatives against some or all of MCF-7, SGC-7901 and H446 exhibited moderate antiproliferative activity (Fig. 67 and Table 56). Structure 205e against MCF-7 showed the most potent anticancer activity. Structures 205d, 205e, and 205f which contained a chloro group displayed better antitumor activity against MCF-7, SGC-7901, and H446 compared to structures 205a, 205b, and 205c which contained a methyl group (Fig. 67 and Table 56). In addition, structure 205e against H446 showed the best antitumor activity. Structures 206a, 206b, 206c, 206d, 206e, 206f, and 206 g were only active toward SGC-7901 cells (Fig. 67 and Table 56). Structures 207a, 207b, 207c, 207d, 207e, 207f, and 207 g against all cancer cell lines exhibited more potent activity compared to structures unsubstituted at the same position (Fig. 67 and Table 56) (Shi et al., 2016)

In 2017, the anticancer activity of ten derivatives containing thiazole scaffold was evaluated by Gomha et al against 1 cancer cell line with respect to cisplatin as a reference drug. Among the ten structures tested, structures 208 and 209 showed the best anticancer activity compared to the reference drug (Fig. 68). It seems that the number of thiazole rings is effective on the activity, especially the fewer number of them which causes a dramatic drop in activity. Moreover, the cytotoxic activity depends on the 1,3,4-Thiadiazole ring (Gomha et al., 2017)

Pansare and co-workers evaluated the anticancer activity of 14 derivatives containing thiazole scaffold against 2 human breast cancer cells line with respect to adriamycin as a reference drug.

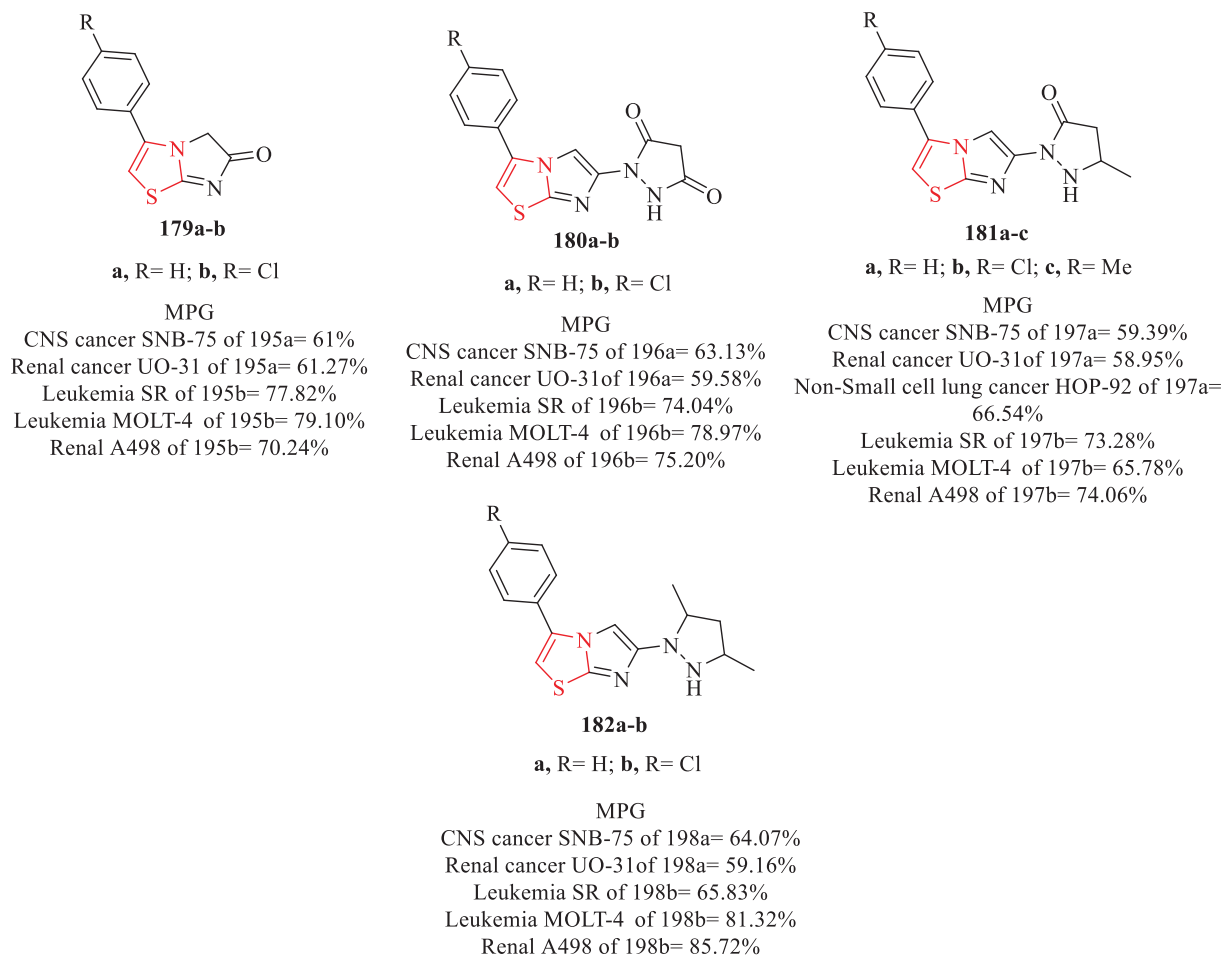


Fig. 55. Chemical structures 179a-b, 180a-b, 181a-c, and 182a-b and their anticancer activity (MPG = Mean percentage growth) (Ali et al., 2014)

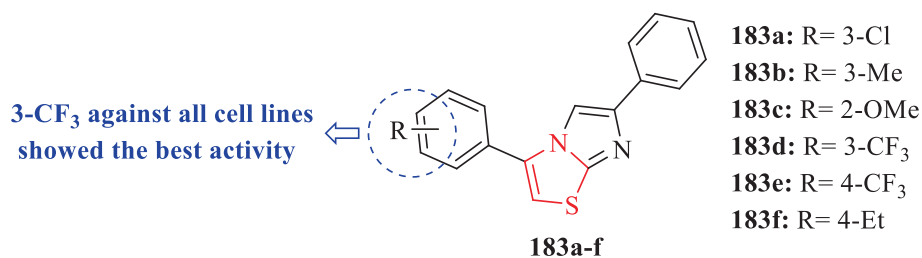


Fig. 56. Chemical structures 183a-f (Koppireddi et al., 2014)

Table 47  
MIC<sub>50</sub> values (μM) of the structures 183a-f (Koppireddi et al., 2014)

Cpd. no.	MIC <sub>50</sub> values (μM)			
	HeLa <sup>1</sup>	A549 <sup>2</sup>	MDAMB-231 <sup>3</sup>	THP1 <sup>4</sup>
183a	14.0 ± 3.06	15.0 ± 3.1		21.7 ± 1.2
183b	13.7 ± 1.02	40.2 ± 4.03		
183c	9.5 ± 1.09	39.0 ± 2.9		
183d	6.5 ± 0.56	8.9 ± 0.46	10.9 ± 0.44	17.4 ± 1.34
183e	8.5 ± 2.43	21.5 ± 0.2		
183f	11.3 ± 1.53	44.8 ± 1.21		
Doxorubicin	6.0 ± 0.7	3.4 ± 0.9	2.0 ± 1.0	3.5 ± 0.8

<sup>1</sup> HeLa = Human cervical carcinoma cells; <sup>2</sup>A549 = Human lung adenocarcinoma epithelial cells;

<sup>3</sup> MDA-MB-231 = Human breast carcinoma cells; <sup>4</sup>THP1 = Human leukemic cells.

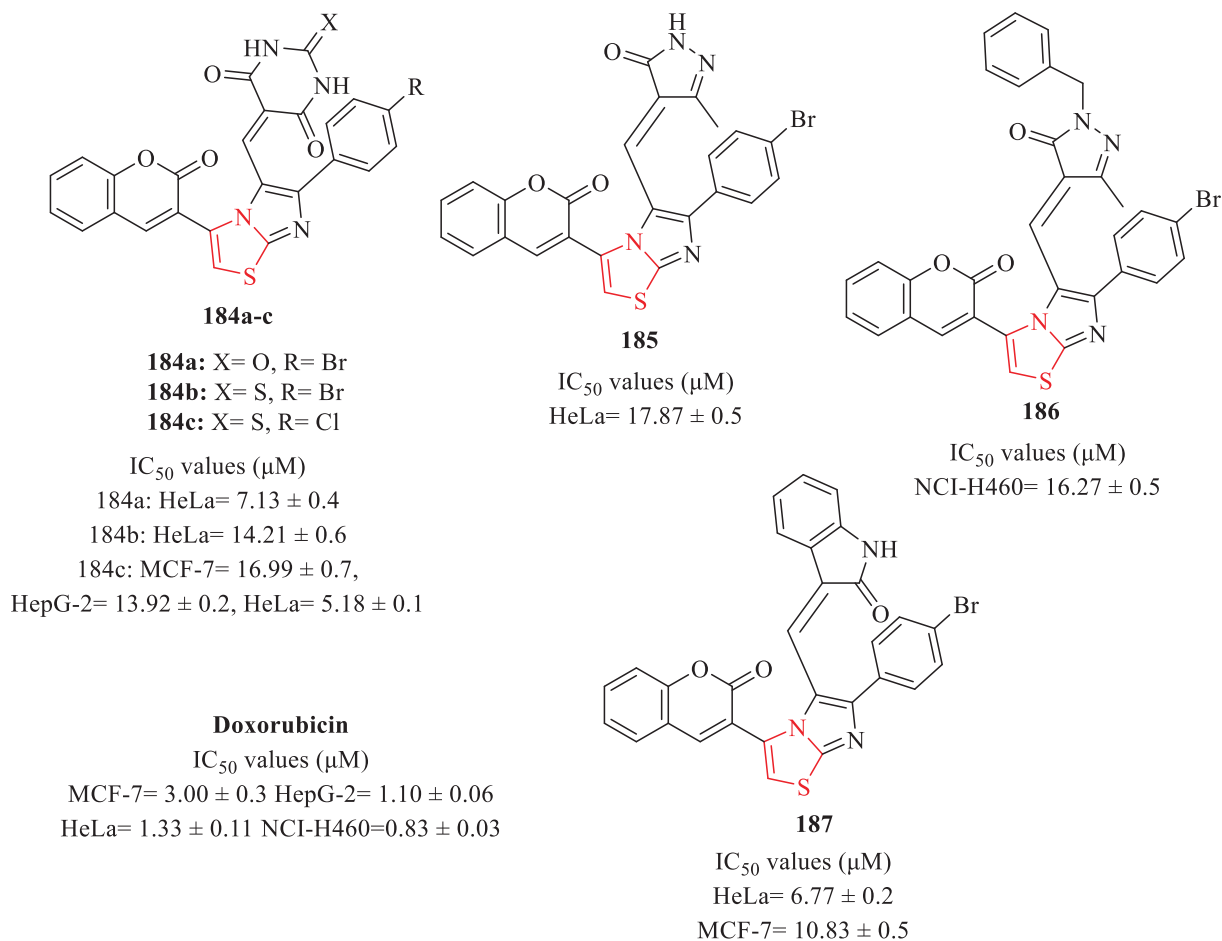


Fig. 57. Chemical structures 184a-c, and 185–187 and their IC<sub>50</sub> values (Gali et al., 2014)

Among fourteen derivatives, structures 210a, 210b, 210c, 210d, and 210e against both cancer cell lines displayed the most activity (Fig. 69 and Table 57) (Pansare et al., 2017)

The anticancer activity of a series of derivatives containing thiazole scaffold against 4 cancer cell lines with respect to doxorubicin as a reference drug was evaluated by Mirza et al. Structures 211a, 211b, 211c, 211d, 211e, 211f, 212a, and 212b against MCF-7 were active (Fig. 70 and Table 58). Structures 211a, 211b, 211c, 211d, 211e, and 211f against HCT-116 exhibited anticancer activity (Fig. 70 and Table 58). In addition, structures 211a, 211b, 211c, 211d, 211e, 211f, and 212a against HeLa showed activity. It seems that structure 211a is the best structure compared to other structures (Fig. 70 and Table 58) (Mirza et al., 2017)

In 2018, the in vitro anticancer activity of a series of pyrimidine-thiazole derivatives was evaluated against 3 cancer cell lines with respect to erlotinib as a reference drug by Sharma et al. Among all derivatives that were tested, structured 213b, 213c, 213d, 213e, and 213f against all cancer cell lines at 1 μM concentration showed high activity (Fig. 71 and Table 59). Structure 213d against MCF-7 and A375 had remarkable cytotoxic activity. In addition, structures 213b, 213c, 213d, 213e, and 213f exhibited good activity against A375 (Fig. 71 and Table 59). Two structures (213a and 213f) against MCF-7 and HeLa showed good activity. The activity of structures 213b, 213c, 213d, 213e, and 213f against MCF-7 and A375 had comparable to the reference drug (Fig. 71 and Table 59).

Also, the same structures had comparable inhibitory activities against MCF-7. Structure 213f against MCF-7, A375, and HeLa showed better anticancer activity (Sharma et al., 2018)

Sateesh Kumar and Umadevi evaluated in vitro anticancer activity of a series of derivatives containing thiazole scaffold against 4 cancer cells with respect to combretastatin-A4 as a reference drug. Most of the structures against the 4 cell lines showed moderate to excellent activity. Structure 214g against HT-29, A549, and MCF-7 showed strong activity, and structure 214d against MCF-7 displayed high activity (Fig. 72 and Table 60). In contrast, structure 214f containing nitro group at the same position showed low activity. Moreover, structures 214b and 214c against MCF-7 and A549 had more potent activity. Also, structure 214e against MCF-7 and A549 exhibited comparable activity (Fig. 72 and Table 60). Generally, structures 214a, 214b, 214c, 214d, 214f, and 214g demonstrated more potent activity (Sateesh Kumar and Umadevi, 2018)

The antitumor activity of a series of pyrazolines containing thiazole scaffold was investigated against 1 cancer cell line with respect to cisplatin as a reference drug by Edrees et al. According to the cytotoxic activity results, structure 215b had the highest cytotoxic activity. After that, structures 215a and 216 displayed excellent activity (Fig. 73 and Table 61) (Edrees et al., 2018)

In 2019, the anticancer activity of a series of derivatives containing thiazole scaffold against 4 cancer cell lines with respect

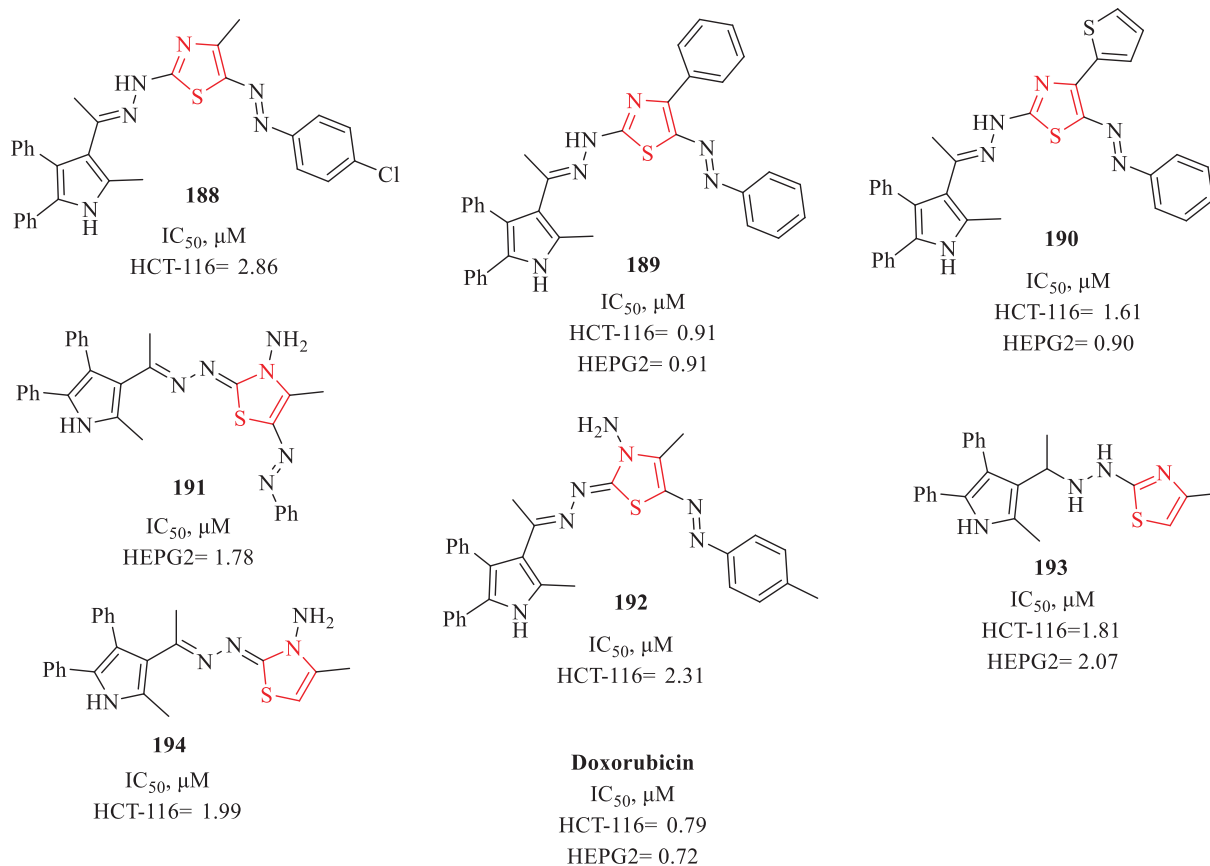


Fig. 58. Chemical structures 188–194 and their IC<sub>50</sub> values (Gomha et al., 2015)

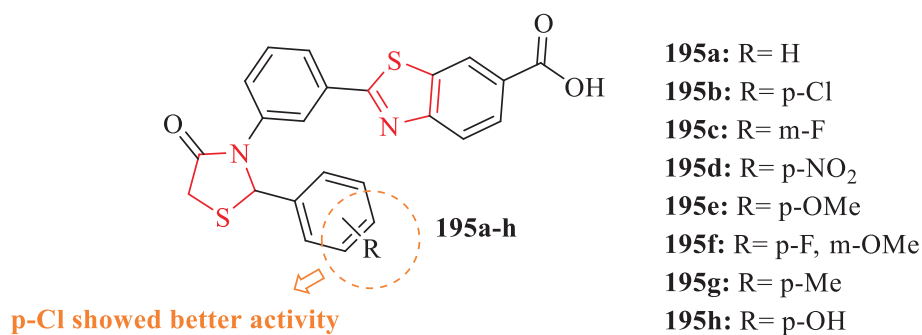


Fig. 59. The structures of thiazolidinone substituted benzothiazole-6-carboxylic derivatives (195a-h) (Prabhu et al., 2015)

Table 48

Anticancer activity of the structures 195b, 195e, 195 g, and 195 h (Prabhu et al., 2015)

Cpd. no.	Compound concentration (μmol/L)				IC <sub>50</sub>
	% Growth inhibition				
	5	12.5	25	40	
<b>195b</b>	50.7	66.8	80.8	96.8	9.768
<b>195e</b>	45.7	70.8	77.9	88.45	14.566
<b>195 g</b>	40.8	66.7	70.7	82.68	16.456
<b>195 h</b>	44.9	68.8	76.9	81.7	17.768
<b>Cisplatin</b>	64.2	75.3	86.9	99.7	28.427

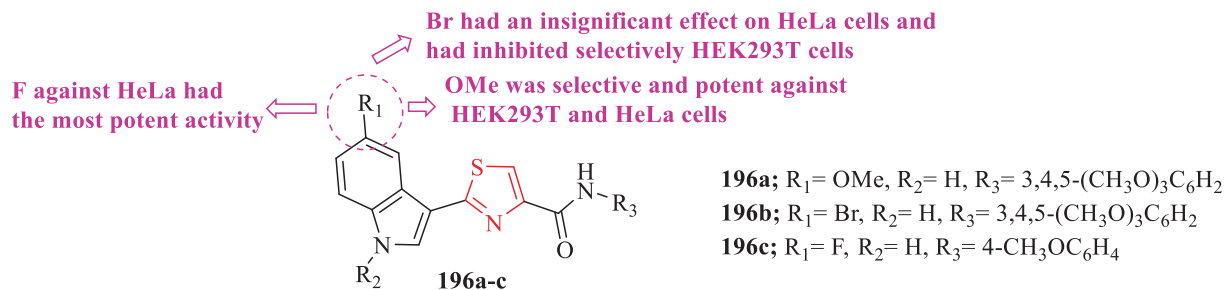


Fig. 60. Chemical structures 196a-c (Tantak et al., 2015)

Table 49

IC<sub>50</sub> values of the structures 196a-c (Tantak et al., 2015)

Cpd. no.	In vitro cytotoxicity (without FBS) IC <sub>50</sub> (μM)		In vitro cytotoxicity (with FBS) IC <sub>50</sub> (μM)	
	HEK 293 T	HeLa	HEK 293 T	HeLa
<b>196a</b>	8.60 ± 0.91	29.64 ± 1.44	8.74 ± 1.26	9.98 ± 0.01
<b>196b</b>	>100	55.79 ± 4.73	>100	93.03 ± 3.96
<b>196c</b>	12.10 ± 0.61	3.41 ± 0.07		33.48 ± 0.98
<b>Doxorubicin</b>	0.84 ± 0.05	0.45 ± 0.06	0.75 ± 0.03	0.43 ± 0.10

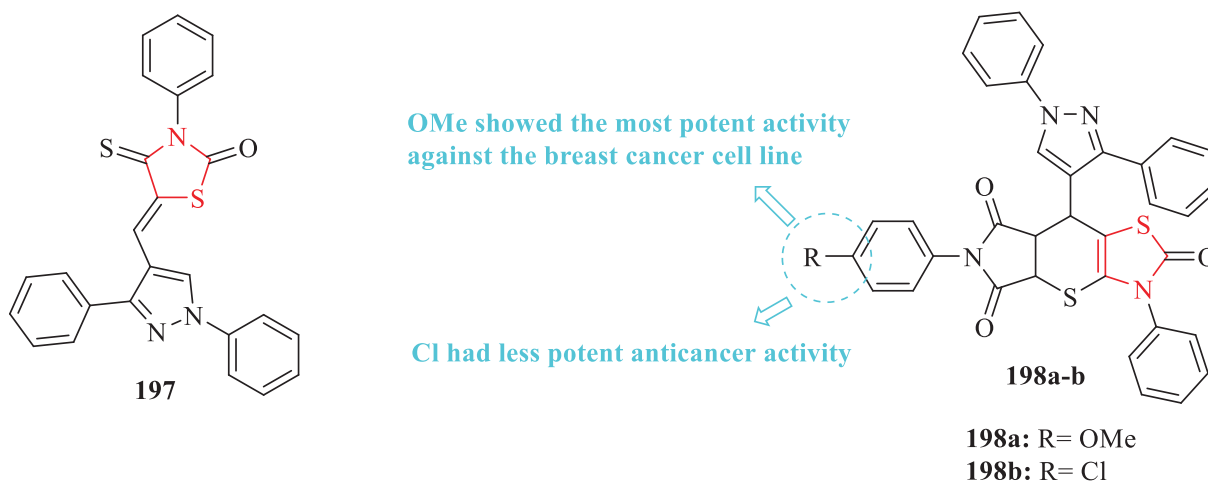


Fig. 61. Chemical structures 197 and 198a-b (Metwally et al., 2015)

Table 50

IC<sub>50</sub> values of the structures 197 and 198a-b (Metwally et al., 2015)

Cpd. no.	IC <sub>50</sub> in μg/mL	
	MCF-7	HEPG-2
<b>197</b>	19.3	10.6
<b>198a</b>	12.3	21.4
<b>198b</b>	35.9	21.3

to etoposide as a reference drug was evaluated by Yakantham and co-workers. Four structures (217a, 217d, 217e, and 217f) displayed higher anticancer activity against A549, MCF-7, A2780, and Colo-205 (Fig. 74 and Table 62). Notably, structure 217f had the most

promising activity. Structure 217b (with 3,5-dimethoxyphenyl substituent) showed low activity against A549, A2780, and Colo-205 compared to structure 217a with 3,4,5-trimethoxyphenyl substituent (Fig. 74 and Table 62). Moving along the same line, structure 217c (4-methoxy) showed lower activity than structure 217b against A549, MCF-7, A2780, and Colo-205 (Fig. 74 and Table 62). Finally, structure 217f against four cell lines displayed the highest activity (Fig. 74 and Table 62) (Yakantham et al., 2019)

Sayed et al. evaluated the anticancer activity of a series of derivatives against 1 cancer cell line with respect to doxorubicin as a reference drug. Five structures (218, 219, 220, 221, and 222) were tested against HepG-2 (Fig. 75 and Table 63). Structure 220 against HepG-2 had higher antitumor inhibitory activity (Fig. 75 and Table 63). Structure 222 had higher antitumor activity compared to structure 237 (Fig. 75 and Table 63) (Sayed et al., 2019)

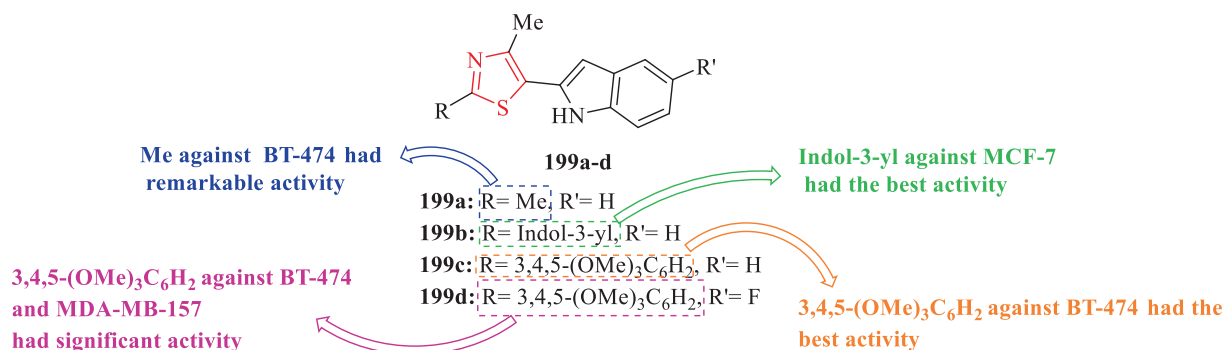


Fig. 62. Chemical structures 199a-d (Vaddula et al., 2016)

Table 51  
IC<sub>50</sub> values of the structures 199a-d (Vaddula et al., 2016).

Cpd. no.	IC <sub>50</sub> in $\mu\text{M}$		
	BT-474	MCF-7	MDA-MB-157
<b>199a</b>	30		
<b>199b</b>		10	
<b>199c</b>	20		
<b>199d</b>	30		30
<b>Doxorubicin</b>	0.3–0.4		

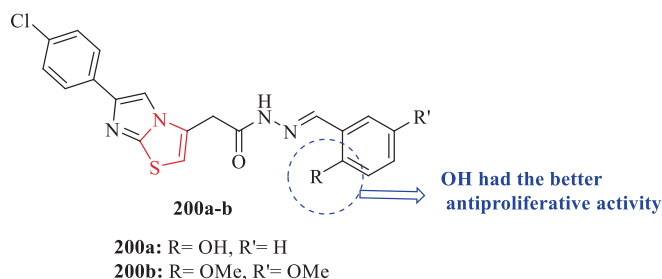


Fig. 63. Chemical structures 200a-b (Karaman and Ulusoy Güzeldemirci, 2016)

The antiproliferative activity of 15 derivatives containing thiazole scaffold was investigated against 4 cancer cell lines with respect to crizotinib as a reference drug by Zhang et al. Structure 223a against A549, Hela, HT29, and Karpas299 had the best anticancer activity compared to other structures (Fig. 76 and Table 64).

Table 52  
Anticancer activity of the structures 200a-b (Karaman and Ulusoy Güzeldemirci, 2016)

Panel/cell line	Comparison of in vitro tumor cell GI								
	200a			Cisplatin			Sorafenib		
	Log <sub>10</sub> GI <sub>50</sub>	Log <sub>10</sub> TGI	Log <sub>10</sub> LC <sub>50</sub>	Log <sub>10</sub> GI <sub>50</sub>	Log <sub>10</sub> TGI	Log <sub>10</sub> LC <sub>50</sub>	Log <sub>10</sub> GI <sub>50</sub>	Log <sub>10</sub> TGI	Log <sub>10</sub> LC <sub>50</sub>
<b>Leukemia</b>									
HL-60(TB)	-5.78	-5.07	>-4.00	-5.18	-4.047	-4	-5.793	-4.595	-4
K-562	-5.47	>-4.00	>-4.00	-4.577	-4.062	-4	-5.547	-4	-4
SR	-6.22	>-4.00	>-4.00	-5.113	-4.266	-4	-5.515	-4.885	-4
<b>Prostate cancer</b>									
DU-145	-5.57	>-4.00	>-4.00	-5.165	-4.324	-4	-5.476	-4.899	-4.353
Cpd. no.	Growth %								
	DU-145			K-562	SR		HL-60 (TB)		
<b>200a</b>	-8.65			51.07	-11.51		-3.50		
<b>200b</b>	55.11				32.07				

Structures 223b, 223c and 223d against A549, Hela, HT29, and Karpas299 demonstrated good activity (Fig. 76 and Table 64). Two structures (223e and 223f) were perfectly inactive on all cells (Zhang et al., 2019)

Abu-Melha et al. investigated the anticancer activity of 14 derivatives containing thiazole scaffold against 3 cancer cell lines with respect to doxorubicin as a reference drug. Most derivatives showed antitumor activity, especially structures 224 and 225 which had the most potent activity against HepG-2, HCT-116, and MCF-7 (Fig. 77 and Table 65) (Abu-Melha et al., 2019)

The in vitro anticancer activity of 18 derivatives against 5 cancer cell lines with respect to 5-FU as a reference drug was investigated by Afifi et al. Structures 226 and 228 against 5 cell lines had broad spectrum activity (Fig. 78 and Table 66). Structure 228 against A549 had the most potent activity, followed by structures 226 and 227. Further, structure 228 against MCF-7 showed significant activity, while structure 226 displayed moderate activity (Fig. 78 and Table 66). Structures 228 and 226 showed high activity against HepG-2. Moreover, higher cytotoxic potency against Caco-2 compared to the reference drug was shown by structure 228, while structures 226 and 227 showed moderate activity (Fig. 78 and Table 66). Structure 226 exhibited higher anticancer activity compared to the reference drug against PC3. Pyrazole carboxaldehydes (231a, 231b, and 231c) and their rhodanine condensation products (229a, 229b, 229c, 230a, 230b, and 230c) did not illustrate pronounced anticancer activity (Fig. 78) (Afifi et al., 2019)

Sultanova et al. investigated the anticancer activity of 15 derivatives against 4 cancer cell lines with respect to doxorubicin as a reference drug. Structures 232c and 232d showed pronounced cytotoxic activities, especially towards the Jurkat and HEK293 cell lines (Fig. 79 and Table 67). In addition, structures containing 2-

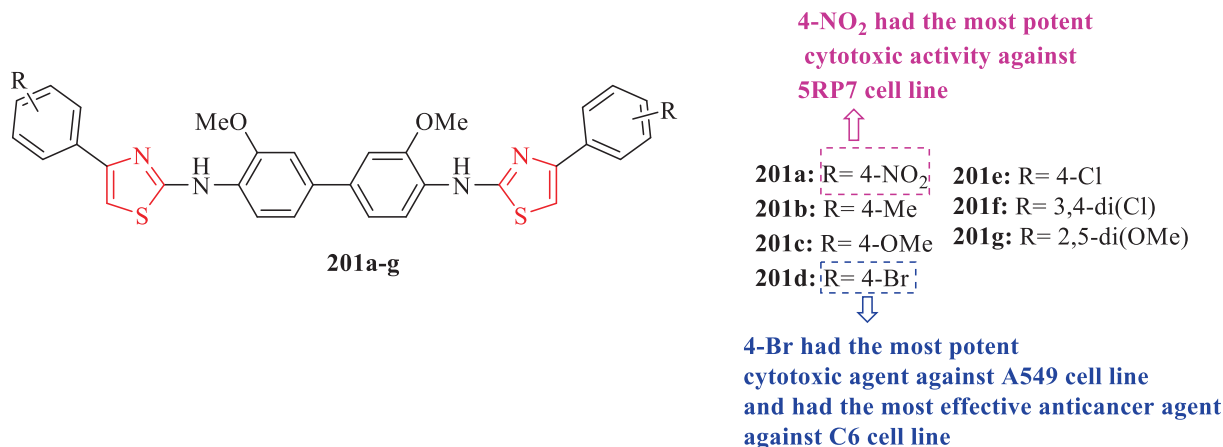


Fig. 64. Chemical structures 201a-g (Turan-Zitouni et al., 2016)

Table 53

IC<sub>50</sub> values of the structures 201a-g (Turan-Zitouni et al., 2016)

Cpd. no.	IC <sub>50</sub> (μg/mL)		
	A549 cell lines	C6 cell lines	5RP7 cell lines
<b>201a</b>	82.3 ± 2.5	33.3 ± 5.8	5.83 ± 1.04
<b>201b</b>	98.3 ± 7.6	21.0 ± 1.7	
<b>201c</b>	58.3 ± 7.6	28.7 ± 1.2	13.33 ± 1.53
<b>201d</b>	37.3 ± 6.8	11.3 ± 1.2	68.33 ± 22.55
<b>201e</b>		146.7 ± 5.8	
<b>201f</b>	146.7 ± 20.8		
<b>201g</b>			12.33 ± 0.58
<b>Mitoxantrone</b>	15.7 ± 4.0	11.0 ± 1.7	0.73 ± 0.06

allyl- (232b), 2-acetyl- (232a), and 2-methyl- (232e) aminothiazoles showed moderate cytotoxic activity (Fig. 79 and Table 67) (Sultanova et al., 2021)

Mahmoud and co-workers investigated the in vitro anticancer activity of 22 derivatives against 2 cancer cells with respect to doxorubicin as a reference drug. Among all derivatives, Structures 237a, 237d, 237c, 237b, 234a, 237e, 236a, 236c, and 236e had much better cytotoxic activities than the reference drug against HCT-116 (Fig. 80 and Table 68). Structure 233 in comparison with derivatives 234 and 235, there was only one structure (234a) that was higher activity than it against the HCT-116 and MCF-7 (Fig. 80 and Table 68). Nineteen structures (233, 234a-d, 235a-e, 236a-e, and 237a-d) exhibited higher activity compared to the reference drug against MCF-7 (Mahmoud et al., 2021)

Table 54

IC<sub>50</sub> values of the structures 202a-k (Lei et al., 2016)

Cpd. no.	IC <sub>50</sub> (μM)		
	HT-29	MKN-45	H460
<b>202a</b>	0.18 ± 0.02	0.06 ± 0.01	0.01 ± 0.003
<b>202b</b>	0.26 ± 0.03	0.02 ± 0.005	0.05 ± 0.007
<b>202c</b>			0.08 ± 0.006
<b>202d</b>		0.22 ± 0.02	0.15 ± 0.02
<b>202e</b>	0.21 ± 0.03	0.03 ± 0.005	0.09 ± 0.02
<b>202f</b>	0.70 ± 0.05	0.04 ± 0.005	0.14 ± 0.03
<b>202g</b>			0.09 ± 0.02
<b>202h</b>	0.46 ± 0.04	0.04 ± 0.004	0.06 ± 0.02
<b>202i</b>			0.08 ± 0.02
<b>202j</b>			0.12 ± 0.03
<b>202k</b>			0.10 ± 0.02
<b>Foretinib</b>	0.18 ± 0.02	0.031 ± 0.004	0.18 ± 0.04

The anticancer activity of some derivatives against 2 cancer cells with respect to cisplatin as a reference drug was investigated by Farghaly et al. Structures 238, 239, 240, and 241 against HCT-116 and HepG2 exhibited excellent antitumor activity (Fig. 81 and Table 69). Structure 239 showed good activity against HCT-116 and HepG2 compared to structures 240 and 241 (Fig. 81 and Table 69) (Farghaly et al., 2021)

In 2020, the anticancer activity of novel bithiazole derivatives against 3 cancer cells with respect to doxorubicin as a reference drug was evaluated by Latif et al. Structures 249c and 249a showed

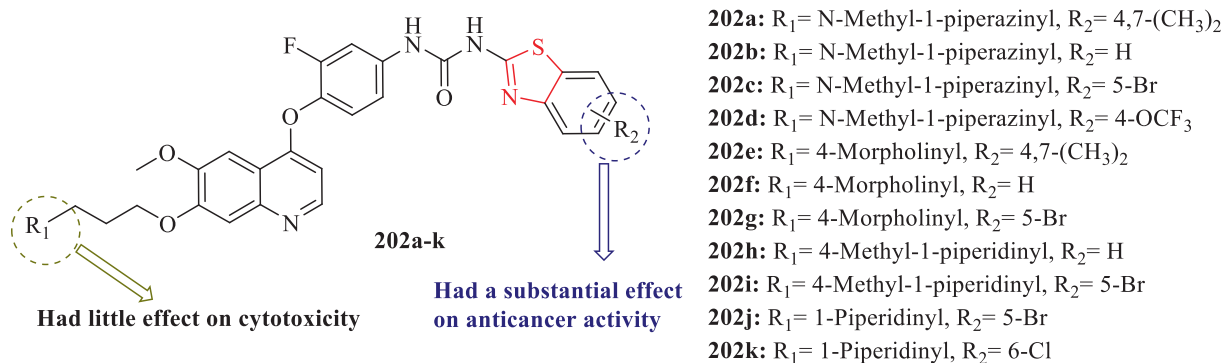


Fig. 65. Chemical structures 202a-k (Lei et al., 2016)

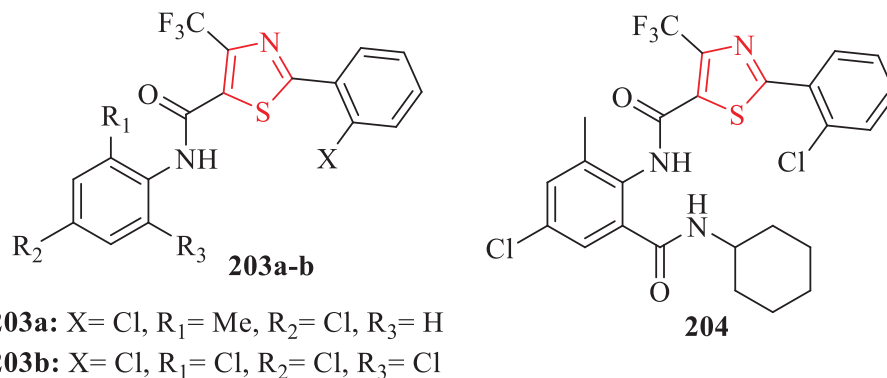


Fig. 66. Chemical structures 203a-b and 204 (Cai et al., 2016)

**Table 55**  
 Anticancer activity of the structures 203a-b and 204 (Cai et al., 2016)

Cpd. no.	% inhibitory	
	A-549	HCT-8
<b>203a</b>	48	
<b>203b</b>	40	
<b>204</b>		40
<b>5-Fluorouracil</b>	57	79

more potent anticancer activity against HCT-116 (Fig. 82 and Table 70). Structures 249a, 242b, and 242a had remarkably more potent activity against MCF-7 (Fig. 82 and Table 70). In addition,

structures 246, 245a, 247b, 249c, 249b, 245b, 248, 243, and 249a showed higher activity toward the reference drug against HepG2 human liver cancer cells (Fig. 82 and Table 70). Structures 246, 245a, 249b, 245b, and 248 did not active against human breast cancer and colon but were active against human liver cancer (Fig. 82 and Table 70). further, structures 247a and 247b against MCF-7 and HCT-116 had significant cytotoxic effects (Fig. 82 and Table 70). In the case of 249a–c derivatives, structures 249a and 249c against the 3 tested cells displayed the most activity (Fig. 82 and Table 70) (Latif et al., 2020)

Bayazeed and Alnoman investigated in vitro anticancer activity of novel thiazole derivatives against 4 cell lines with respect to 5-Fluorouracil as a reference drug by the MTT assay. Structure 250c against breast cancer cell lines showed higher activity (Fig. 83

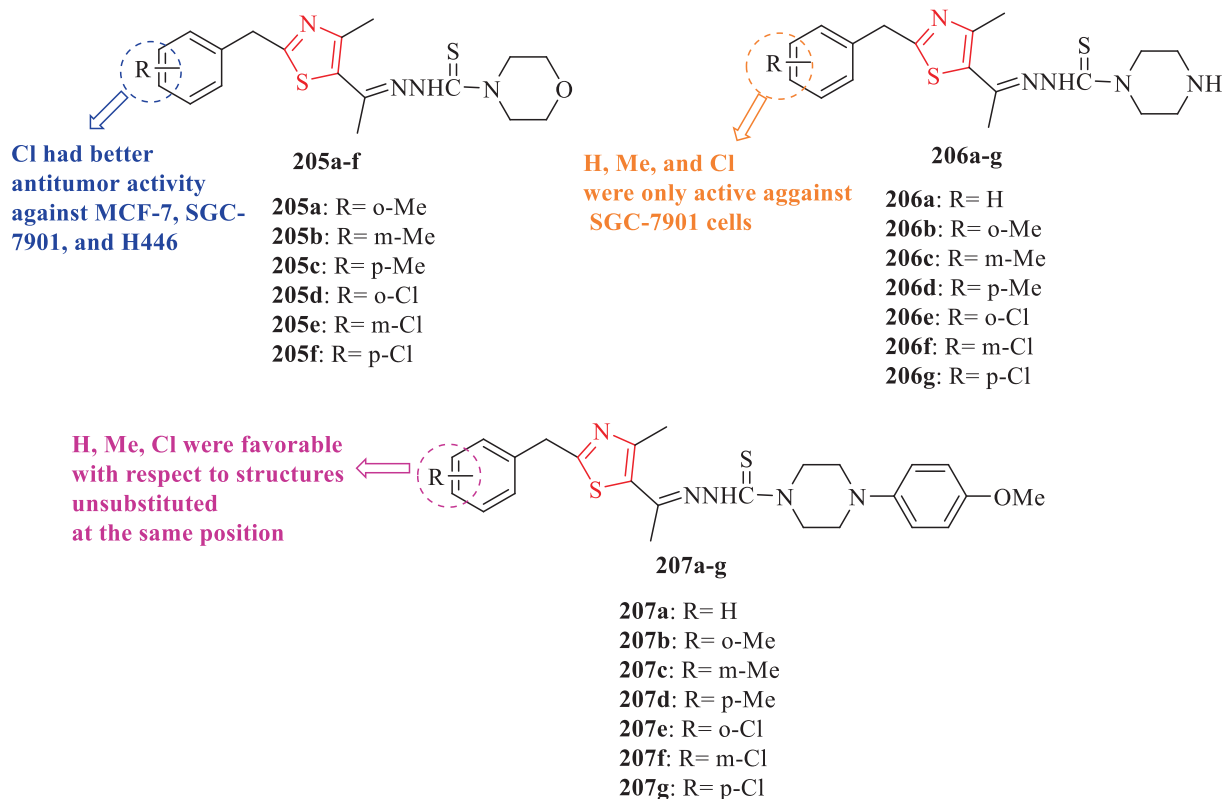


Fig. 67. Chemical structures 205a-f, 206a-g, and 207a-g (Shi et al., 2016)

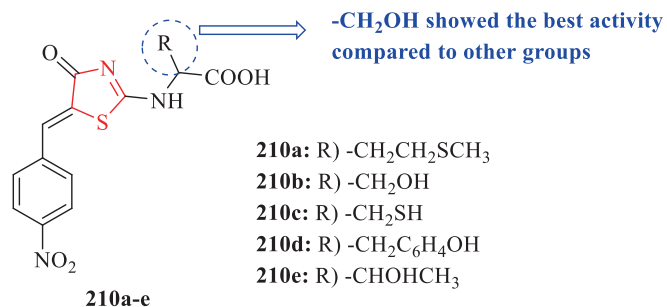
**Table 56**  
IC<sub>50</sub> values of the structures 205a-f, 206a-g, and 207a-g (Shi et al., 2016)

Cpd. no.	IC <sub>50</sub> (μM)		
	SGC-7901	H446	MCF-7
205a	45.91	48.37	20.52
205b	64.06	>100	57.07
205c	33.29	40.32	53.97
205d	25.09	21.13	17.74
205e	16.55	10.33	5.49
205f	26.47	34.05	11.11
206a	>100		
206b	18.25		
206c	33.04		
206d	71.99		
206e	>100		
206f	31.03		
206g	>100		
207a	65.95	>100	38.28
207b	18.54	56.13	15.04
207c	30.21	71.19	39.51
207d	21.35	81.79	49.61
207e	16.50	>100	34.65
207f	38.49	83.95	45.43
207g	11.58	35.03	23.29
Cisplatin	1.74	2.23	6.53

and Table 71). Structures 250a, 250b, and 251c had the most potent activity against 4 cell lines (Fig. 83 and Table 71). Structures 251a, 251b, and 251c had less activity than structures 250a, 250b, and 250c, but had strong activity against breast cancer cell lines (Fig. 83 and Table 71) (Bayazeed and Alnoman, 2020)

Suma et al. investigated the anticancer activity of some chalcone-linked thiazole-imidazopyridine derivatives against 4 cancer cells with respect to etoposide as a reference drug. Among all derivatives, structure 252a against 4 cell lines exhibited more potent activity (Fig. 84 and Table 72). In addition, structures 252b, 252c, 252d, and 252e showed significant activity against all cell lines (Fig. 84 and Table 72). In the case of 252a-e derivatives, Structure 252b (3,5-dimethoxy) displayed just lower activity toward structure 252a (3,4,5-trimethoxy) (Fig. 84 and Table 72). Also, Structure 252c (4-methoxy) had decreased activity on all cell lines toward structure 252a (3,4,5-trimethoxy) and 252b (3,5-dimethoxy) (Fig. 84 and Table 72) (Suma et al., 2020)

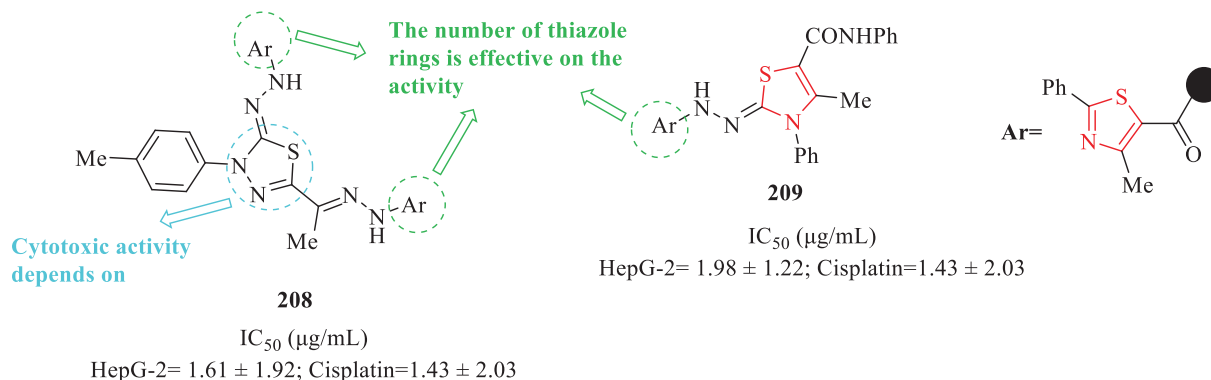
Ansari et al. investigated the anticancer activity of some derivatives containing thiazole scaffold against 3 cell lines with respect to etoposide as a reference drug by the MTT assay. Structures 254a and 254b against MCF-7 demonstrated the best inhibitory

**Fig. 69.** Chemical structures 210a-e (Pansare et al., 2017)**Table 57**  
IC<sub>50</sub> values of the structures 210a-e (Pansare et al., 2017)

Cpd. no.	IC <sub>50</sub> (μM)	
	MCF-7	BT-474
210a	7.5	8.6
210b	1.4	0.6
210c	7.2	6.1
210d	4.1	10.1
210e	1.6	1.2
Adriamycin	0.9	0.5

(Fig. 85 and Table 73). The activity of structure 254a was better than the reference drug against MCF-7. Also, structure 254b against A549 had the most potent activity. Structures 253a, 253b, 253c, and 253d against SKOV3 had the most activity (Fig. 85 and Table 73). Moreover, by comparing structures 254b and 255 can be understood that the insertion of methylene between 4-chlorophenyl moiety and thiazole-2(3H)-thione ring is effective for making the potent activity against MCF-7 and A549 (Fig. 85 and Table 73) (Ansari et al., 2020)

Farghaly et al. investigated in vitro antitumor activity of some thiazole derivatives against 3 cell lines with respect to doxorubicin as a reference drug. Structures 257c, 257d, and 256 had potent activity and showed less toxicity against WI-38 with high selectivity index (Fig. 86 and Table 74). Structure 257a against 3 cells exhibited the best activity. In addition, structure 257d had more activity against 3 cells (Fig. 86 and Table 74). Also, two structures (257b and 257c) had comparable antitumor activity against 3 cells (Fig. 86 and Table 74) (Farghaly et al., 2020)

**Fig. 68.** Chemical structures 208–209 and their IC<sub>50</sub> values (Gomha et al., 2017)

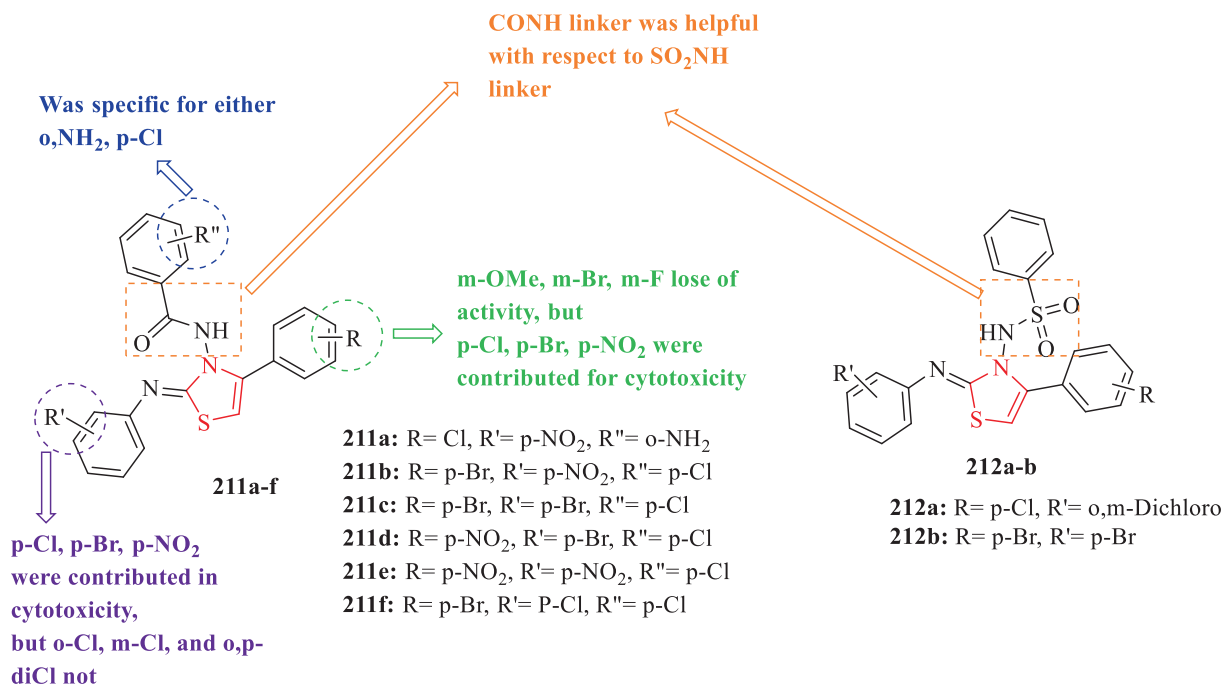


Fig. 70. Chemical structures 211a-f and 212a-b (Mirza et al., 2017)

Table 58

IC<sub>50</sub> values of the structures 211a-f and 212a-b (Mirza et al., 2017)

Cpd. no.	(IC <sub>50</sub> ± SEM) <sup>1</sup> (μM)		
	MCF-7	HCT-116	HeLa
<b>211a</b>	5.37 ± 0.56	16.99 ± 0.94	48.02 ± 0.98
<b>211b</b>	10.96 ± 0.33	41.48 ± 1.08	8.28 ± 0.21
<b>211c</b>	13.23 ± 1.6	40.03 ± 2.09	7.8 ± 0.07
<b>211d</b>	11.79 ± 0.58	34.17 ± 0.87	7.82 ± 0.12
<b>211e</b>	26.47 ± 1.09	40.51 ± 0.60	7.95 ± 0.10
<b>211f</b>	14.53 ± 0.23	40.06 ± 0.32	8.77 ± 0.27
<b>212a</b>	46.72 ± 1.80		19.86 ± 0.11
<b>212b</b>	40.21 ± 4.15		
<b>Doxorubicin</b>	1.56 ± 0.05	1.09 ± 0.1	0.7 ± 0.08

<sup>1</sup> IC<sub>50</sub> Values are expressed as mean ± standard error of mean.

The in vitro anticancer activity of some novel thiazole derivatives against 3 cell lines with respect to doxorubicin as a reference drug was investigated by Ghoneim and Ali Hassan, using the MTT assay (Fig. 87 and Table 75). Structures 258, 259, 260, and 261 showed better activity against HCT-116 toward the reference drug (Fig. 87 and Table 75). In the case of PC-3, structures 260 and 261 showed lower IC<sub>50</sub> than the reference drug (Fig. 87 and Table 75). Also, all structures had high IC<sub>50</sub> against HepG-2 (Ghoneim and Ali Hassan, 2022)

Sayed et al. investigated in vitro anticancer activity of some novel structures containing thiazole scaffold against 3 cancer cells with respect to harmine and cisplatin as reference drugs which was synthesized via the one-pot reaction, using the MTT colorimetric assay. The results revealed that structures 262a, 262b, and 263 against HCT-116 had growth inhibition activity toward reference drugs (Fig. 88 and Table 76). In addition, three structures (263, 262b, and 262a) displayed significant activity against HT-29

toward both reference drugs (Fig. 88 and Table 76). In the case of HepG2 cell lines, structures 262b, 262a, 263, and 264 showed the most activity toward both reference drugs (Sayed et al., 2020)

The anticancer activity of a series of amide-based thiazole-pyrimidines against 4 cancer cells with respect to etoposide as a reference drug was evaluated by Bandaru et al, using the MTT method. According to the structure-activity relationship studies, structure 265a against 4 cells exhibited remarkable activity (Fig. 89 and Table 77). Structure 265b showed potent activity against 4 cells. Structure 265c in comparison to structure 265b showed slightly decreased activity against 4 cells (Fig. 89 and Table 77). Also, structure 265d against 4 cells displayed lower activity compared to structures 265b and 265c. Structure 265f against A2780, MCF-7, and A549 demonstrated moderate activity (Fig. 89 and Table 77). In addition, Structure 265g in comparison to Structure 265f exhibited potentially improved activity against 4 cells (Fig. 89 and Table 77). Structure 265e against 4 cell lines

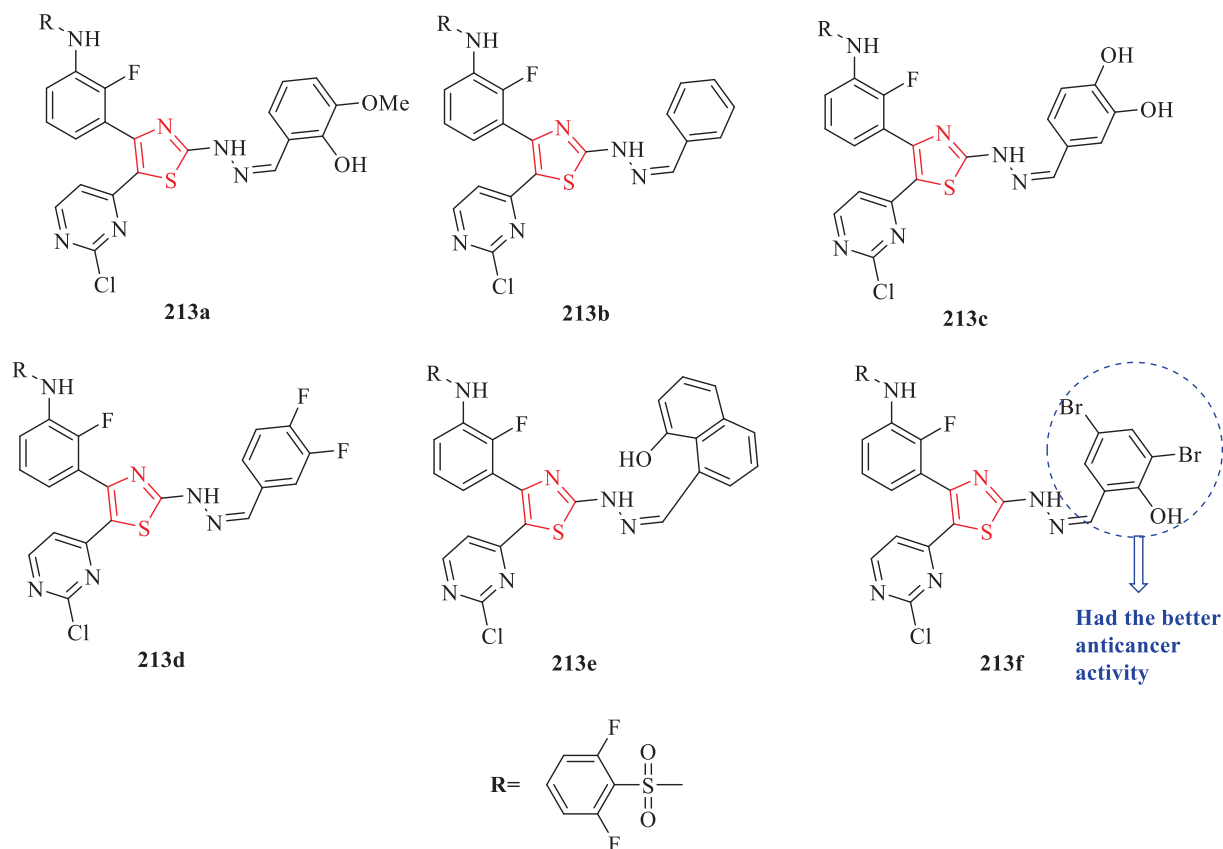


Fig. 71. Chemical structures 213a-f (Sharma et al., 2018)

Table 59

IC<sub>50</sub> values of the structures 213a-f (Sharma et al., 2018)

Cpd. no.	IC <sub>50</sub> Values [μM]		
	A375	HeLa	MCF-7
213a		26.32 ± 1.95	8.562 ± 1.19
213b	1.768 ± 0.12	NA	7.781 ± 2.36
213c	2.532 ± 0.31	NA	8.674 ± 0.91
213d	1.456 ± 0.21	NA	6.328 ± 1.15
213e	1.208 ± 0.04	NA	5.632 ± 0.67
213f	1.819 ± 0.17	24.6 ± 2.21	6.478 ± 0.96
Erlotinib	3.60	41.80	15.55

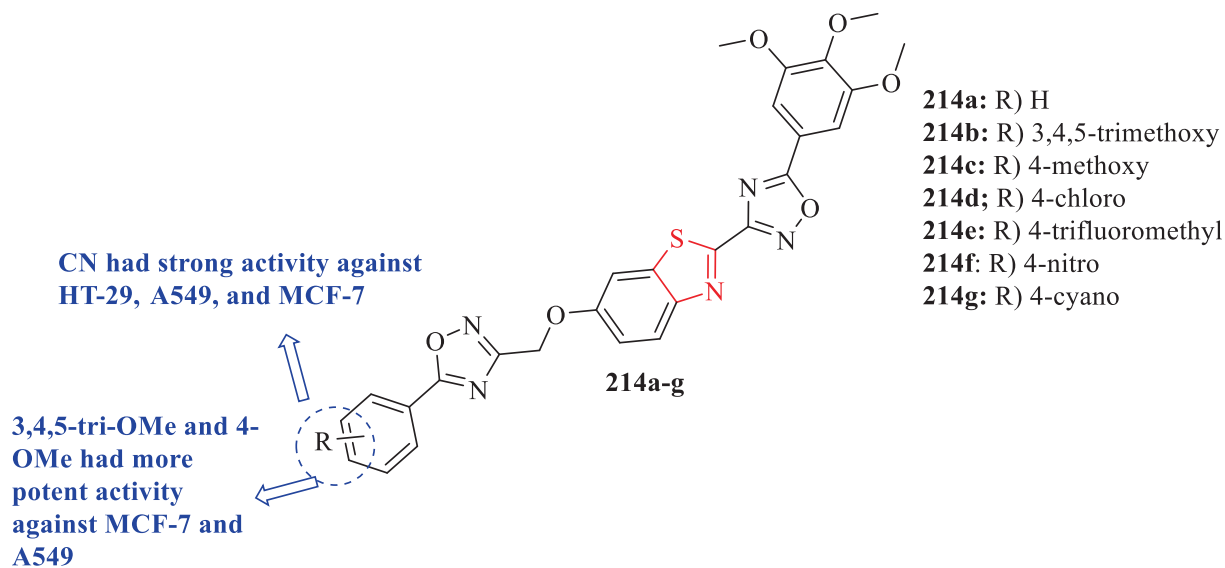
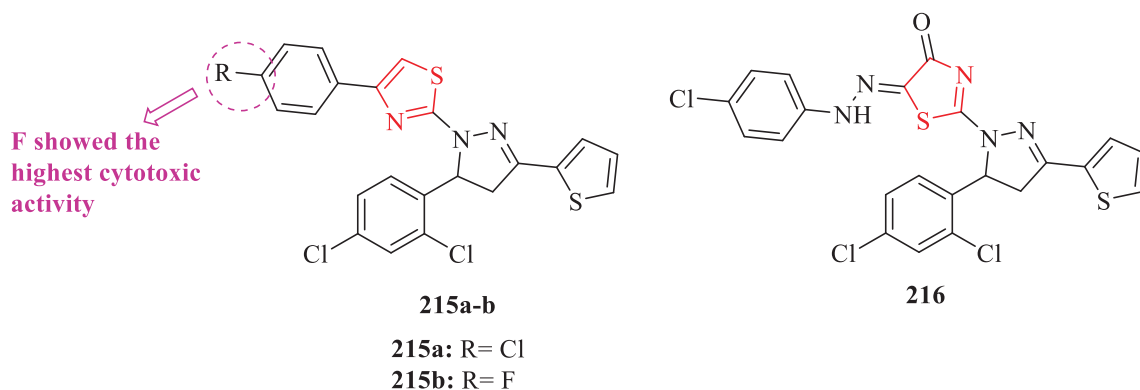
NA: Compound showing IC<sub>50</sub> value greater than 50 μM/mL.

Fig. 72. Chemical structures 214a-g (Sateesh Kumar and Umadevi, 2018)

**Table 60**  
IC<sub>50</sub> values of the structures 214a-g (Sateesh Kumar and Umadevi, 2018).

Cpd. no.	IC <sub>50</sub> μM <sup>1</sup>		
	A549	MCF-7	HT-29
214a	0.23 ± 0.013	1.67 ± 0.17	
214b	0.11 ± 0.01	0.78 ± 0.024	
214c	0.13 ± 0.01	0.70 ± 0.038	
214d		0.90 ± 0.022	
214e	1.56 ± 0.17	1.95 ± 0.18	
214f		14.6 ± 3.89	
214 g	1.89 ± 0.19	0.20 ± 0.029	0.76 ± 0.022
Combretastatin-A4	0.11 ± 0.02	0.18 ± 0.021	0.93 ± 0.034

<sup>1</sup> Each data represents as mean ± S.D values.



**Fig. 73.** Chemical structures 215a-b and 216 (Edrees et al., 2018)

**Table 61**  
IC<sub>50</sub> values of the structures 215a-b and 216 (Edrees et al., 2018)

Cpd. no.	IC <sub>50</sub> (μM) HepG2
215a	2.98 ± 1.8
215b	1.70 ± 8.2
216	3.54 ± 1.8
Cisplatin	0.90 ± 1.1

had slightly improved activity. Generally, six structures (265a, 265b, 265c, 265d, 265e, and 265 g) had very promising activity (Fig. 89 and Table 77) (Bandaru et al., 2022)

Gomha and co-workers investigated the anticancer activity of a series of novel thiazole–thiophene derivatives against the MCF-7 tumor cells and the LLC-Mk2 normal cell line with respect to cisplatin as a reference drug, using the MTT method. According to the results, most of the derivatives had variable activity. Structures

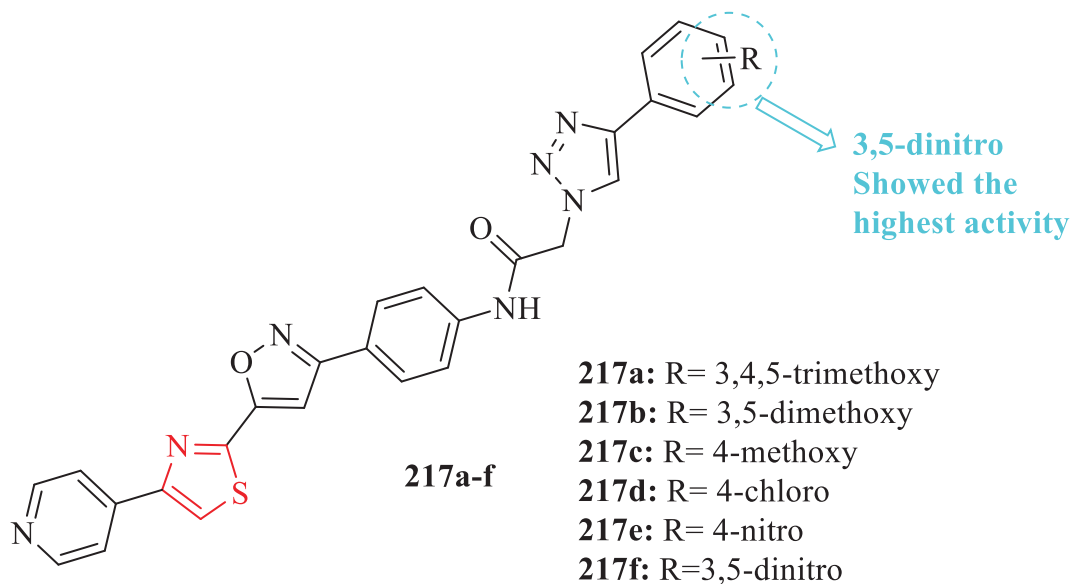


**Fig. 74.** Chemical structures 217a-f (Yakantham et al., 2019)



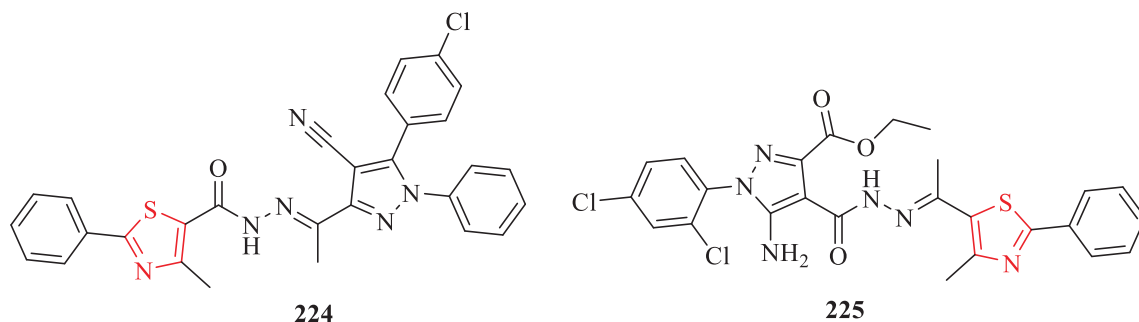


Fig. 77. Chemical structures of 224 and 225 (Abu-Melha et al., 2019)

Table 65

IC<sub>50</sub> values of 224 and 225 (Abu-Melha et al., 2019)

Cpd. no.	IC <sub>50</sub> (g/mL)		
	HepG-2	HCT-116	MCF-7
224	4.24 ± 0.3	7.35 ± 0.4	2.99 ± 0.2
225	7.4 ± 0.2	11.8 ± 0.5	3.77 ± 0.2
Doxorubicin	0.36 ± 0.04	0.49 ± 0.07	0.35 ± 0.03

268a and 266 against MCF-7 demonstrated significant activity (Fig. 90 and Table 78). Structure 268a with an acetyl group (Ac) showed higher activity compared to structure 268b with an ester group (CO<sub>2</sub>Et) (Fig. 90 and Table 78). Also, Structures 267a and 267b showed poor antitumor activity (Gomha et al., 2022)

Liu et al. evaluated the anticancer activity of a series of thiazole-based stilbene derivatives against 3 cancer cell lines with respect to etoposide and CPT as reference drugs, using the MTT method. The results revealed that structures 269a, 269b, 269c, 269d, 269f,

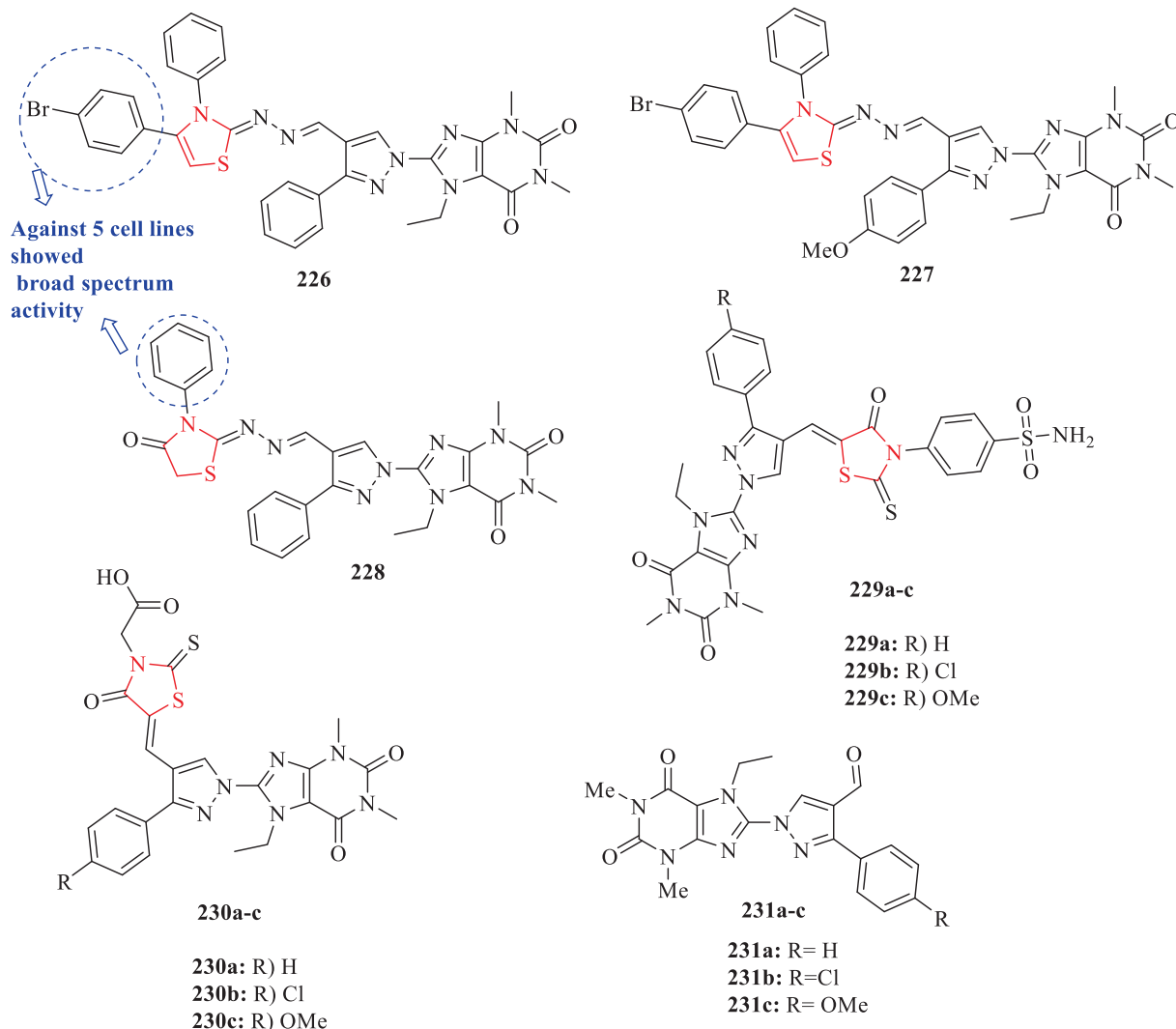
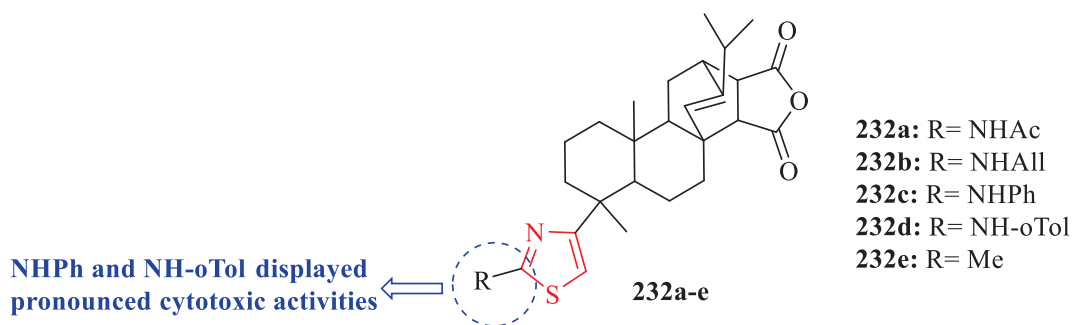


Fig. 78. Chemical structures 226–228, 229a–c, 230a–c, and 231a–c (Afifi et al., 2019)

**Table 66**  
IC<sub>50</sub> values of the structures 226–228 (Afifi et al., 2019)

Cpd. no.	IC <sub>50</sub> (μM)				
	A549	MCF-7	HepG-2	Caco-2	PC3
226	36.51	95.39	74.72	94.25	44.30
227	64.48			109.28	
228	18.85	23.43	23.08	23.08	18.50
5-FU	83.03	93.79	96.86	112.24	82.26

**Fig. 79.** Chemical structures 232a-e (Sultanova et al., 2021)**Table 67**  
IC<sub>50</sub> values of the structures 232a-e (Sultanova et al., 2021)

Cpd. no.	IC <sub>50</sub> (μM)			
	HEK293	Jurkat	HepG2	SH-SY5Y
232a	25.14 ± 0.72	27.65 ± 1.47	47.19 ± 2.63 (p = 0.00002) <sup>1</sup>	17.77 ± 1.94 (p = 0.003) <sup>1</sup>
232b	20.30 ± 0.08	25.26 ± 2.49 (p = 0.01) <sup>1</sup>	37.97 ± 1.00 (p = 0.00003) <sup>1</sup>	23.29 ± 5.61
232c	15.13 ± 3.15	22.21 ± 5.61	57.04 ± 1.40 (p = 0.00001) <sup>1</sup>	9.73 ± 1.55
232d	5.36 ± 2.10	9.60 ± 0.52	41.20 ± 5.93 (p = 0.00002) <sup>1</sup>	11.67 ± 0.10
232e	22.76 ± 7.61	14.65 ± 1.76 (p = 0.05) <sup>1</sup>	76.37 ± 1.63 (p = 0.00001) <sup>1</sup>	26.75 ± 3.49
Doxorubicin	1.90 ± 0.04	5.42 ± 0.38	7.21 ± 0.16	0.22 ± 0.005

<sup>1</sup> Corresponding cell line versus HEK293 cells. IC<sub>50</sub> values differences for certain cell lines proved by one-way ANOVA with Dunnett's Post Hoc test.

and 269 g had potent cytotoxicity against MCF-7 toward both reference drugs (Fig. 91 and Table 79). Structure 269a against MCF-7 demonstrated the highest cytotoxicity activity. In addition, structures 269a, 269b, 269c, 269e, 269f, 269 g, 269 k and 269 m showed high cytotoxicity against HCT116 (Fig. 91 and Table 79). Also, structure 269b exhibited the highest cytotoxicity against HCT116. Structures 269a, 269b, 269c, 269e, and 269 g were tested against HEK293T and the results showed all structures had possess a degree of cytotoxicity, while CPT had potent cytotoxicity (Fig. 91 and Table 79). It seems that derivatives containing fluorine-substituted (269a-d) displayed higher cytotoxicity than derivatives containing chlorinated and brominated against MCF-7 and HCT116 (Fig. 91 and Table 79). Structures 269 k, 269 l, and 269 m containing a hydroxy group had raised cytotoxicity against MCF-7 and HCT116 than structures 269 h, 269i, and 269j containing a meth-

oxy group, which revealed that a hydroxy group was effective for improving the cytotoxicity (Fig. 91 and Table 79) (Liu et al., 2022)

Al-Warhi et al. evaluated the in vitro antiproliferative activity of a series of new thiazolyl-pyrazoline derivatives against 2 cancer cells with respect to staurosporine and erlotinib as reference drugs. In the case of A549, structures 270f and 270b exhibited the most potent activity toward both reference drugs (Fig. 92 and Table 80). In addition, Structures 270j and 270i demonstrated moderate in vitro anti-proliferative activities toward the reference drugs. In the case of the T-47D, Structures 270j, 270i, 270f, and 270b displayed more potent antiproliferative activity toward the reference drugs (Fig. 92 and Table 80). Moreover, structures 270c and 270d had moderate cytotoxic activity. Structures 270c, 270 g, and 270j which contain p-methoxyphenyl on the phenyl ring showed potent to moderate antiproliferative activity against A549 and T-47D

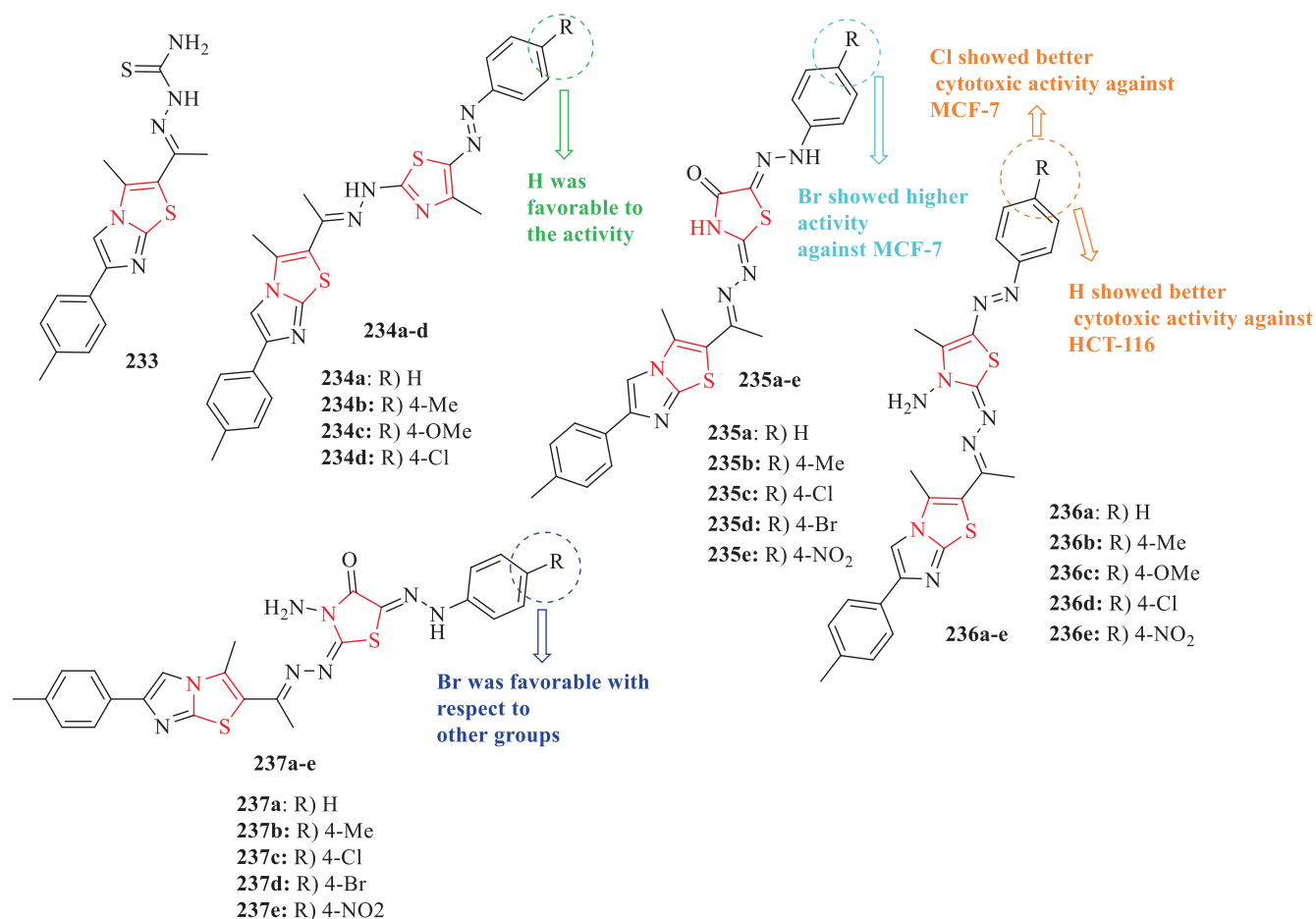


Fig. 80. Chemical structures 233, 234a-d, 235a-e, 236a-e, and 237a-e (Mahmoud et al., 2021)

Table 68

IC<sub>50</sub> values of 233, 234a-d, 235a-e, 236a-e, and 237a-e (Mahmoud et al., 2021)

Cpd. no.	IC <sub>50</sub> (μM) ± SD	
	HCT-116	MCF-7
233	8.8 ± 3.9	4.7 ± 2.7
234a	6.2 ± 2.7	2.4 ± 1.5
234b		4.5 ± 2.1
234c		3.9 ± 2.1
234d		3.8 ± 1.9
235a		3.4 ± 1.9
235b		3.2 ± 3.1
235c		3.2 ± 2.1
235d		2.4 ± 1.8
235e		5.3 ± 2.5
236a	8.0 ± 2.9	2.2 ± 1.7
236b		3.6 ± 1.5
236c	8.5 ± 3.1	2.3 ± 1.9
236d		1.4 ± 0.4
236e	8.9 ± 2.5	4.2 ± 2.1
237a	1.1 ± 1.5	6.3 ± 3.6
237b	5.6 ± 2.5	6.6 ± 3.1
237c	1.8 ± 1.9	6.2 ± 2.9
237d	1.1 ± 1.3	1.9 ± 0.3
237e	7.3 ± 3.6	
Doxorubicin	9.4 ± 3.9	6.7 ± 2.1

(Fig. 92 and Table 80). structures 270b with hydroxyl substituent, 270c with methoxy substituent, and 270d with chloro substituent showed better anti-proliferative activity against A549 and T-47D

than structure 270a with hydrogen substituent (Fig. 92 and Table 80). Also, structures 270f with hydroxyl substituent, 270 g with methoxy substituent, and 270 h with chloro substituent showed better anti-proliferative activity against T-47D than Structure 270e with hydrogen substituent (Fig. 92 and Table 80). In the case of the MCF-10A, the cytotoxic activity of structures 270b, 270f, 270i, and 270j was evaluated to explore their selectivity (Fig. 92 and Table 80). The results revealed that the structures had non-significant toxicity toward the MCF-10A (Al-Warhi et al., 2022)

The anticancer activity of a new series of nano-sized fluorinated thiazoles against 1 cancer cell with respect to cisplatin as a reference drug was investigated by Alsaedi et al. Structures 272 and 271c showed the most anticancer activity, while structures 271a and 271e exhibited the least activity in this series (Fig. 93 and Table 81). In addition, structure 271d displayed moderate activity. In the case of 270a-d, structures 270a and 270c showed moderate activity, while structure 270d had weak activity (Fig. 93 and Table 81). In general, structure 271c was more strong than the reference drug, and structures 270b and 271b had good activity (Fig. 93 and Table 81) ((Alsaedi et al., 2022)

El-Naggar et al. investigated the anticancer activity of a series of hydrazinyl-thiazole derivatives against 3 cancer cells with respect to roscovitine as a reference drug. Structures 273b and 273a showed the most cytotoxic activity against three cells (Fig. 94 and Table 82). In addition, structure 273d against HCT-116 and MCF-7 was more selective, while structure 273e was more selective against the three cells, and structure 273f was more selective

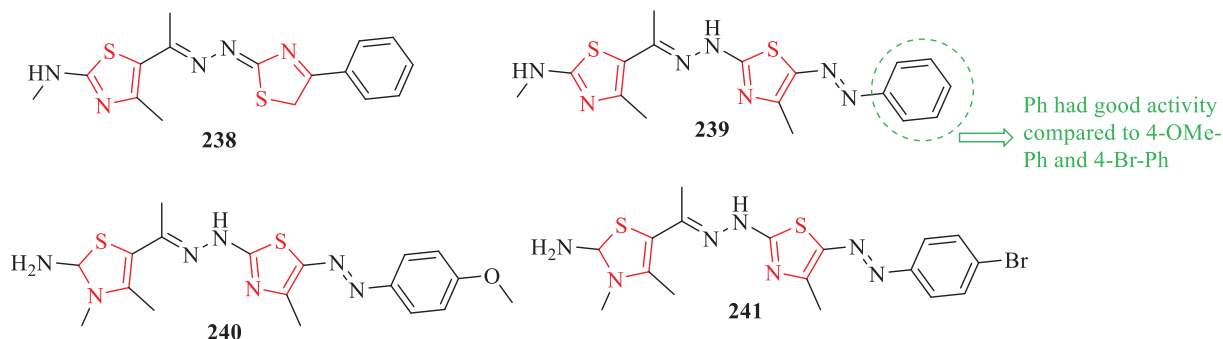


Fig. 81. Chemical structures 238–241 (Farghaly et al., 2021)

Table 69

IC<sub>50</sub> values of the structures 238–241 (Farghaly et al., 2021)

Cpd. no.	IC <sub>50</sub> (μg/mL)	
	HCT-116	HepG2
238	15	25
239	6.7	5
240	18	30
241	12	23
Cisplatin	2	3.7

against HCT-116 than HePG-2 and MCF-7 (Fig. 94 and Table 82). It seems that the presence of the methoxy (273a) and methyl (273c) groups as electron donating group and chlorine (273d) group as electron withdrawing group at position 4 of the phenyl ring enhance cytotoxic activity against 3 cell lines (Fig. 94 and Table 82). Some structures were chosen for in vitro inhibition of epidermal growth factor receptor (EGFR) and aromatase (ARO) enzymes with respect to erlotinib and letrozole as reference drugs. According to the results, structure 273d was the most active EGFR inhibitor toward erlotinib (Fig. 94 and Table 82). Also, the same structure

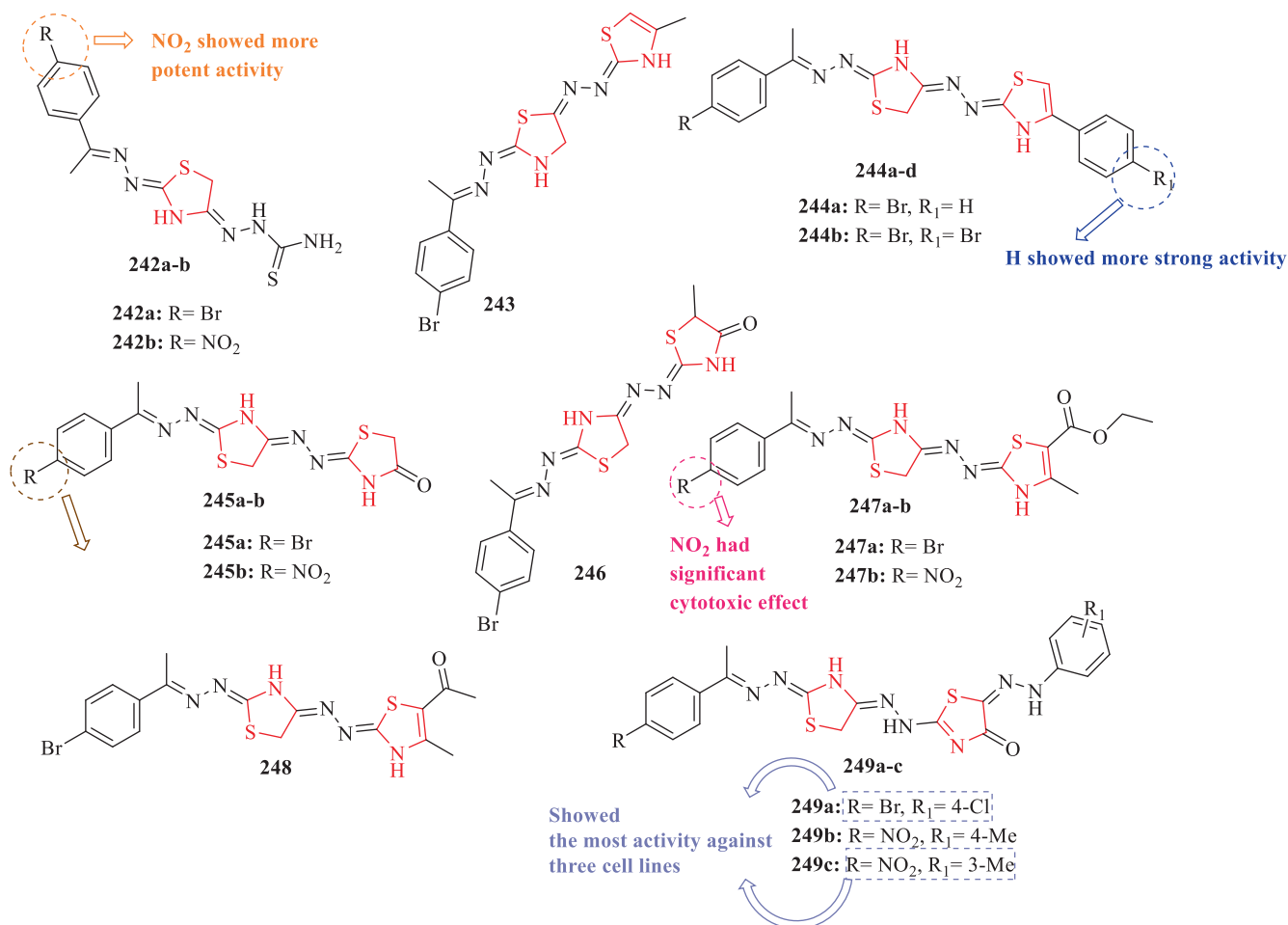
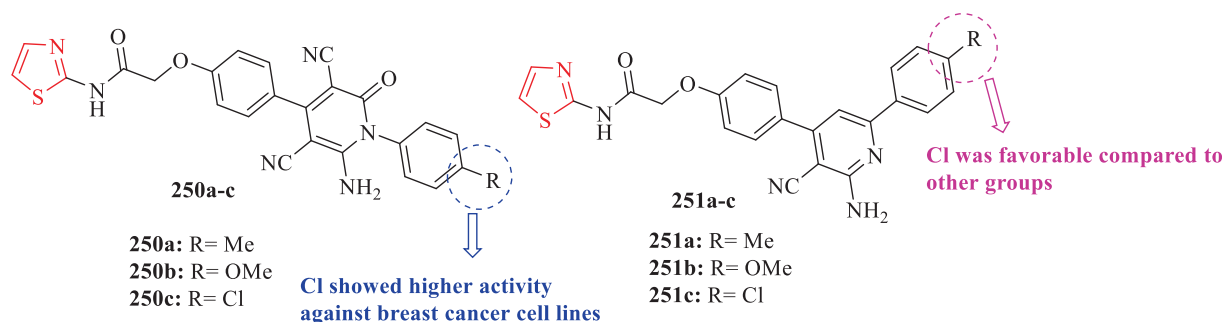


Fig. 82. Chemical structures 242a–b, 243, 244a–b, 245a–b, 246, 247a–b, 248, and 249a–c (Latif et al., 2020)

**Table 70**IC<sub>50</sub> values of the structures 242a-b, 243, 244a-b, 245a-b, 246, 247a-b, 248, and 249a-c (Latif et al., 2020)

Cpd. no.	IC <sub>50</sub> (μM)		
	HCT-116	MCF-7	HepG2
242a		19.9 ± 2.3	
242b		16.3 ± 2.1	
243			30.0 ± 3.2
244a	16.3 ± 3.1		
244b	17.1 ± 2.5		
245a			28.0 ± 3.5
245b			29.5 ± 3.6
246			23.5 ± 2.3
247a	13.5 ± 1.8	24.7 ± 3.8	
247b	13.2 ± 2.1	21.4 ± 3.3	
248			28.8 ± 3.5
249a	11.5 ± 1.5	14.4 ± 1.8	29.9 ± 3.5
249b			30.8 ± 3.3
249c	11.4 ± 1.7	20.7 ± 3.2	29.5 ± 3.9
Doxorubicin	12.0 ± 2.1	20.5 ± 2.1	29.4 ± 3.5
			32.7 ± 3.2

**Fig. 83.** Chemical structures 250a-c and 251a-c (Bayazeed and Alnoman, 2020)**Table 71**IC<sub>50</sub> values of the structures 250a-c and 251a-c (Bayazeed and Alnoman, 2020)

Cpd. no.	IC <sub>50</sub> (μM)			
	PC3	HepG2	Hep-2	MCF-7
250a	32.46 ± 2.15	20.34 ± 0.15	18.37 ± 0.13	11.03 ± 0.23
250b	30.57 ± 0.11	16.20 ± 0.03	13.52 ± 0.10	8.40 ± 0.16
250c	18.10 ± 0.01	13.18 ± 0.02	11.27 ± 0.05	5.71 ± 0.15
251a	37.48 ± 0.63	32.27 ± 0.44	27.13 ± 0.11	21.09 ± 0.27
251b	38.56 ± 0.81	29.32 ± 0.66	24.72 ± 0.73	17.41 ± 0.62
251c	24.82 ± 0.03	17.19 ± 0.07	18.23 ± 0.27	12.57 ± 0.49
5-Fu	8.30 ± 0.23	7.19 ± 0.45	5.22 ± 0.82	6.14 ± 0.31

had the most potent ARO inhibitory action but had less potent than letrozole (El-Naggar et al., 2022)

The in vitro anticancer activity and cytotoxic activity of 13 derivatives containing thiazole scaffold against 5 cancer cells and 1 human normal cell with respect to doxorubicin and cisplatin as reference drugs was evaluated by Bhandare et al. Structure 274 with three heterocyclic rings exhibited anticancer activity against HeLa, MCF-7, A2780, and BGC-823 (Fig. 95 and Table 83). However, The conversion of structure 274 into structures 275 and 276 remarkably improved the anticancer activity (Fig. 95 and Table 83). Structure 276 had the highest activity against BGC-823. Comparison between structures of 277a-e and 278a-e exhibited structures of 278a-e series had modest activity compared to cisplatin. In the

case of 277a-e, structure 277e had excellent activity against MCF-7 (Fig. 95 and Table 83). In the case of 278a-e, the additional carbonyl group dwindled the important interactions, one of which was electronic and another reason was steric. These reasons caused low activity in the structures 278a-e series (Fig. 95 and Table 83). In the case of the results of the L02, the results showed that all structures were non-toxic ((Bhandare et al., 2022)

According to the analyzes carried out on structures with antibacterial and antifungal properties, depending on the type of structure, electron-withdrawing or electron-donating groups are effective in improving their properties, for example, in structures 20a-f and 21a-f, the presence of electron groups Killing agents such as nitro increase the activity of imam, while electron-donating

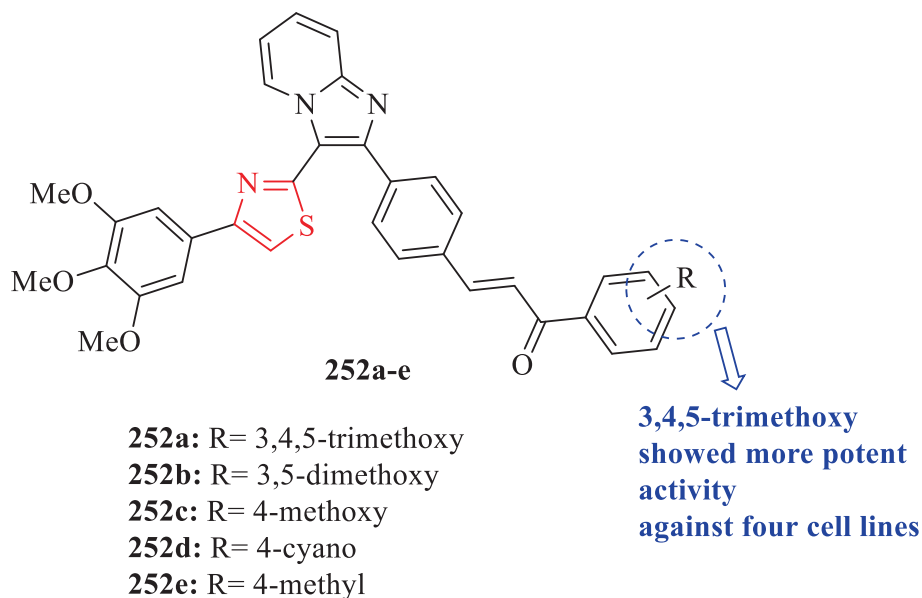


Fig. 84. Chemical structures 252a-e (Suma et al., 2020)

Table 72

IC<sub>50</sub> values of the structures 252a-e (Suma et al., 2020)

Cpd. no.	IC <sub>50</sub> (μM)			
	MCF-7	A549	DU-145	MDA MB-231
<b>252a</b>	0.18 ± 0.094	0.66 ± 0.071	1.03 ± 0.45	0.065 ± 0.0082
<b>252b</b>	0.44 ± 0.018	1.23 ± 0.37	1.12 ± 0.25	0.95 ± 0.066
<b>252c</b>	1.98 ± 0.52	2.10 ± 1.66	2.44 ± 1.32	1.81 ± 0.84
<b>252d</b>	2.33 ± 1.73	2.17 ± 1.50	1.90 ± 0.88	2.02 ± 0.99
<b>252e</b>	1.73 ± 0.11	1.69 ± 0.32	1.33 ± 0.45	3.22 ± 2.48
<b>Etoposide</b>	2.11 ± 0.024	3.08 ± 0.135	1.97 ± 0.45	1.91 ± 0.84

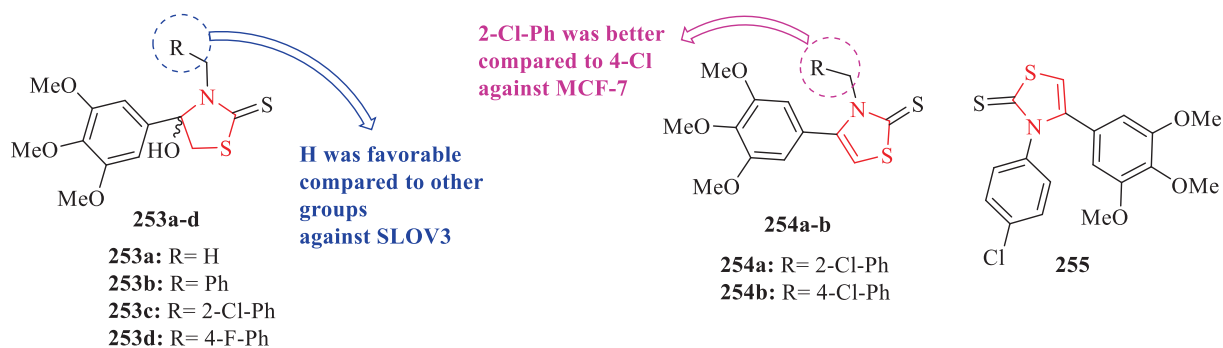


Fig. 85. Chemical structures 253a-d, 254a-b, and 255 (Ansari et al., 2020)

Table 73

IC<sub>50</sub> values of the structures 253a-d, 254a-b, and 255 (Ansari et al., 2020)

Cpd. no.	IC <sub>50</sub> (μg/mL) <sup>1</sup>		
	A549	MCF-7	SKOV3
<b>253a</b>			4.23 ± 0.14 (13.4)
<b>253b</b>			5.38 ± 0.16 (13.8)
<b>253c</b>			5.13 ± 0.18 (12.1)
<b>253d</b>			5.05 ± 0.22 (12.4)
<b>254a</b>		1.14 ± 0.18 (2.8)	
<b>254b</b>	2.72 ± 0.15 (6.7)	2.41 ± 0.11 (5.9)	
<b>255</b>	6.04 ± 0.23 (15.4)	6.63 ± 0.08 (16.9)	
<b>Etoposide</b>	3.52 ± 0.23 (6.0)	3.37 ± 0.24 (5.7)	5.41 ± 0.06 (9.2)

<sup>1</sup> the related IC<sub>50</sub> values in μM are shown into parentheses below the values in μg/mL.

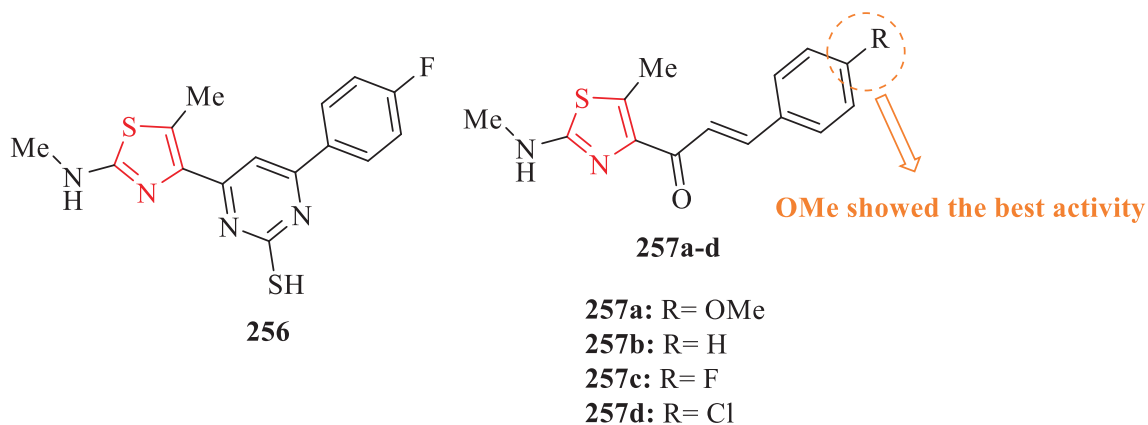


Fig. 86. Chemical structures 256 and 257a-d (Farghaly et al., 2020)

Table 74

IC<sub>50</sub> values of the structures 256 and 257a-d (Farghaly et al., 2020)

Cpd. no.	IC <sub>50</sub> (μM)				Selectivity index <sup>2</sup>		
	HepG-2	A549	MCF-7	WI-38 <sup>1</sup>	HepG-2	A549	MCF-7
<b>256</b>	3.5 ± 0.19	2.37 ± 0.12	4.11 ± 0.3	107.66 ± 1.7	35.88	45.42	26.19
<b>257a</b>	1.56 ± 0.07	1.39 ± 0.061	1.97 ± 0.09	137.35 ± 1.05	88.04	98.8	69.7
<b>257b</b>	4.53 ± 0.35	3.78 ± 0.2	4.9 ± 0.39				
<b>257c</b>	3.79 ± 0.21	3.17 ± 0.15	4.14 ± 0.35	93.44 ± 1.49	24.65	29.47	22.57
<b>257d</b>	2.29 ± 0.11	2.01 ± 0.1	2.38 ± 0.14	121.29 ± 2.3	52.96	60.34	50.96
<b>Doxorubicin</b>	3.54 ± 0.2	3.19 ± 0.14	4.39 ± 0.31				

<sup>1</sup> The data are expressed as the mean ± SD of 3 independent experiments and The cytotoxicity of 256, 257a, 257c and 257d on the normal WI-35 cell line was detected using the MTT assay.

<sup>2</sup> Selectivity index (SI) = IC<sub>50</sub> on WI-38 / IC<sub>50</sub> on cancer cells.

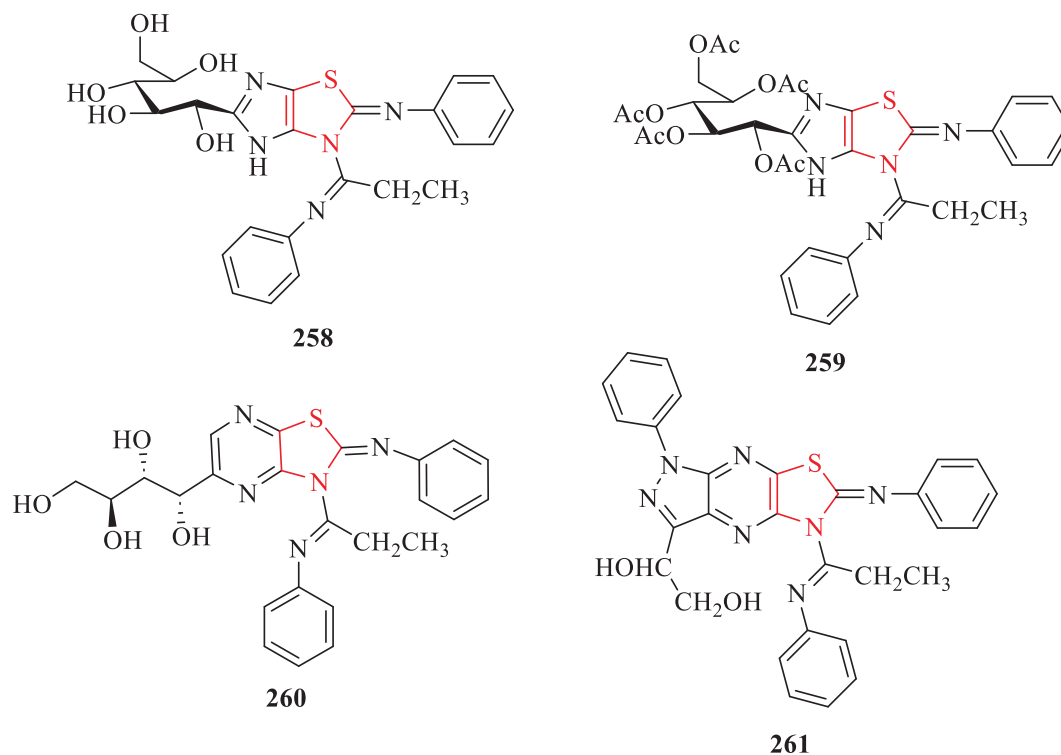


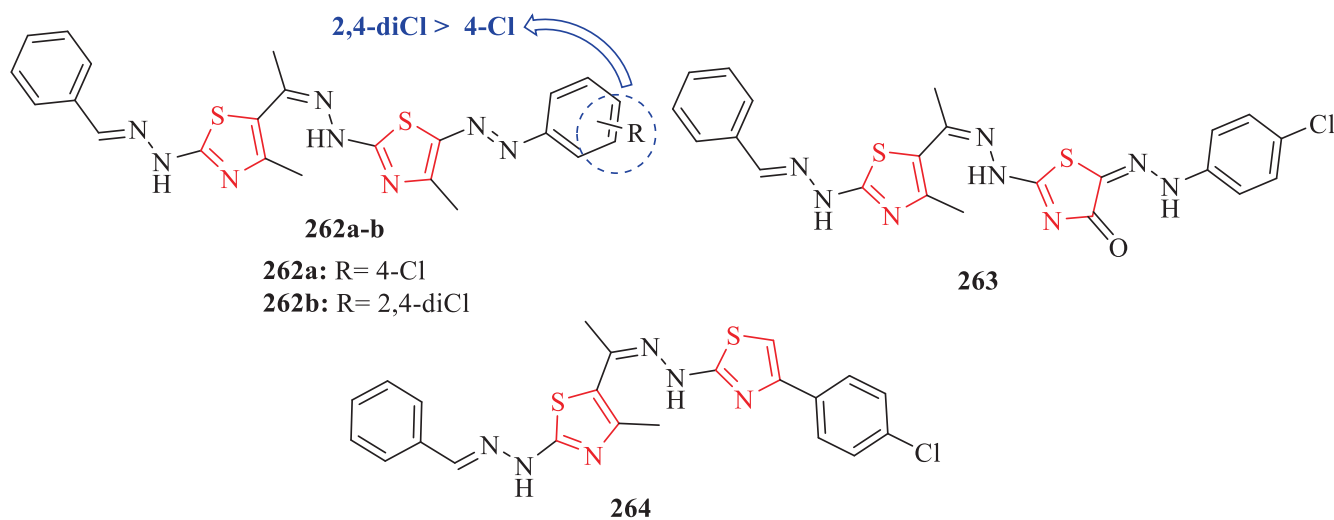
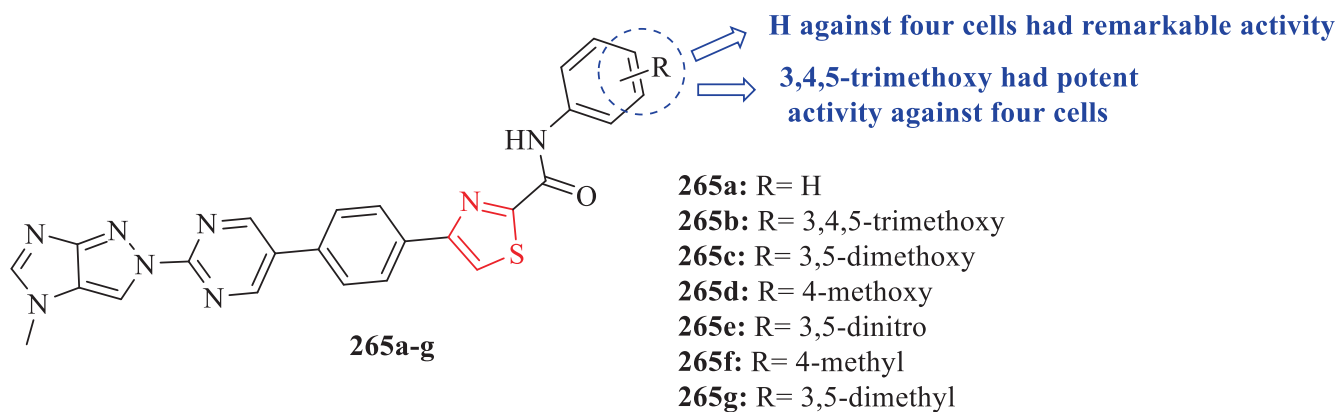
Fig. 87. Chemical structures 258–261 (Ghoneim and Ali Hassan, 2022)

**Table 75**  
IC<sub>50</sub> values of the structures 258–261 (Ghoneim and Ali Hassan, 2022)

Cpd. no.	IC <sub>50</sub> (nM) ± SD		
	HCT-116	PC-3	HepG-2
<b>258</b>	119 ± 4.1		133.5 ± 4.8
<b>259</b>	94.8 ± 3.6		284.1 ± 3.8
<b>260</b>	91.2 ± 1.7	119.8 ± 3.8	175.9 ± 2.8
<b>261</b>	106.2 ± 2.8	111.5 ± 3.7	333.9 ± 9.8
<b>Doxorubicin</b>	126.8 ± 8.8	129.6 ± 2.3	116.9 ± 5.7

**Table 76**  
IC<sub>50</sub> values of the structures 262a-b, and 263–264 (Sayed et al., 2020)

Cpd. no.	IC <sub>50</sub> (μM)		
	HCT-116	HepG2	HT-29
<b>262a</b>	3.80 ± 0.80	2.94 ± 0.62	7.24 ± 0.62
<b>262b</b>	3.65 ± 0.90	2.31 ± 0.43	4.13 ± 0.51
<b>263</b>	3.16 ± 0.90	4.57 ± 0.85	3.47 ± 0.79
<b>264</b>		9.86 ± 0.78	
<b>Harmine</b>	2.40 ± 0.12	2.54 ± 0.82	4.59 ± 0.67
<b>Cisplatin</b>	5.18 ± 0.94	9.41 ± 0.63	11.68 ± 1.54

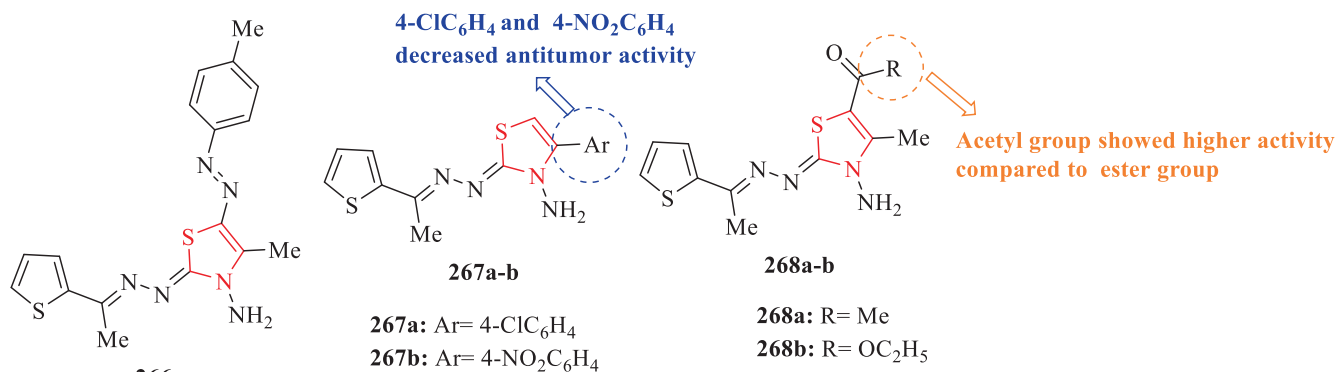
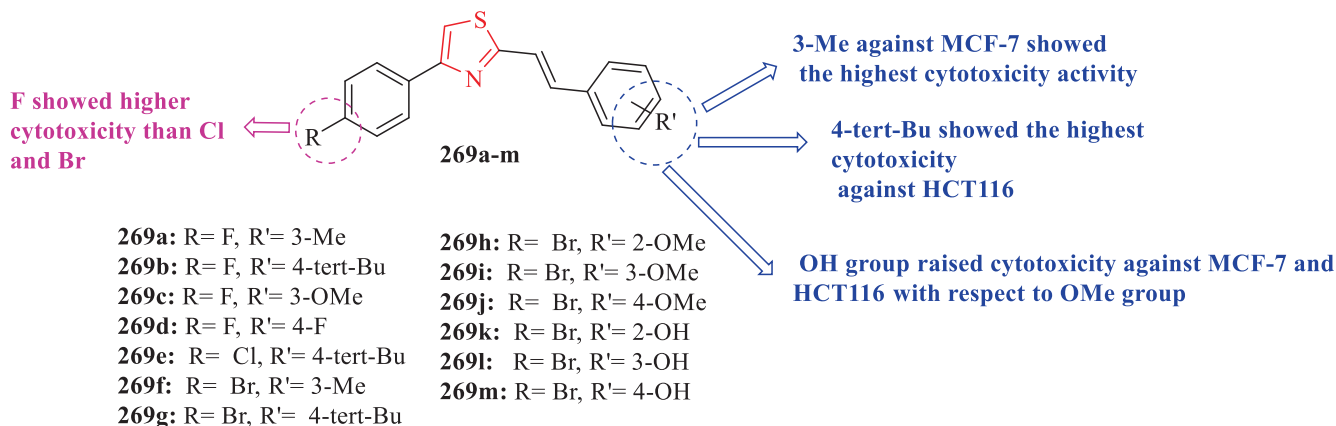
**Fig. 88.** Chemical structures 262a-b, and 263–264 (Sayed et al., 2020)**Fig. 89.** Chemical structures 265a-g (Bandaru et al., 2022)**Table 77**  
IC<sub>50</sub> values of the structures 265a-g (Bandaru et al., 2022)

Cpd. no.	IC <sub>50</sub> (μM)			
	A549	MCF-7	Colo-205	A-2780
<b>265a</b>	1.46 ± 0.17	0.74 ± 0.054	2.35 ± 1.34	2.01 ± 0.35
<b>265b</b>	0.043 ± 0.006	0.87 ± 0.045	0.12 ± 0.038	0.33 ± 0.071
<b>265c</b>	0.24 ± 0.043	1.28 ± 0.27	2.66 ± 1.58	2.14 ± 1.32
<b>265d</b>	2.77 ± 1.98	3.44 ± 2.31	2.93 ± 2.11	2.35 ± 1.77
<b>265e</b>	0.52 ± 0.019	0.39 ± 0.056	0.16 ± 0.044	0.79 ± 0.037
<b>265f</b>	4.56 ± 2.53	7.38 ± 3.72	Not active	10.52 ± 5.98
<b>265 g</b>	0.96 ± 0.074	0.28 ± 0.058	1.55 ± 0.64	2.67 ± 1.40
<b>Etoposide</b>	3.25 ± 0.132	2.38 ± 0.027	0.12 ± 0.015	1.36 ± 0.28

**Table 78**  
IC<sub>50</sub> values of the structures 266, 267a-b, and 268a-b (Gomha et al., 2022)

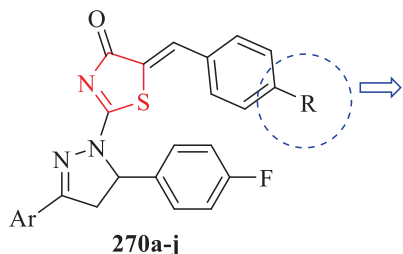
Cpd. no.	IC <sub>50</sub> (μM) MCF-7
266	10.2 ± 0.8
267a	38.2 ± 1.4
267b	54.8 ± 1.6
268a	11.5 ± 0.7
268b	16.3 ± 1.4
Cisplatin	13.3 ± 0.61

groups such as methyl and methoxy decrease it. Also, in the structures of 36a-j, this is the opposite, and the electron-donating groups such as methoxy are preferred over the electron-withdrawing groups of chlorine, which increases the activity of these structures. However, these electron-killing groups increase antifungal and antibacterial activity. The position of the groups has also been effective in increasing and decreasing the activity, for example, the combination of 40d with the placement of the flora group in position three has shown more suitable activity.

**Fig. 90.** Chemical structures 266, 267a-b, and 268a-b (Gomha et al., 2022)**Fig. 91.** Chemical structures 269a-m (Liu et al., 2022)**Table 79**  
IC<sub>50</sub> values of the structures 269a-m (Liu et al., 2022)

Cpd. no.	Cytotoxicity (IC <sub>50</sub> , μM)		
	MCF-7	HCT116	HEK293T
269a	0.78 ± 0.12	1.48 ± 0.16	10.15 ± 0.68
269b	6.31 ± 0.51	0.62 ± 0.09	12.02 ± 2.45
269c	9.85 ± 0.47	4.99 ± 0.80	25.16 ± 1.52
269d	4.14 ± 0.40		
269e	7.22 ± 0.40	2.87 ± 0.26	18.67 ± 1.37
269f		2.09 ± 0.15	
269g	3.78 ± 1.66	1.39 ± 0.16	21.78 ± 3.80
269h	>100	>100	
269i	45.82 ± 4.47	40.30 ± 7.80	
269j	>100	>100	
269k	39.18 ± 1.79	4.15 ± 0.76	
269l	22.79 ± 1.40	9.99 ± 0.19	
269m	38.01 ± 5.82	2.86 ± 0.46	
CPT	0.34 ± 0.026	0.012 ± 0.001	0.10 ± 0.003
Etoposide	24.68 ± 3.12	18.95 ± 1.35	

- 270a:** Ar= p-Me-C<sub>6</sub>H<sub>4</sub>, R= H  
**270b:** Ar= p-Me-C<sub>6</sub>H<sub>4</sub>, R= OH  
**270c:** Ar= p-Me-C<sub>6</sub>H<sub>4</sub>, R= OMe  
**270d:** Ar= p-Me-C<sub>6</sub>H<sub>4</sub>, R= Cl  
**270e:** Ar= p-OMe-C<sub>6</sub>H<sub>4</sub>, R= H  
**270f:** Ar= p-OMe-C<sub>6</sub>H<sub>4</sub>, R= OH  
**270g:** Ar= p-OMe-C<sub>6</sub>H<sub>4</sub>, R= OMe  
**270h:** Ar= p-OMe-C<sub>6</sub>H<sub>4</sub>, R= Cl  
**270i:** Ar= 2-thienyl, R= OH  
**270j:** Ar= 2-thienyl, R= OMe



**OH, OMe, and Cl showed better anti-proliferative activity against A549 and T-47D with respect to H**

**Fig. 92.** Chemical structures 270a-j (Al-Warhi et al., 2022)

**Table 80**

IC<sub>50</sub> values of the structures 270a-j (Al-Warhi et al., 2022)

Cpd. no.	IC <sub>50</sub> (μM)	
	A549	T-47D
<b>270a</b>	66.50 ± 3.38	17.10 ± 1.03
<b>270b</b>	4.41 ± 0.59	1.15 ± 0.56
<b>270c</b>	11.72 ± 1.06	9.30 ± 0.07
<b>270d</b>	43.11 ± 3.70	7.06 ± 0.43
<b>270e</b>		77.10 ± 4.68
<b>270f</b>	3.92 ± 0.18	0.88 ± 0.05
<b>270g</b>	21.73 ± 1.96	14.4 ± 0.87
<b>270h</b>		55.10 ± 3.34
<b>270i</b>	8.10 ± 0.37	1.66 ± 0.1
<b>270j</b>	6.53 ± 0.23	0.75 ± 0.05
<b>Staurosporine</b>	4.29 ± 0.72	6.83 ± 1.03
<b>Erlotinib</b>	5.73 ± 0.69	8.14 ± 0.97

**Table 81**

IC<sub>50</sub> values of the structures 270a-d, 271a-e, and 272 ((Alsaedi et al., 2022)

Cpd. no.	IC <sub>50</sub> values (μg/ml)
	MDA-MB-231
<b>270a</b>	28.8 ± 1.9
<b>270b</b>	13.4 ± 0.85
<b>270c</b>	55.8 ± 3.8
<b>270d</b>	408 ± 19.8
<b>271a</b>	97.1 ± 4.9
<b>271b</b>	14.9 ± 0.97
<b>271c</b>	2.97 ± 0.32
<b>271d</b>	27.2 ± 1.7
<b>271e</b>	366 ± 21.4
<b>272</b>	7.7 ± 0.41
<b>Cisplatin</b>	4.33 ± 0.12

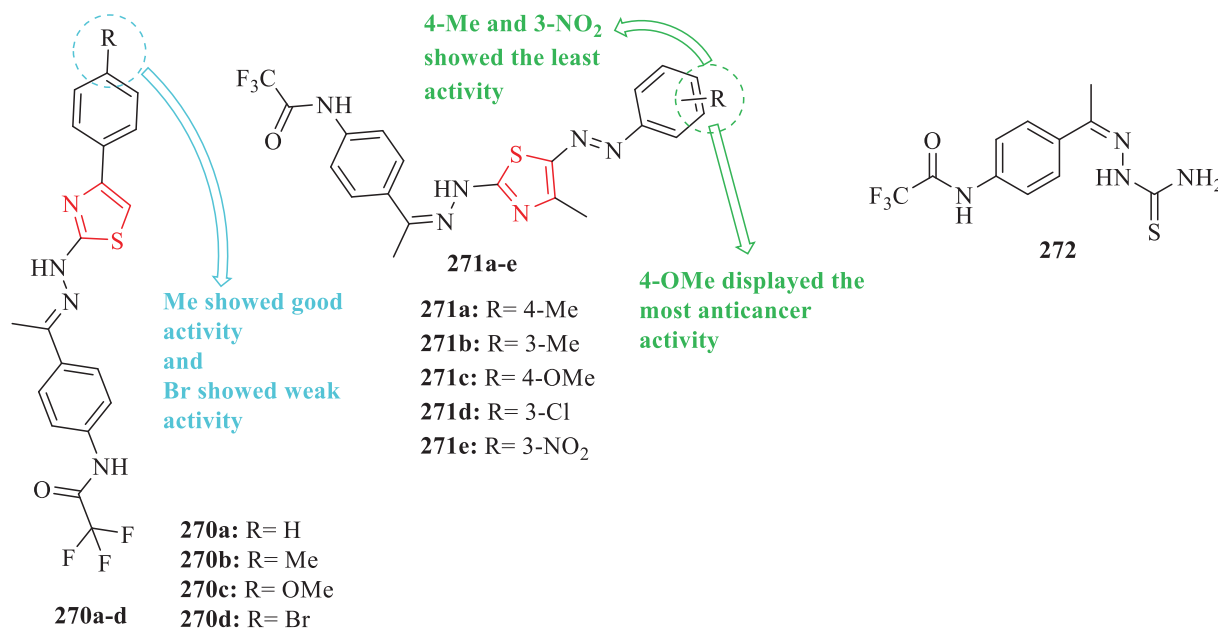


**Fig. 93.** Chemical structures 270a-d, 271a-e, and 272 (Alsaedi et al., 2022)

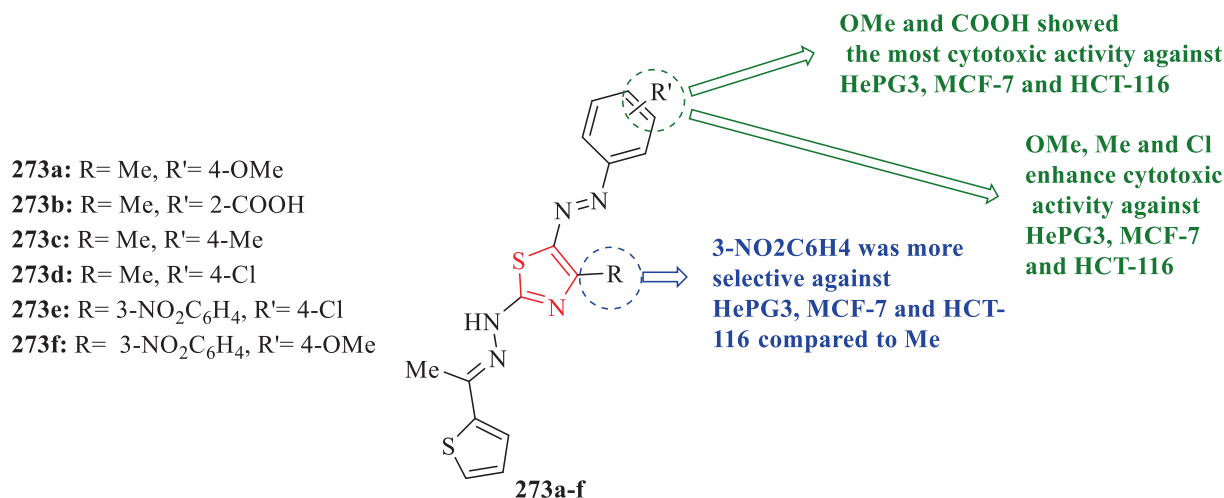


Fig. 94. Chemical structures 273a-f (El-Naggar et al., 2022)

Table 82

IC<sub>50</sub> values of the structures 273a-f (El-Naggar et al., 2022)

Cpd. no.	IC <sub>50</sub> (μM) <sup>1</sup>			EGFR inhibition IC <sub>50</sub> (nM) <sup>1</sup>	ARO inhibition IC <sub>50</sub> (nM) <sup>1</sup>
	HePG2	MCF-7	HCT-116		
<b>273a</b>	3.81 ± 0.2	7.19 ± 0.6	8.22 ± 0.7		
<b>273b</b>	11.34 ± 0.9	7.29 ± 0.5	6.87 ± 0.3		
<b>273c</b>	33.57 ± 2.3	21.68 ± 1.9	26.85 ± 2.1		
<b>273d</b>	6.73 ± 0.6	10.87 ± 0.9	13.79 ± 1.2	82.8 ± 0.004	98.6 ± 0.006
<b>273e</b>	9.29 ± 0.8	18.38 ± 1.4	22.17 ± 1.8		
<b>273f</b>	17.91 ± 1.5	10.33 ± 0.8	8.93 ± 0.6		
<b>Roscovitine</b>	13.82 ± 1.15	9.32 ± 0.49	12.24 ± 1.17		
<b>Erlotinib</b>				62.4 ± 0.005	NT <sup>2</sup>
<b>Letrozole</b>				NT <sup>2</sup>	79 ± 0.005

<sup>1</sup> IC<sub>50</sub> values are the mean ± S.D. of three separate experiments.

<sup>2</sup> NT: Compounds not tested.

Even increasing the number of thiazole rings improves the antibacterial and antifungal activity, like the structure of 68d.

In terms of anti-inflammatory activity, the structures hybridized with thiazole showed remarkable characteristics, such as structure 113, which has a coumarin appendage, and increased the anti-inflammatory properties of this compound. Also, the presence of an ester group attached to the thiazole ring is preferable to an acidic group and increases the anti-inflammatory properties of the structures (structures 120a-h, 125b, and 126d).

Regarding the anticancer activity of different structures, the number of thiazole rings is effective, and by increasing the number of these rings, the anticancer activity improves, such as the structures of 208 and 209. The type of linker is also very important, for example, linker CONH is more effective than linker SO<sub>2</sub>NH (Structures 211a-f and 212a-b, respectively). Therefore, special attention should be paid to the type of linker and the groups connected to it in the design of the structures. Also, electron-withdrawing groups are preferred over electron-donating groups and are more effective on the anti-cancer property of the structures (for example 217f and 201 a). Also, the existence of hybridized structures with thiazole is also effective on the anticancer property and increases the anticancer property of the desired compounds, similar to the structures 274 and 275.

## 5. Future remarks

According to the contents mentioned above, we suggest that you focus on the structures containing the thiazole ring hybridized

with other structures such as pyrimidine, imidazole, pyrazole, triazole, piperazine, pyrrole, pyridine, furan, coumarin, and etc. Examine the electron-donating and electron-withdrawing groups at the same time to determine the greater influence of each group. Also, research should move towards clinicalization, and only laboratory results do not help the development of structures, because the interaction of structures in the body environment is different from the laboratory, and its results help the development of these types of structures for better design of advanced drugs. Linkers are very important in interactions because they can help in structure interaction if they are designed and studied correctly. Therefore, we suggest that in the synthesis and design of structures with anti-microbial, anti-inflammatory and anti-cancer properties, attention should be paid to the type of linkers and groups used, and a lot of research is still needed in this field to improve the conditions of the structures.

## Funding

This research did not receive any specific grant from funding agencies in the public, commercial, or not-for-profit sectors.

## Declaration of Competing Interest

The authors declare that they have no known competing financial interests or personal relationships that could have appeared to influence the work reported in this paper.

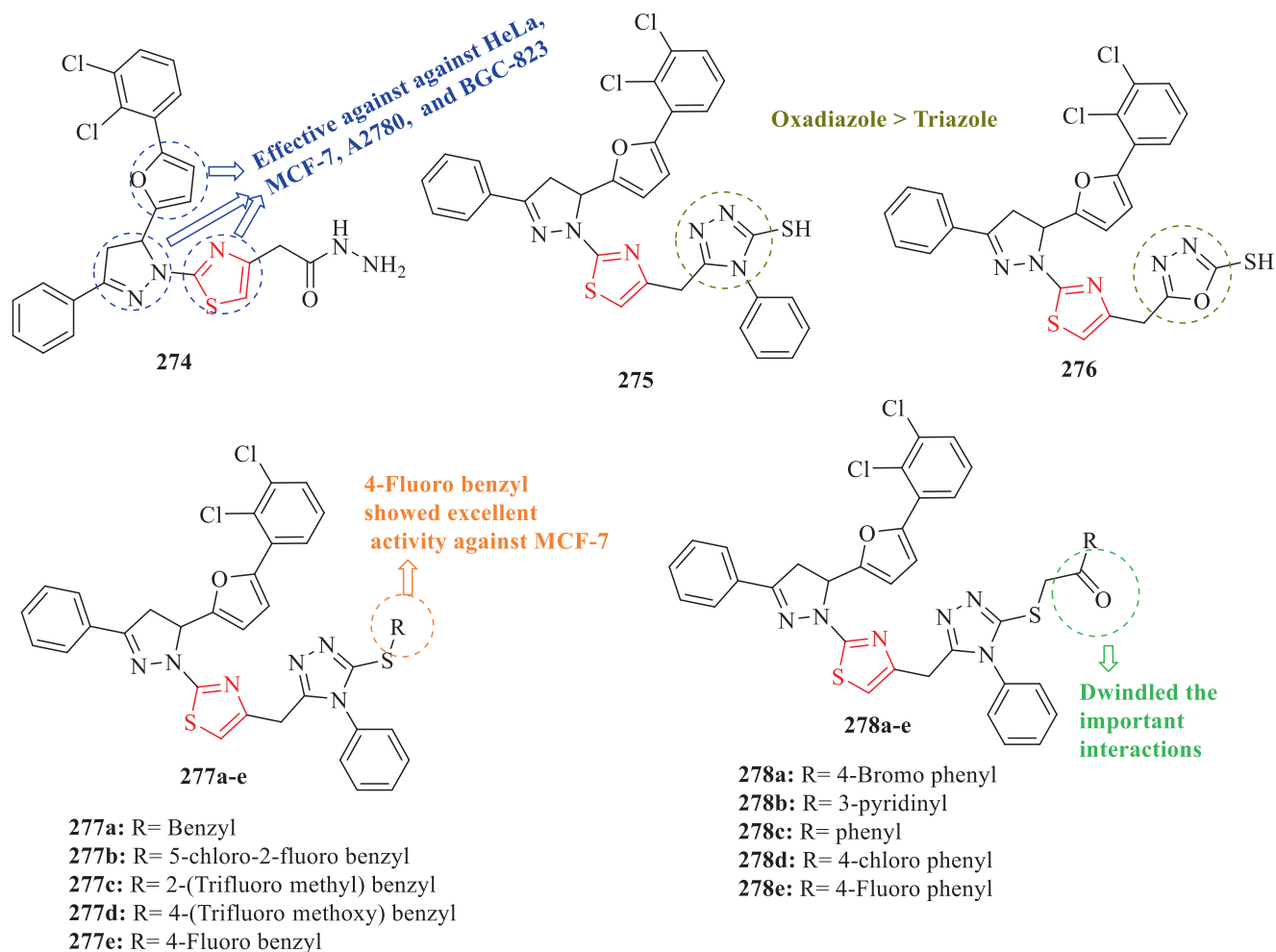


Fig. 95. Chemical structures 274–276, 277a-e, and 278a-e ((Bhandare et al., 2022)

Table 83

IC<sub>50</sub> values of the structures 274–276, 277a-e, and 278a-e (Bhandare et al., 2022).

Cpd. no.	IC <sub>50</sub> ± SD, μM				
	HeLa	A549	MCF-7	A2780	BGC-823
<b>274</b>	4.23 ± 0.23	2.18 ± 0.45	1.65 ± 0.44	2.12 ± 0.32	1.34 ± 0.11
<b>275</b>	4.86 ± 0.49	1.21 ± 0.92	2.50 ± 0.42	3.03 ± 1.54	1.20 ± 0.56
<b>276</b>	2.24 ± 0.48	1.39 ± 0.33	3.76 ± 0.54	1.56 ± 0.34	0.49 ± 1.45
<b>277a</b>	5.02 ± 0.34	3.98 ± 0.32	3.43 ± 0.33	2.88 ± 1.55	2.87 ± 0.55
<b>277b</b>	5.11 ± 0.55	2.87 ± 0.44	3.12 ± 0.65	3.12 ± 0.55	2.08 ± 0.55
<b>277c</b>	3.98 ± 0.54	2.09 ± 0.54	4.14 ± 0.58	5.76 ± 0.87	1.66 ± 0.54
<b>277d</b>	5.23 ± 0.67	3.84 ± 0.48	2.74 ± 0.32	1.57 ± 0.54	2.54 ± 0.65
<b>277e</b>	1.43 ± 0.77	1.22 ± 0.45	0.65 ± 0.53	2.12 ± 0.44	1.45 ± 0.28
<b>278a</b>	7.23 ± 0.47	4.48 ± 0.84	2.34 ± 0.54	2.78 ± 0.56	1.22 ± 0.37
<b>278b</b>	6.09 ± 0.33	1.59 ± 0.42	2.60 ± 0.48	3.93 ± 0.57	1.28 ± 0.30
<b>278c</b>	6.45 ± 1.84	4.58 ± 0.11	2.94 ± 0.21	6.32 ± 1.25	3.35 ± 0.16
<b>278d</b>	5.13 ± 0.35	1.25 ± 0.87	2.89 ± 0.35	5.51 ± 2.32	3.31 ± 0.54
<b>278e</b>	4.71 ± 0.24	3.11 ± 0.64	1.72 ± 1.98	4.33 ± 1.59	1.97 ± 0.91
<b>Doxorubicin</b>	1.03 ± 0.22	0.67 ± 0.13	0.73 ± 0.25	0.95 ± 0.31	1.08 ± 0.15
<b>Cisplatin</b>	5.65 ± 0.21	1.83 ± 0.62	1.85 ± 0.46	2.39 ± 0.47	0.98 ± 0.25

## References

- Abdelazeem, A.H., El-Saadi, M.T., Said, E.G., Youssif, B.G., Omar, H.A., El-Moghazy, S. M., 2017. Novel diphenylthiazole derivatives with multi-target mechanism: Synthesis, docking study, anticancer and anti-inflammatory activities. *Bioorg. Chem.* 75, 127–138. <https://doi.org/10.1016/j.bioorg.2017.09.009>.
- Abdel-Aziz, S.A., Taher, E.S., Lan, P., El-Koussi, N.A., Salem, O.I., Gomaa, H.A., Youssif, B.G., 2022. New pyrimidine/thiazole hybrids endowed with analgesic, anti-inflammatory, and lower cardiotoxic activities: Design, synthesis, and COX-2/5EH dual inhibition. *Arch. Pharm.* 355 (7), 2200024. <https://doi.org/10.1002/ardp.202200024>.
- Abdel-Wahab, B.F., Khidre, R.E., Awad, G.E., 2017. Design and Synthesis of Novel 6-(5-Methyl-1 H-1, 2, 3-triazol-4-yl)-5-[(2-(thiazol-2-yl) hydrazono) methyl] imidazo [2, 1-b] thiazoles as Antimicrobial Agents. *J. Heterocycl. Chem.* 54 (1), 489–494. <https://doi.org/10.1002/jhet.2610>.
- Abu-Hashem, A.A., Al-Hussain, S.A., Zaki, M.E., 2020. Synthesis of novel benzodifuranyl; 1, 3, 5-triazines; 1, 3, 5-oxadiazepines; and thiazolopyrimidines derived from visnaginone and khellinone as anti-inflammatory and analgesic agents. *Molecules* 25 (1), 220. <https://doi.org/10.3390/molecules25010220>.
- Abu-Melha, S., Edrees, M.M., Salem, H.H., Kheder, N.A., Gomha, S.M., Abdelaziz, M.R., 2019. Synthesis and biological evaluation of some novel thiazole-based heterocycles as potential anticancer and antimicrobial agents. *Molecules* 24 (3), 539. <https://doi.org/10.3390/molecules24030539>.
- Affi, O.S., Shaaban, O.G., Abd El Razik, H.A., El, S.E.D.A.S., Ashour, F.A., El-Tombary, A. A., Abu-Serie, M.M., 2019. Synthesis and biological evaluation of purine-pyrazole hybrids incorporating thiazole, thiazolidinone or rhodanine moiety as 15-LOX inhibitors endowed with anticancer and antioxidant potential. *Bioorg. Chem.* 87, 821–837. <https://doi.org/10.1016/j.bioorg.2019.03.076>.
- Ali, A.R., El-Bendary, E.R., Ghaly, M.A., Shehata, I.A., 2014. Synthesis, in vitro anticancer evaluation and in silico studies of novel imidazo [2, 1-b] thiazole derivatives bearing pyrazole moieties. *Eur. J. Med. Chem.* 75, 492–500. <https://doi.org/10.1016/j.ejmech.2013.12.010>.
- Ali, S.H., Sayed, A.R., 2021. Review of the synthesis and biological activity of thiazoles. *Synth. Commun.* 51 (5), 670–700. <https://doi.org/10.1080/00397911.2020.1854787>.
- Al-Mutairi, A.A., Hafez, H.N., El-Gazzar, A.R.B., Mohamed, M.Y., 2022. Synthesis and antimicrobial, anticancer and anti-oxidant activities of novel 2, 3-dihydropyrido [2, 3-d] pyrimidine-4-one and pyrrolo [2, 1-b][1, 3] benzothiazole derivatives via microwave-assisted synthesis. *Molecules* 27 (4), 1246. <https://doi.org/10.3390/molecules27041246>.
- Alsaedi, A.M., Farghaly, T.A., Shaaban, M.R., 2022. Fluorinated azole anticancer drugs: Synthesis, elaborated structure elucidation and docking studies. *Arab. J. Chem.* 15, (5). <https://doi.org/10.1016/j.arabjc.2022.103782> 103782.
- Althagafi, I., El-Metwaly, N., Farghaly, T.A., 2019. New series of thiazole derivatives: synthesis, structural elucidation, antimicrobial activity, molecular modeling and MOE docking. *Molecules* 24 (9), 1741. <https://doi.org/10.3390/molecules24091741>.
- Altintop, M.D., Özdemir, A., Turan-Zitouni, G., Ilgin, S., Atlı, Ö., Demirci, F., Kaplançıklı, Z.A., 2014. Synthesis and in vitro evaluation of new nitro-substituted thiazolyl hydrazone derivatives as anticandidal and anticancer agents. *Molecules* 19 (9), 14809–14820. <https://doi.org/10.3390/molecules190914809>.
- Al-Warhi, T., El Kerdawy, A.M., Sajid, M.A., Albohy, A., Elsayed, Z.M., Aljaeed, N., Elkaeed, E.B., Eldehna, W.M., Abdel-Aziz, H.A., Abdelmoaz, M.A., 2022. Novel 2-(5-Aryl-4, 5-dihydropyrazol-1-yl) thiazol-4-one as EGFR inhibitors: synthesis, biological assessment and molecular docking insights. *Drug Des. Devel. Ther.*, 1457–1471. <https://doi.org/10.2147/DDDT.S356988>.
- Ankali, K.N., Rangaswamy, J., Shalavadi, M., Naik, N., Krishnamurthy, G., 2021. Synthesis and molecular docking of novel 1, 3-thiazole derived 1, 2, 3-triazoles and in vivo biological evaluation for their anti anxiety and anti inflammatory activity. *J. Mol. Struct.* 1236., <https://doi.org/10.1016/j.molstruc.2021.130357> 130357.
- Ansari, M.I., Khan, S.A., 2017. Synthesis and antimicrobial activity of some novel quinoline-pyrazoline-based coumarinyl thiazole derivatives. *Med. Chem. Res.* 26, 1481–1496. <https://doi.org/10.1007/s00044-017-1855-4>.
- Ansari, M., Shokrzadeh, M., Karima, S., Rajaei, S., Fallah, M., Ghassemi-Barghi, N., Ghasemian, M., Emami, S., 2020. New thiazole-2 (3H)-thiones containing 4-(3, 4, 5-trimethoxyphenyl) moiety as anticancer agents. *Eur. J. Med. Chem.* 185., <https://doi.org/10.1016/j.ejmech.2019.111784> 111784.
- Ayati, A., Emami, S., Moghimi, S., Foroumadi, A., 2019. Thiazole in the targeted anticancer drug discovery. *Future Med. Chem.* 11 (16), 1929–1952. <https://doi.org/10.4155/fmc-2018-0416>.
- Bandaru, C.M., Poojith, N., Jadav, S.S., Basaveswara Rao, M.V., Babu, K.S., Sreenivasulu, R., Alluri, R., 2022. Design, synthesis, anticancer evaluation, and molecular docking studies of thiazole-pyrimidine linked amide derivatives. *Polycycl. Aromat. Compd.* 42 (8), 5368–5384. <https://doi.org/10.1080/10406638.2021.1939067>.
- Basha, S.S., Ramachandra Reddy, P., Padmaja, A., Padmavathi, V., Mouli, K.C., Vijaya, T., 2015. Synthesis and antimicrobial activity of 3-aryol-4-heteroaryl pyrroles and pyrazoles. *Med. Chem. Res.* 24, 954–964. <https://doi.org/10.1007/s00044-014-1169-8>.
- Bayazeed, A.A., Alnoman, R.B., 2020. Synthesis of New Thiazole-Pyridine Hybrids and Their Anticancer Activity. *Russ. J. Gen. Chem.* 90, 2004–2011. <https://doi.org/10.1134/S1070363220100254>.
- Bhandare, R.R., Munikrishnappa, C.S., Kumar, G.S., Konidala, S.K., Sigalappalli, D.K., Vaishnav, Y., Chinnam, S., Yasin, H., Al-karmalawy, A.A., Shaik, A.B., 2022. Multistep synthesis and screening of heterocyclic tetraads containing furan, pyrazoline, thiazole and triazole (or oxadiazole) as antimicrobial and anticancer agents. *J. Saudi Chem. Soc.* 26, (3). <https://doi.org/10.1016/j.jscs.2022.101447> 101447.
- Bueno, J.M., Carda, M., Crespo, B., Cuñat, A.C., De Cozar, C., León, M.L., Marco, J.A., Roda, N., Sanz-Cervera, J.F., 2016. Design, synthesis and antimalarial evaluation of novel thiazole derivatives. *Bioorg. Med. Chem. Lett.* 26 (16), 3938–3944. <https://doi.org/10.1016/j.bmcl.2016.07.010>.
- Cai, W.X., Liu, A.L., Li, Z.M., Dong, W.L., Liu, X.H., Sun, N.B., 2016. Synthesis and anticancer activity of novel thiazole-5-carboxamide derivatives. *Appl. Sci.* 6 (1), 8. <https://doi.org/10.3390/app6010008>.
- Deb, P.K., Kaur, R., Chandrasekaran, B., Bala, M., Gill, D., Kaki, V.R., Akkinapalli, R.R., Mailavaram, R., 2014. Synthesis, anti-inflammatory evaluation, and docking studies of some new thiazole derivatives. *Med. Chem. Res.* 23, 2780–2792. <https://doi.org/10.1007/s00044-013-0861-4>.
- Desai, N.C., Bhatt, N., Somani, H., 2015. Synthesis, characterization, and antimicrobial activity of some novel thiazole clubbed 1, 3, 4-oxadiazoles. *Med. Chem. Res.* 24, 258–266. <https://doi.org/10.1007/s00044-014-1108-8>.
- Deshineni, R., Velpula, R., Koppu, S., Pilli, J., Chellamella, G., 2020. One-pot multi-component synthesis of novel ethyl-2-(3-(2-(4-(4-aryl) thiazol-2-yl) hydrazono) methyl)-4-hydroxy/isobutoxyphenyl)-4-methylthiazole-5-carboxylate derivatives and evaluation of their in vitro antimicrobial activity. *J. Heterocycl. Chem.* 57 (3), 1361–1367. <https://doi.org/10.1002/jhet.3872>.
- Edrees, M.M., Melha, S.A., Saad, A.M., Kheder, N.A., Gomha, S.M., Muhammad, Z.A., 2018. Eco-friendly synthesis, characterization and biological evaluation of some novel pyrazolines containing thiazole moiety as potential anticancer and antimicrobial agents. *Molecules* 23 (11), 2970. <https://doi.org/10.3390/molecules23112970>.
- El-Hagrassey, E.A., Abdel-Latif, E., Abdel-Fattah, G.M., 2022. Synthesis and efficiency of new pyridine, chromene and thiazole containing compounds as antimicrobial and antioxidant agents. *Bull. Chem. Soc. Ethiop.* 36 (1), 137–148. <https://doi.org/10.4314/bcse.v36i1.12>.
- El-Kady, M., Abbas, E.M., Salem, M.S., Kassem, A.F., Abd El-Moez, S.I., 2016. Synthesis and antimicrobial evaluation of novel 1, 3-thiazoles and unsymmetrical azines. *Res. Chem. Intermed.* 42, 3333–3349. <https://doi.org/10.1007/s11164-015-2214-z>.
- El-Naggar, A.M., Zidan, A., Elkaeed, E.B., Taghour, M.S., Badawi, W.A., 2022. Design, synthesis and docking studies of new hydrazinyl-thiazole derivatives as anticancer and antimicrobial agents. *J. Saudi Chem. Soc.* 26, (4). <https://doi.org/10.1016/j.jscs.2022.101488> 101488.
- Farghaly, T.A., Masaret, G.S., Muhammad, Z.A., Harras, M.F., 2020. Discovery of thiazole-based-chalcones and 4-hetarylthiazoles as potent anticancer agents: Synthesis, docking study and anticancer activity. *Bioorg. Chem.* 98., <https://doi.org/10.1016/j.bioorg.2020.103761> 103761.
- Fadda, A.A., Soliman, N.N., Bayoumy, N.M., 2019. Antimicrobial properties of some new synthesized benzothiazole linked carboxamide, acetohydrazide, and sulfonamide systems. *Journal of Heterocyclic Chemistry* 56 (9), 2369–2378.
- Farghaly, T.A., El-Metwaly, N., Al-Soliemy, A.M., Katouah, H.A., Muhammad, Z.A., Sabour, R., 2021. Synthesis, molecular docking and antitumor activity of new dithiazoles. *Polycycl. Aromat. Compd.* 41 (8), 1591–1607. <https://doi.org/10.1080/10406638.2019.1689512>.
- Flefel, E.M., Sayed, H.H., Hashem, A.I., Shalaby, E.A., El-Sofany, W., Abdel-Megeid, F. M., 2014. Pharmacological evaluation of some novel synthesized compounds derived from spiro (cyclohexane-1, 2'-thiazolidines). *Med. Chem. Res.* 23, 2515–2527. <https://doi.org/10.1007/s00044-013-0830-y>.
- Gali, R., Banothu, J., Porika, M., Velpula, R., Bavantula, R., Abbagan, S., 2014. Synthesis and in vitro cytotoxic activity of novel coumarinylimidazo [2, 1-b] thiazole derivatives. *RSC Adv.* 4 (96), 53812–53819. <https://doi.org/10.1039/C4RA11428K>.
- Ghoneim, A.A., Ali Hassan, A.G., 2022. An Efficient Procedure of Synthesis Acyclic C-Glycosides of Thiazolo [4, 5-b] Pyrazine and Imidazo [4, 5-d] Thiazole with Expected Anti-Cancer Activities. *Polycycl. Aromat. Compd.* 42 (6), 3328–3338. <https://doi.org/10.1080/10406638.2020.1866035>.
- Gomha, S.M., Riyadh, S.M., Mahmoud, E.A., Elaasser, M.M., 2015. Synthesis and anticancer activity of arylazothiazoles and 1, 3, 4-thiadiazoles using chitosan-grafted-poly (4-vinylpyridine) as a novel copolymer basic catalyst. *Chem. Heterocycl. Compd.* 51, 1030–1038. <https://doi.org/10.1007/s10593-016-1815-9>.
- Gomha, S.M., Abdelaziz, M.R., Kheder, N.A., Abdel-Aziz, H.M., Alterary, S., Mabbkhot, Y.N., 2017. A facile access and evaluation of some novel thiazole and 1, 3, 4-thiadiazole derivatives incorporating thiazole moiety as potent anticancer agents. *Chem. Cent. J.* 11 (1), 1–8. <https://doi.org/10.1186/s13065-017-0335-8>.
- Gomha, S.M., Riyadh, S.M., Huwaimel, B., Zayed, M.E., Abdellattif, M.H., 2022. Synthesis, molecular docking study, and cytotoxic activity against MCF cells of new thiazole-thiophene scaffolds. *Molecules* 27 (14), 4639. <https://doi.org/10.3390/molecules27144639>.
- Grozav, A., Porumb, I.D., Găină, L.I., Filip, L., Hanganu, D., 2017. Cytotoxicity and Antioxidant Potential of Novel 2-(2-((1 H-indol-5yl) methylene)-hydrazinyl)-thiazole Derivatives. *Molecules* 22 (2), 260. <https://doi.org/10.3390/molecules22020260>.
- Haiba, M.E., Abd El-Karim, S.S., Gouhar, R.S., El-Zahar, M.I., El-Awdan, S.A., 2014. Synthesis and evaluation of anti-inflammatory and analgesic activity of some substituted thiazolyl and thiazolidinonyl tetrahydronaphthalene derivatives. *Med. Chem. Res.* 23, 3418–3435. <https://doi.org/10.1007/s00044-014-0926-z>.

- Han, Y., Huang, D., Xu, S., Li, L., Tian, Y., Li, S., Chen, C., Li, Y., Sun, Y., Hou, Y., Sun, Y., 2021. Ligand-based optimization to identify novel 2-aminobenzo [d] thiazole derivatives as potent sEH inhibitors with anti-inflammatory effects. *Eur. J. Med. Chem.* 212. <https://doi.org/10.1016/j.ejmech.2020.113028>
- Holmes, A.H., Moore, L.S., Sundsfjord, A., Steinbakk, M., Regmi, S., Karkey, A., Guerin, P.J., Pidcock, L.J., 2016. Understanding the mechanisms and drivers of antimicrobial resistance. *Lancet* 387 (10014), 176–187. [https://doi.org/10.1016/S0140-6736\(15\)00473-0](https://doi.org/10.1016/S0140-6736(15)00473-0)
- J. Chem. Ed. 87, 1348.
- Jagdale, S., Chavan, A., Shinde, A., Sisode, V., Bobade, V.D., Mhaske, P.C., 2020. Synthesis and antimicrobial evaluation of new thiazolyl-1, 2, 3-triazolyl-alcohol derivatives. *Med. Chem. Res.* 29, 989–999. <https://doi.org/10.1007/s00044-020-02540-5>
- Jain, S., Pattnaik, S., Pathak, K., Kumar, S., Pathak, D., Jain, S., Vaidya, A., 2018. Anticancer potential of thiazole derivatives: a retrospective review. *Mini Rev. Med. Chem.* 18 (8), 640–655. <https://doi.org/10.2174/1389557517666171123211321>
- Kamat, V., Santosh, R., Poojary, B., Nayak, S.P., Kumar, B.K., Sankaranarayanan, M., Faheem, S., Khanapure, S., Barretto, D.A., Vootla, S.K., 2020. Pyridine- and thiazole-based hydrazides with promising anti-inflammatory and antimicrobial activities along with their in silico studies. *ACS Omega* 5 (39), 25228–25239. <https://doi.org/10.1021/acsomega.0c03386>
- Kamble, R.D., Meshram, R.J., Hese, S.V., More, R.A., Kamble, S.S., Gacche, R.N., Dawane, B.S., 2016. Synthesis and in silico investigation of thiazoles bearing pyrazoles derivatives as anti-inflammatory agents. *Comput. Biol. Chem.* 61, 86–96. <https://doi.org/10.1016/j.compbiolchem.2016.01.007>
- Karaman, B., Ulusoy Güzeldemirci, N., 2016. Synthesis and biological evaluation of new imidazo [2, 1-b] thiazole derivatives as anticancer agents. *Med. Chem. Res.* 25, 2471–2484. <https://doi.org/10.1007/s00044-016-1684-x>
- Kartsev, V., Geronikaki, A., Zubenko, A., Petrou, A., Ivanov, M., Glamočlija, J., Sokovic, M., Divaeva, L., Morkovnik, A., Klimenko, A., 2022. Synthesis and antimicrobial activity of new heteroaryl (aryl) thiazole derivatives molecular docking studies. *Antibiotics* 11 (10), 1337. <https://doi.org/10.3390/antibiotics11101337>
- Kaur, N., 2018a. Solid-phase synthesis of sulfur containing heterocycles. *J. Sulfur Chem.* 39 (5), 544–577. <https://doi.org/10.1080/17415993.2018.1457673>
- Kaur, N., 2018b. Photochemical mediated reactions in five-membered O-heterocycles synthesis. *Synth. Commun.* 48 (17), 2119–2149. <https://doi.org/10.1080/00397911.2018.1485165>
- Kaur, N., Ahlawat, N., Verma, Y., Grewal, P., Bhardwaj, P., Jangid, N.K., 2021. Silver-assisted Syntheses of Fused Five-membered N-heterocycles. *Curr. Org. Chem.* 25 (19), 2232–2256. <https://doi.org/10.2174/1385272825666210716144555>
- Kaur, N., Kishore, D., 2014. Nitrogen-containing six-membered heterocycles: solid-phase synthesis. *Synth. Commun.* 44 (9), 1173–1211. <https://doi.org/10.1080/00397911.2012.760129>
- Khidre, R.E., Radini, I.A.M., 2021. Design, synthesis and docking studies of novel thiazole derivatives incorporating pyridine moiety and assessment as antimicrobial agents. *Sci. Rep.* 11 (1), 7846. <https://doi.org/10.1038/s41598-021-86424-7>
- Khloya, P., Kumar, S., Kaushik, P., Surain, P., Kaushik, D., Sharma, P.K., 2015. Synthesis and biological evaluation of pyrazolylthiazole carboxylic acids as potent anti-inflammatory-antimicrobial agents. *Bioorg. Med. Chem. Lett.* 25 (6), 1177–1181. <https://doi.org/10.1016/j.bmcl.2015.02.004>
- Koppireddi, S., Chilaka, D.R.K., Avula, S., Komsani, J.R., Kotamraju, S., Yadla, R., 2014. Synthesis and anticancer evaluation of 3-aryl-6-phenylimidazo [2, 1-b] thiazoles. *Bioorg. Med. Chem. Lett.* 24 (23), 5428–5431. <https://doi.org/10.1016/j.bmcl.2014.10.030>
- Kumar, S., Aggarwal, R., Kumar, V., Sadana, R., Patel, B., Kaushik, P., Kaushik, D., 2016. Solvent-free synthesis of bacillamide analogues as novel cytotoxic and anti-inflammatory agents. *Eur. J. Med. Chem.* 123, 718–726. <https://doi.org/10.1016/j.ejmech.2016.07.033>
- Kumar, G., Singh, N.P., 2021. Synthesis, anti-inflammatory and analgesic evaluation of thiazole/oxazole substituted benzothiazole derivatives. *Bioorg. Chem.* 107. <https://doi.org/10.1016/j.bioorg.2020.104608>
- Latif, N.A., Abbas, E.M.H., Farghaly, T.A., Awad, H.M., 2020. Synthesis, characterization, and anticancer screening of some new bithiazole derivatives. *Russ. J. Org. Chem.* 56, 1096–1107. <https://doi.org/10.1134/S1070428020060202>
- Lei, H., Hu, G., Wang, Y., Han, P., Liu, Z., Zhao, Y., Gong, P., 2016. Design, Synthesis, and Biological Evaluation of 4-Phenoxyquinoline Derivatives Containing Benzo [d] thiazole-2-yl Urea as c-Met Kinase Inhibitors. *Arch. Pharm.* 349 (8), 651–661. <https://doi.org/10.1002/ardp.201600003>
- Li, J.R., Li, D.D., Wang, R.R., Sun, J., Dong, J.J., Du, Q.R., Fang, F., Zhang, W.M., Zhu, H.L., 2014. Design and synthesis of thiazole derivatives as potent FabH inhibitors with antibacterial activity. *Eur. J. Med. Chem.* 75, 438–447. <https://doi.org/10.1016/j.ejmech.2013.11.020>
- Liao, G.P., Zhou, X., Xiao, W., Xie, Y., Jin, L.H., 2017. Synthesis and Antimicrobial Activity of Novel 2-Substituted Phenoxy-N-(4-substituted Phenyl-5-(1H-1, 2, 4-triazol-1-yl) thiazol-2-yl) acetamide Derivatives. *J. Heterocycl. Chem.* 54 (2), 1506–1513. <https://doi.org/10.1002/jhet.2737>
- Liaras, K., Geronikaki, A., Glamočlija, J., Čirić, A., Soković, M., 2014. Thiazole-based aminopyrimidines and N-phenylpyrazolines as potent antimicrobial agents: synthesis and biological evaluation. *MedChemComm* 5 (7), 915–922. <https://doi.org/10.1039/C4MD00124A>
- Lino, C.L., de Souza, I.G., Borelli, B.M., Matos, T.T.S., Teixeira, I.N.S., Ramos, J.P., de Souza Fagundes, E.M., de Oliveira Fernandes, P., Maltarollo, V.G., Johann, S., de Oliveira, R.B., 2018. Synthesis, molecular modeling studies and evaluation of antifungal activity of a novel series of thiazole derivatives. *Eur. J. Med. Chem.* 151, 248–260. <https://doi.org/10.1016/j.ejmech.2018.03.083>
- Liu, J.C., Chen, B., Yang, J.L., Weng, J.Q., Yu, Q., Hu, D.X., 2022. Design, synthesis and cytotoxicity of thiazole-based stilbene analogs as novel DNA topoisomerase IB inhibitors. *Molecules* 27 (3), 1009. <https://doi.org/10.3390/molecules27031009>
- Maghraby, M.T.E., Abou-Ghadi, O.M., Abdel-Moty, S.G., Ali, A.Y., Salem, O.I., 2020. Novel class of benzimidazole-thiazole hybrids: The privileged scaffolds of potent anti-inflammatory activity with dual inhibition of cyclooxygenase and 15-lipoxygenase enzymes. *Bioorg. Med. Chem.* 28, (7). <https://doi.org/10.1016/j.bmc.2020.115403>
- Mahmoud, H.K., Gomha, S.M., Farghaly, T.A., Awad, H.M., 2021. Synthesis of thiazole linked imidazo [2, 1-b] thiazoles as anticancer agents. *Polycycl. Aromat. Compd.* 41 (8), 1608–1622. <https://doi.org/10.1080/10406638.2019.1689514>
- Metwally, N.H., Badawy, M.A., Okpy, D.S., 2015. Synthesis and anticancer activity of some new thiopyrano [2, 3-d] thiazoles incorporating pyrazole moiety. *Chem. Pharm. Bull.* 63 (7), 495–503. <https://doi.org/10.1248/cpb.c14-00885>
- Mirza, S., Naqvi, S.A., Khan, K.M., Salar, U., Choudhary, M.I., 2017. Facile synthesis of novel substituted aryl-thiazole (SAT) analogs via one-pot multi-component reaction as potent cytotoxic agents against cancer cell lines. *Bioorg. Chem.* 70, 133–143. <https://doi.org/10.1016/j.bioorg.2016.12.003>
- Mohareb, R., Al-Omran, F., Abdelaziz, M., Ibrahim, R., 2017. Anti-inflammatory and Anti-ulcer Activities of New Fused Thiazole Derivatives Derived from 2-(2-Oxo-2H-chromen-3-yl) thiazol-4 (5H)-one. *Acta Chim. Slov.* 64 (2), 349–364. <https://doi.org/10.17344/acsi.2017.3200>
- Moldovan, C.M., Oniga, O., Parvu, A., Tipericiu, B., Verite, P., Pîrnău, A., Crișan, O., Bojiță, M., Pop, R., 2011. Synthesis and anti-inflammatory evaluation of some new acyl-hydrazones bearing 2-aryl-thiazole. *Eur. J. Med. Chem.* 46 (2), 526–534. <https://doi.org/10.1016/j.ejmech.2010.11.032>
- Nofal, Z.M., Soliman, E.A., Abd El-Karim, S.S., El-Zahar, M.I., Srour, A.M., Sethumadhavan, S., Maher, T.J., 2014. Synthesis of some new benzimidazole-thiazole derivatives as anticancer agents. *J. Heterocycl. Chem.* 51 (6), 1797–1806. <https://doi.org/10.1002/jhet.1886>
- Othman, I.M., Alamshany, Z.M., Tashkandi, N.Y., Nossier, E.S., Anwar, M.M., Radwan, H.A., 2022. Chemical synthesis and molecular docking study of new thiazole, thiophene, and thieno [2, 3-d] pyrimidine derivatives as potential antiproliferative and antimicrobial agents. *J. Mol. Struct.* 1270. <https://doi.org/10.1016/j.molstruc.2022.133926>
- Pansare, D.N., Shelke, R.N., Shinde, D.B., 2017. A Facial Synthesis and Anticancer Activity of (Z)-2-((5-(4-nitrobenzylidene)-4-oxo-4, 5-dihydrothiazol-2-yl) amino)-substituted Acid. *J. Heterocycl. Chem.* 54 (6), 3077–3086. <https://doi.org/10.1002/jhet.2919>
- Patel, J.J., Morja, M.I., Chikhaliya, K.H., 2020. An efficient synthesis of designed 4-thiazolidinone fused pyrimidine derivatives as potent antimicrobial agents. *J. Heterocycl. Chem.* 57 (10), 3531–3543. <https://doi.org/10.1002/jhet.4070>
- Pawar, C.D., Sarkate, A.P., Karnik, K.S., Bahekar, S.S., Pansare, D.N., Shelke, R.N., Jawale, C.S., Shinde, D.B., 2016. Synthesis and antimicrobial evaluation of novel ethyl 2-(2-(4-substituted) acetamido)-4-substituted-thiazole-5-carboxylate derivatives. *Bioorg. Med. Chem. Lett.* 26 (15), 3525–3528. <https://doi.org/10.1016/j.bmcl.2016.06.030>
- Petrou, A., Fesatidou, M., Geronikaki, A., 2021. Thiazole ring—a biologically active scaffold. *Molecules* 26 (11), 3166. <https://doi.org/10.3390/molecules26113166>
- Prabhu, P.P., Panneerselvam, T., Shastry, C.S., Sivakumar, A., Pande, S.S., 2015. Synthesis and anticancer evaluation of 2-phenyl thiazolidinone substituted 2-phenyl benzothiazole-6-carboxylic acid derivatives. *J. Saudi Chem. Soc.* 19 (2), 181–185. <https://doi.org/10.1016/j.jscs.2012.02.001>
- Prakash, T.B., Reddy, G.D., Padmaja, A., Padmavathi, V., 2014. Synthesis and antimicrobial activity of amine linked bis-and tri-heterocycles. *Eur. J. Med. Chem.* 82, 347–354. <https://doi.org/10.1016/j.ejmech.2014.06.001>
- Reddy, S.M., Rao, D.S., Madhu, K., Subramanyam, C., Kumari, P.G., Raju, C.N., 2018. 2-(Benzo [d] thiazol-2-yl) phenyl-4-nitrophenyl alkyl/aryl substituted phosphoramidates: synthesis, characterization and antimicrobial activity evaluation. *Phosphorus Sulfur Silicon Relat. Elem.* 193 (3), 136–140. <https://doi.org/10.1080/10426507.2017.1392960>
- Rostom, S.A., Faidallah, H.M., Radwan, M.F., Badr, M.H., 2014. Bifunctional ethyl 2-amino-4-methylthiazole-5-carboxylate derivatives: synthesis and in vitro biological evaluation as antimicrobial and anticancer agents. *Eur. J. Med. Chem.* 76, 170–181. <https://doi.org/10.1016/j.ejmech.2014.02.027>
- Saliyeva, L., Holota, S., Grozav, A., Yakovychuk, N., Litvinchuk, M., Sliyva, N., Vovk, M., 2021. Synthesis and evaluation of antimicrobial and anti-inflammatory activity of 6-arylidene-2-methyl-2, 3-dihydroimidazo [2, 1-b][1, 3] thiazoles. *Appl. Chem* 12, 292–303. <https://doi.org/10.33263/BRIAC121.292303>
- Sani, M., Zanda, M., 2022. Recent advances in the synthesis and medicinal chemistry of SF5 and SF4Cl compounds. *Synthesis* 54 (2022), 4184–4209. <https://doi.org/10.1055/a-1845-9291>
- Sateesh Kumar, P., Umadevi, P., 2018. Novel bis (1, 2, 4-oxadiazolyl) Fused thiazole derivatives: synthesis and anticancer activity. *Russ. J. Gen. Chem.* 88, 2611–2615. <https://doi.org/10.1134/S107036321812023X>
- Sayed, A.R., Gomha, S.M., Abdelrazek, F.M., Farghaly, M.S., Hassan, S.A., Metz, P., 2019. Design, efficient synthesis and molecular docking of some novel thiazolyl-pyrazole derivatives as anticancer agents. *BMC chemistry* 13 (1), 1–13. <https://doi.org/10.1186/s13065-019-0632-5>
- Sayed, A.R., Gomha, S.M., Taher, E.A., Muhammad, Z.A., El-Seedi, H.R., Gaber, H.M., Ahmed, M.M., 2020. One-pot synthesis of novel thiazoles as potential anticancer agents. *Drug Des. Devel. Ther.*, 1363–1375. <https://doi.org/10.2147/DDDT.S221263>

- Shabaan, S.N., Baaiu, B.S., Abdel-Aziem, A., Abdel-Aziz, M.S., 2021. Ultrasound-assisted green synthesis and antimicrobial assessment of 1, 3-thiazoles and 1, 3, 4-thiadiazines. *Green Chem. Lett. Rev.* 14 (4), 679–688. <https://doi.org/10.1080/17518253.2021.1999508>.
- Shankerrao, S., Bodke, Y.D., Santoshkumar, S., 2017. Synthesis and antimicrobial activity of some imidazothiazole derivatives of benzofuran. *Arab. J. Chem.* 10, S554–S558. <https://doi.org/10.1016/j.arabjc.2012.10.018>.
- Sharma, A., Gudala, S., Ambati, S.R., Mahapatra, S.P., Raza, A., Payra, S., Jha, A., Kumar, A., Penta, S., Banerjee, S., 2018. On-Water NiFe<sub>2</sub>O<sub>4</sub> nanoparticle-catalyzed one-pot synthesis of biofunctionalized pyrimidine-thiazole derivatives: in silico binding affinity and in vitro anticancer activity studies. *ChemistrySelect* 3 (39), 11012–11019. <https://doi.org/10.1002/slct.201801414>.
- Sharma, D., Kumar, S., Narasimhan, B., Ramasamy, K., Lim, S.M., Shah, S.A.A., Mani, V., 2019a. Synthesis, molecular modelling and biological significance of N-(4-(4-bromophenyl) thiazol-2-yl)-2-chloroacetamide derivatives as prospective antimicrobial and antiproliferative agents. *BMC Chem.* 13, 1–14. <https://doi.org/10.1186/s13065-019-0564-0>.
- Sharma, D., Kumar, S., Narasimhan, B., Ramasamy, K., Lim, S.M., Shah, S.A.A., Mani, V., 2019b. 4-(4-Bromophenyl)-thiazol-2-amine derivatives: synthesis, biological activity and molecular docking study with ADME profile. *BMC Chem.* 13 (1), 1–16. <https://doi.org/10.1186/s13065-019-0575-x>.
- Shi, H.B., Hu, W.X., Zhang, W.M., Wu, Y.F., 2016. Synthesis of 5-acetyl-2-arylamino-4-methylthiazole thiosemicarbazones under microwave irradiation and their in vitro anticancer activity. *J. Chem. Res.* 40 (2), 67–72. <https://doi.org/10.3184/174751916X14519928918516>.
- Shinde, R.R., Gaikwad, D., Farooqui, M., 2020. Synthesis and antimicrobial activity of 2-(4-(benzo [d] thiazol-5-ylsulfonyl) piperazine-1-yl)-N-substituted acetamide derivatives. *J. Heterocycl. Chem.* 57 (11), 3907–3917. <https://doi.org/10.1002/jhet.4099>.
- Sirakanyan, S., Kartsev, V., Spinelli, D., Geronikaki, A., Petrou, A., Ivanov, M., Glamoclija, J., Sokovic, M., Hakobyan, E., Hovakimyan, A., 2021. Synthesis and antimicrobial activity of new 2-piperazin-1-yl-N-1, 3-thiazol-2-ylacetamides of cyclopenta [c] pyridines and pyrano [3, 4-c] pyridines. *Arch. Pharm.* 354 (1), 2000208. <https://doi.org/10.1002/ardp.202000208>.
- Ss, P., Nb, K., Rekha, T., Padmaja, A., Padmavathi, V., 2021. Molecular properties prediction, synthesis, and antimicrobial activity of bis (azolyl) sulfonamidoacetamides. *Arch. Pharm.* 354 (8), e2000483–e. <https://doi.org/10.1002/ardp.202000483>.
- Sukanya, S.H., Venkatesh, T., Rao, S.A., Joy, M.N., 2022. Efficient L-Proline catalyzed synthesis of some new (4-substituted-phenyl)-1, 5-dihydro-2H-pyrimido [4, 5-d][1, 3] thiazolo [3, 2a]-pyrimidine-2, 4 (3H)-diones bearing thiazolopyrimidine derivatives and evaluation of their pharmacological activities. *J. Mol. Struct.* 1247. <https://doi.org/10.1016/j.molstruc.2021.131324> 131324.
- Sultanova, R.M., Lobov, A.N., Shumadalova, A.V., Meshcheryakova, S.A., Zileeva, Z.R., Khusnutdinova, N.S., Vakhitov, V.A., Vakhitova, Y.V., 2021. Synthesis of new 1, 3-thiazol derivatives of maleopimaric acid as anticancer, antibacterial and antifungal agents. *Nat. Prod. Res.* 35 (8), 1340–1348. <https://doi.org/10.1080/14786419.2019.1648459>.
- Suma, V.R., Sreenivasulu, R., Rao, M.V.B., Subramanyam, M., Ahsan, M.J., Alluri, R., Rao, K.R.M., 2020. Design, synthesis, and biological evaluation of chalcone-linked thiazole-imidazopyridine derivatives as anticancer agents. *Med. Chem. Res.* 29, 1643–1654. <https://doi.org/10.1007/s00044-020-02590-9>.
- Tantak, M.P., Wang, J., Singh, R.P., Kumar, A., Shah, K., Kumar, D., 2015. 2-(3'-Indolyl)-N-arylthiazole-4-carboxamides: synthesis and evaluation of antibacterial and anticancer activities. *Bioorg. Med. Chem. Lett.* 25 (19), 4225–4231. <https://doi.org/10.1016/j.bmcl.2015.07.105>.
- Thakare, P., Shinde, A., Dakhane, S., Chavan, A., Bobade, V.D., Mhaske, P.C., 2021. Synthesis and biological evaluation of novel 4-(6-substituted quinolin-4-yl)-N-aryl thiazol-2-amine derivatives as potential antimicrobial agents. *J. Heterocycl. Chem.* 58 (9), 1867–1877. <https://doi.org/10.1002/jhet.4317>.
- Toma, A., Mogoşan, C., Vlase, L., Leonte, D., Zaharia, V., 2017. Heterocycles 39. Synthesis, characterization and evaluation of the anti-inflammatory activity of thiazolo [3, 2-b][1, 2, 4] triazole derivatives bearing pyridin-3/4-yl moiety. *Med. Chem. Res.* 26, 2602–2613. <https://doi.org/10.1007/s00044-017-1959-x>.
- Turan-Zitouni, G., Altıntop, M.D., Özdemir, A., Kaplançıklı, Z.A., Çiftçi, G.A., Temel, H. E., 2016. Synthesis and evaluation of bis-thiazole derivatives as new anticancer agents. *Eur. J. Med. Chem.* 107, 288–294. <https://doi.org/10.1016/j.ejmech.2015.11.002>.
- Vaddula, B.R., Tantak, M.P., Sadana, R., Gonzalez, M.A., Kumar, D., 2016. One-pot synthesis and in-vitro anticancer evaluation of 5-(2'-indolyl) thiazoles. *Sci. Rep.* 6 (1), 23401. <https://doi.org/10.1038/srep23401>.
- Wang, S.M., Zha, G.F., Rakesh, K.P., Darshini, N., Shubhavathi, T., Vivek, H.K., Mallesha, N., Qin, H.L., 2017. Synthesis of benzo [d] thiazole-hydrazone analogues: molecular docking and SAR studies of potential H<sup>+</sup>/K<sup>+</sup> ATPase inhibitors and anti-inflammatory agents. *MedChemComm* 8 (6), 1173–1189. <https://doi.org/10.1039/C7MD00111H>.
- Wentrup, C., 2022. Origins of Organic Chemistry and Organic Synthesis. *Eur. J. Org. Chem.* e202101492. <https://doi.org/10.1002/ejoc.202101492>.
- Yakantham, T., Sreenivasulu, R., Alluraiah, G., Tej, M.B., Ramesh Raju, R., 2019. Design, Synthesis, and Anticancer Activity of 1, 2, 3-triazole Liked Thiazole-1, 2-Isloxazole Derivatives. *Russ. J. Gen. Chem.* 89, 2522–2527. <https://doi.org/10.1134/S1070363219120314>.
- Yamsani, N., Sundararajan, R., 2022. Analgesic and anti-inflammatory activities of novel heterocyclic substituted thiazole derivatives. *Rasayan J. Chem.* 15 (1) <https://doi.org/10.31788/RJC.2022.1516737>.
- Yang, X.C., Hu, C.F., Zhang, P.L., Li, S., Hu, C.S., Geng, R.X., Zhou, C.H., 2022. Coumarin thiazoles as unique structural skeleton of potential antimicrobial agents. *Bioorg. Chem.* 124. <https://doi.org/10.1016/j.bioorg.2022.105855> 105855.
- Zhang, Z.H., Wu, H.M., Deng, S.N., Chai, R.X., Mwenda, M.C., Peng, Y.Y., Cai, D., Chen, Y., 2019. Synthesis and biological evaluation of 2, 4-disubstituted thiazole amide derivatives as anticancer agent. *Chem. Pap.* 73, 355–364. <https://doi.org/10.1007/s11696-018-0587-3>.